SHRINK-SWELL DYNAMICS OF VERTISOL CATENAE UNDER DIFFERENT LAND USES

A Dissertation

by

TAKELE MITIKU DINKA

Submitted to the Office of Graduate Studies of
Texas A&M University
in partial fulfillment of the requirements for the degree of

DOCTOR OF PHILOSOPHY

December 2011

Major Subject: Soil Science

Shrink-Swell Dynamics of Vertisol Catenae under Different Land Uses

SHRINK-SWELL DYNAMICS OF VERTISOL CATENAE UNDER DIFFERENT LAND USES

A Dissertation

by

TAKELE MITIKU DINKA

Submitted to the Office of Graduate Studies of
Texas A&M University
in partial fulfillment of the requirements for the degree of

DOCTOR OF PHILOSOPHY

Approved by:

Chair of Committee,	Cristine Morgan
Committee Members,	Tom Hallmark
	Daren Harmel
	Robert Lascano
	Kevin McInnes
Head of Department,	David Baltensberger

December 2011

Major Subject: Soil Science

ABSTRACT

Shrink-Swell Dynamics of Vertisol Catenae under Different Land Uses.

(December 2011)

Takele Mitiku Dinka, B.S., Mekelle University, Ethiopia;

M.S., Wageningen University, The Netherlands

Chair of Advisory Committee: Dr. Cristine Morgan

Because of the dynamic nature of shrinking and swelling of soils that are classified as Vertisols, partitioning of rainfall into infiltration and runoff in a Vertic watershed is more temporally and spatially unique than in most other watersheds. Hydrology models that account for realistic representation of crack dynamics are rarely used because the spatial and temporal patterns of cracking across a catena and under different land uses are poorly understood. The objectives of the study were to: 1) determine if variability in soil cracking on a Vertisol catena, having the same soil and land cover, could be explained by shrink-swell potential of the soil and changes in soil water content; 2) characterize the temporal and spatial variability of the shrinkage of a Vertisol under different land uses; and 3) determine the relationship between specific volume and water content of soils, particularly between saturation and field capacity. The research was conducted in Vertisol catenae of the Houston Black and Heiden soil series. The catenae were located within the Grassland, Soil and Water Research Laboratory, in Riesel Texas. Soil samples were taken to characterize the general properties of the soils. In situ bi-weekly measurements of vertical soil movements and soil water contents were made over a two-year span. Because the shrink-swell potential was high at most landscape positions, soil water content was the primary factor driving the spatial and temporal variability of soil shrinking and swelling. The measured relationship between the amount of soil subsidence and water loss generally agreed with what would be theoretically expected. Maximum soil subsidence was 120 mm in the grazed pasture, 75 mm in the native prairie, and 76 mm in the row cropped field. Shrinkage of the whole soil was not equidimensional and the study generally indicates more horizontal shrinkage than vertical shrinkage. Laboratory analysis showed an appreciable change in the volume of soils between saturation and field capacity, which further suggested that a layer of soil layer can subside up to 4% while drying from saturation to field capacity, which indicates that the common laboratory measure of shrink swell potential does not capture the complete shrink-swell behavior of soils.

ACKNOWLEDGEMENTS

Above all, always and forever, I thank my God for being so merciful in my life, especially during my studies.

The final output of my study comes to end with the contribution of different institutions and people.

This research was supported by many sources of funding, including the Texas AgriLife Research, a Cooperative Agreement with the United States Department of Agriculture-Natural Resource Conservation Service (USDA-NRCS) Texas Soil Survey; the National Science Foundation; and Texas Water Research Institute.

I would like to thank my Ph.D. committee chair, Dr. Cristine Morgan, and my committee members, Dr. Daren Harmel, Dr. Tom Hallmark, Dr. Robert Lascano, and Dr. Kevin McInnes, for their guidance and support throughout the course of this research.

My appreciation goes to Drs. Cristine Morgan and Kevin McInnes, who have worked so hard to shape my research and improve my ability to think critically and see issues from different points of view.

Special thanks is extended to Dr. Andrea Kishne, Katrina Wilke, Leonardo Rivera, Scott Stanislav, and Dr. Cristine Morgan, for their crucial assistance during fieldwork, especially for their endurance of working outside during the hot and humid summer weather.

Thanks also go to my friends and colleagues, and the Department faculty and staff, for making my time at Texas A&M University a great experience. I also want to extend my gratitude to workers at USDA-ARS Riesel Watersheds for their support during my fieldwork.

Finally, thanks to my mom Asiya, to my dad Mitiku, to my sisters Sofiya, Nefisa, and Buzunesh, and to my brothers Endale and Buzuhayehu, for their encouragement and prayers during my studies.

NOMENCLATURE

b	Surface shrinkage ratio
COLE	Coefficient of Linear Extensibility
h	Thickness of a soil layer
h_{fc}	Maximum thickness of a soil layer
kPa	Killo pascal
$m_{w,i}$	Mass of water at a given water potential
$m_{t,i}$	Total mass of soil at a given water potential
$m_{w,,sat}$	Mass of water at saturation
$m_{t,sat}$	Total mass of soil at saturation
m_d	Mass of solid soil
USDA	United States Department of Agriculture
V_{cr}	Soil crack volume
V_d	Volume of soil clod after oven dry
V_m	Volume of soil clod at -33.3 kPa or field capacity
V_s	Volume of solid soil
$V_{t,i}$	The total volume of soil at a given water potential
$V_{t,sat}$	Volume of bulk soil at saturation
$V_{v,i}$	The volume of void at a given water potential
$V_{v,sat}$	Volume of void at saturation
W	Profile water content per unit land area

W_{max}	Maximum profile water content per unit land area
Z_i	Soil layer height at a given time relative to a monument
Z_{max}	Maximum soil layer height relative to a monument
ΔV	Change in soil volume
ΔZ	Soil subsidence relative to a monument
Δz	Soil subsidence of a soil layer
ΔW	Change in soil water storage
θ	Volumetric water content
θ_{fc}	Volumetric water content at field capacity
θ_s	Volumetric water content at saturation
ω_i	Gravimetric water content of soil at a given water potential
ρ_w	Density of water
ρ_p	Particle density of soil
$\rho_{b,t}$	Wet bulk density of soil at a given water potential
$v_{s,t}$	Specific volume of soil at a given water potential

TABLE OF CONTENTS

LIST OF FIGURES

FIGURE Page

FIGURE Page

LIST OF TABLES

CHAPTER I

INTRODUCTION: RESEARCH OVERVIEW

Vertisols that cover roughly 308 million ha globally (Coulombe et al., 1996) and 18 million ha in the U.S (Soil Survey Staff, 1999) shrink when they dry and swell when they wet. Cracks form in Vertisols when they shrink, and these cracks can facilitate rapid transport of surface water into the subsoil, reduce runoff, and enhance flow of water to subsoil and ground water (Bandyopadhyay et al., 2003; Arnold et al., 2005; Júnior and Boesten, 2005). Because of the spatial and temporal variation in cracks, partitioning of rainfall into infiltration and runoff is more variable in a Vertic watershed compared to watersheds with soils that do not shrink and swell, and this variability should be addressed in models used to simulate surface hydrology. Surface hydrology models that directly account for the effect of crack formation and closure on infiltration and runoff are rarely used in Vertisols because the spatial and temporal phenomena of crack formation and closure across catenae are difficult to mathematically and statistically represent.

Estimates of potential shrinkage and cracking of a soil are typically based on a measurement conducted in a laboratory using the coefficient of linear extensibility

---

This dissertation follows the style of Geoderma.

(COLE) (Grossman et al., 1968; Reeve et al., 1980; Bronswijk, 1991; Thomas et al., 2000a). The COLE provides information on how much a soil is expected to shrink as the soil dries. The measured COLE value is published in USDA NRCS Soil Survey Reports, it is a nationally available nationally and useful starting point for estimating shrink-swell dynamics and crack formation in a soil. For hydrology modeling purposes, it is useful to know if COLE and soil water content across a landscape are sufficient information to calculate soil shrinking and associated estimates of crack formation.

To better understand the relationship between the potential of a soil to shrink and water content and other factors that affect crack formation in situ, more direct field measurements of soil shrink swell dynamics, including measurement of the magnitude of vertical subsidence of a soil layer (Bronswijk, 1991; Kirby et al., 2003; Arnold et al., 2005) and geometric measurements of crack width and length (Daniells, 1989; Bandyopadhyay et al., 2003; Kishné et al., 2009 and 2010) have been conducted. While the shrinking and swelling of small soil samples with change in water content has been extensively studied in laboratory settings, application of that information to calculate how a field soil would behave has been limited by a small number of field measurements of shrink-swell phenomenon. Though the basic concepts of field and laboratory shrinkage have been thought out and observed, it is still unclear how other factors such as landscape position and land use affect shrinkage of soil in the field (Johnston and Hill, 1944; Cabidoche and Voltz, 1995; Baer and Anderson, 1997; Miller et al., 2010). The concept that the soil is a continuum of variable soil properties, soil water dynamics, and land uses across a watershed has had limited attention with regard to soil cracking dynamics. To do a better job of modeling cracking behavior for use in hydrology models, the information that is needed to correctly represent crack formation and extent across watershed needs to be identified.

This Ph.D. study mainly focused on a field-based investigation of the influence of soil properties, land uses and landscape positions on shrink-swell dynamics of a Vertisol by measuring the temporal and spatial variability of soil shrinkage and soil water content. All soil shrinkage and soil water measurements were made in situ. Physical and chemical properties of the soil were measured in the laboratory.

A review of literature that discusses the challenges and the limitations associated with crack measurements is presented. This review provides information or more recent applications of technology that may improve the ability of scientists to quantify soil cracking dynamics, non-invasively, and in the field. The first set of experimental results reported in this dissertation, illustrate the influence of soil properties and landscape positions on temporal and spatial variability of soil shrinking and swelling across a Vertisol catena over three years. The second set of experimental results illustrate the temporal and spatial variability of soil shrinking and swelling under different land uses. These two field experiments are followed by laboratory measurements of the degree of swelling of soil at water contents above field capacity (-33.3 kPa water potential). Finally, exploratory field measurements of the spatial distribution of crack orientations across two Vertisol catenae of different land uses are presented. That field survey shows the potential impact of crack orientation on Vertisol hydrology.

CHAPTER II

REVIEW PAPER: CHALLENGES AND LIMITATIONS IN STUDY OF SHRINK-SWELL AND CRACK DYNAMICS OF VERTISOL

Introduction

According to USDA soil classification, Vertisols are clayey soils (≥ 30 % clay) that have deep, wide cracks for some time during the year and have slickensides within 1 m of the mineral soil surface. Vertisols cover roughly 308 million ha globally (Coulombe et al., 1996) and 18 million ha in the U.S (Soil Survey Staff, 1999). Coverage by Vertisols and vertic integrades is estimated be 320 million ha worldwide (Blokhuis, 2006). These soils swell when they wet, shrink when they dry, and form wide cracks during dry seasons. Wide and deep cracks have capacity to enhance rapid flow of water and nutrients into the subsoil, affecting the hydrology of the soils (Arnold et al., 1995; Bandyopadhyay et al., 2003).

Many studies have looked at the dynamics of soil shrinking and swelling and associated crack formation for the purpose of improving hydrology models (Bronswijk, 1991; Mitchell, 1991; Olsen and Haugen, 1998; Arnold et al., 2005; Kishné et al., 2009; Kishné et al., 2010). While the literature is clear on understanding the shrinking and swelling of soil cores and attempts have been made to translate some of the knowledge to field observations of soil shrinkage, a paucity of observations and knowledge of cracking of field soil exists. For example, how a soil is expected to shrink in the field can be modeled, but several assumptions must be made to simulate crack opening, areal density of cracks, crack depth and crack orientation. The difficulty with modeling actual crack dynamics arises, in part, from the inability to accurately measure crack dimensions in the field and at an adequate scale. Moreover, the shrink-swell dynamics and potential of a soil also varies considerably with time and space.

Shrink-swell properties of Vertisols spatially vary with soil properties, micro-climate, topography, vegetation, cropping patterns, and soil management practices (Davidson and Page, 1956; Komornik, 1969; Smith et al., 1985; Dudal and Eswaran, 1988; Lin et al., 1998; Wilding and Tessier, 1998; Thomas et al., 2000b; Vaught et al., 2006). Soil properties important to shrink-swell that vary in space include clay content, clay mineralogy, and water holding capacity (Davidson and Page, 1956; Ross, 1978; Smith et al., 1985; Dudal and Eswaran, 1988; Lin et al., 1998; Azam et al., 2000; Thomas et al., 2000a). High concentrations of clay in a soil, mainly fine clay fraction, result in high specific surface area that helps store water (Wilding and Tessier, 1998). As a result, when the water content of soil increases, the surface area of the fine clay adsorbs water and the bulk volume of soil increases.

Among all factors, the temporal shrinking and swelling of Vertisols is mainly governed by the amount and distribution of water in the soil, which is a function of clay content, weather patterns, landscape positions, and vegetation type. The annual and seasonal variability of weather patterns (evapotranspiration) causes a variation in the amount and temporal and spatial distribution of soil water that affect the shrink-swell dynamics of soils. Soil water may be high at lower positions in the landscape because of sub/surface flow of water, or shallow ground water. In some cases, increased abundance of fine clay particles (high porosity when wet) from weathering and deposition at the lower positions in the landscape may also enhance the overall wetness of the soils. Root patterns and depths vary by vegetation type and can influence evapotranspiration that determines the rate of water extraction from soils and hence soil shrinking. In contrary, roots may change the size and pattern of cracks by holding soil aggregates together, thus limiting shrinkage of bulk soils (Mitchell and Van Genuchten, 1992). The dependency of shrink-swell and crack dynamics on several spatially and temporally variable factors makes field and laboratory measurement and modeling of soil cracks challenging. This challenge ranges from finding the appropriate measurement technique to the experimental design.

Experiments that observed change in void ratio with moisture ratio natural soil clods and small soil cores have established a well known soil shrinkage characteristic curve (SSCC) (Olsen and Haugen, 1998; Cornelis et al., 2006). Four soil shrinkage phases have been defined within SSCC, structural, basic, residual, and zero shrinkage (Haines, 1923; Keen, 1931; Stirk, 1954; Yule and Ritchie, 1980b; Tariq and Durnford, 1993; Cornelis et al., 2006) (Fig. 2.1). In the structural shrinkage phase, there is little change in bulk volume because air enters soil macropores as they drain (Wilding and Tessier, 1998; Cornelis et al., 2006). Basic shrinkage (normal shrinkage) accounts for the majority of soil shrinkage and water is lost from the inter-particle pores and is reported to occur between soil water potentials of −33.3 to < −1500 kPa (Bandyopadhyay, 2003; Yule, 1980a; Cornelis, 2006). The volume of soil shrunken is equal to the volume of water lost from the soil, resulting in a 1:1 relationship between water ratio (ratio of volume of void to volume of solid soil) and void ratio (ratio of volume of water to volume of solid soil) (Wilding and Tessier, 1998; Bandyopadhyay et al., 2003). Residual shrinkage occurs when the change in volume of the soil is < the volume of water lost and air starts to enter inter-particle pores (Stirk, 1954). In the zero shrinkage, the soil volume does not decrease any further with water loss and the increase of air volume in the soil aggregates is equal to water loss (Bronswijk, 1991).

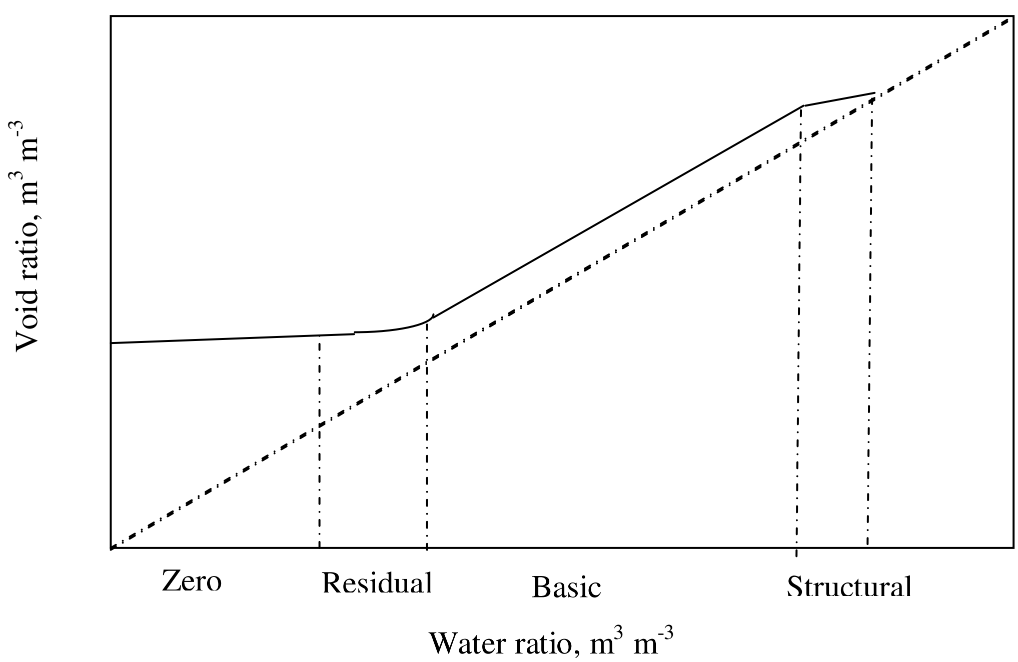

Figure 2.1. Soil shrinkage characteristic curve and the associated shrinkage phases.

Although the significance of incorporating the crack dynamics of Vertisols into hydrology models is well understood, measurements of crack depth, width, orientations, areal density of cracks and crack network, and time of crack opening and closing are challenging. Current estimates of soil cracking usually assume equidimensional shrinkage, in which vertical and horizontal shrinkage are assumed to be equal. Hence, in the field, vertical movement of soil can be measured using rods anchored at different depths in a soil (e.g, Arnold et al., 2005; Baer and Anderson, 1997; Bronswijk, 1991). Measuring horizontal shrinkage is more difficult because of the irregular geometry and spatial distribution of soil cracks (Peng et al., 2006). Combining the equidimensional shrinkage model with field measurements of soil subsidence is not very helpful in estimating crack characteristics. Many assumptions are made to link the measurements of soil subsidence and soil water to estimate or calculate crack information. Due to lack of adequate measurement methods for measuring soil cracking on a representative spatial scale, too few studies have been conducted on soil cracking in the field.

In the literature, little attention is given to examination of techniques used to measure or estimate soil cracks. The purpose of this review is to discuss challenges and limitations of techniques that have been used or might be used to measure soil cracking. Particularly, the techniques are evaluated based on the ability to take frequent and/or continuous measurements, the uncertainty of each measurement, and the scale the measurement represents. Since soil water content is usually measured during, a study of cracking, challenges associated with soil water measurement in a cracking soil also are discussed briefly. This review will help spark discussion and encourage those interested in soil cracking to continue our interdisciplinary search for better measurement techniques.

Measurement Techniques

Past studies of soil swelling and shrinking behavior have involved measurement of the capacity of the soil to make cracks (i.e., soil shrinkage and soil shrink-swell potential) and actual crack dimensions (length, width, depth and orientation). These measurements have been conducted in the laboratory and/or in the field (in situ), each requiring different techniques. The advantages and limitations of field and laboratory measurements techniques are discussed in detail in the following sections.

Field measurement techniques

The most useful insight on soil cracking is likely to be gathered by making crack observations, under actual field conditions. The challenge for such measurements is devising a method that can be used to take measurements at an adequate time and/or spatial scale. Several studies have characterized and quantified the shrink-swell properties of soil and associated crack formation among landscapes, land use types and management systems. Reported methods for measuring shrink-swell dynamics in situ are direct crack width and length measurements made by hand using a ruler (Daniells, 1989; Bandyopadhyay et al., 2003; Kishné et al., 2009), measurement of vertical movement of soils (Aitchenson and Holmes, 1953; Bronswijk, 1991; Baer and Anderson, 1997;

Arnold et al., 2005), surface photography (Peng et al., 2006) and electrical resistivity measurement (Samouëlian et al., 2003; Samouëlian et al., 2004).

Direct crack measurements, can provide information on surface crack density, orientation, and an estimate of crack volume. The measurements are extremely tedious and time consuming for measurements made at appreciable spatial scales. In direct measurement, the depth, width and length of cracks are most often measured using rulers, calipers and tape measures. Kishné et al. (2009; 2010) measured the surface width, length, and location of cracks on a 100-m^2 area (10 m x 10 m) in Texas using a 1-m x 1-m frame with a grid of 0.1-m cell size placed on the soil surface. Though this method resulted in a detailed10-year data set on crack area density, it took 3-4 h to take one measurement from the area during a cracking event (personal communication, Wes Miller). Because measurement takes a long time to collect, these measurements usually only provide snap-shots and the method is not practical for continuous monitoring of soil shrinkage. Additionally, measurements of crack depths and width with depth are prone to high degree of uncertainty. Rivera (2008) graphed hand-measured crack volume data vs. the calculated crack volume based on field-measured soil vertical movement at two different locations. The results of this comparison showed r^2 values of 0.12 and 0.10, but more importantly, the magnitude of the difference was exceptional.

Measurements of vertical shrinkage, made by measuring changes in rod heights anchored at different soil depths, can provide estimates of crack volume (e.g, Arnold et al., 2005; Bronswijk, 1991; Cabidoche and Voltz, 1995). To do so, a monument, which serves as a non-moving reference, is anchored deep below the surface (~ 3 m) or into bedrock. The heights of the rods relative to the monument are measured using surveying equipment, such as a digital level and stadia rod. The changes in heights of the rods are used to track the temporal vertical movement of soil layers. Anchoring rods at different depths provides information about the shrink-swell activity, incrementally with depth. Because the measurement is relatively quick (compared to hand measurement), multiple locations can be measured in one day. Therefore, the rod-based vertical shrinkage measurement allows for multiple locations across a landscape to be monitored. In addition, installation of the rods is rather quick with the use of a hydraulic probe. However, taking a measurement requires two people to be present, hence is labor intensive. Comparison of soil shrinkage layer by layer using this technique may not provide an adequate result unless the soil layers move uniformly across a sample area. Moreover, the use of vertical shrinkage data for hydrology models requires estimation of a crack volume using assumptions such as equidimensional shrinkage. Instead of rods, magnets along a soil profile might also be used to monitor vertical movement of soils. A magnet sensor would sense the location of the installed magnets in the soil profile and help monitor the temporal variation of the location as influenced by the vertical movement of the soil. The benefit of use of the magnets is that the measurement is faster; soil shrinking at different soil layers can be taken at one position and hence comparison of shrinkage based on soil layer is very easy.

Photography has been used to directly quantify density of surface crack area density. Peng et al. (2006) measured soil cracks by digital image analysis and was able to identify crack changes as small as 1.0 mm^2. The digital image analysis method is advantageous because measurements can be taken repeatedly, continuously, and non-destructively. Though its use in the field does not measure crack depth, image analysis helps determine the crack area density at the surface. The benefit of photography is that a time-lapse camera could take short-term temporal variation of cracks and crack opening. Subjectivity related to image processing (Peng et al., 2006) and selection of a representative site can, however, affect results. As outdoor cameras become less expensive, photography becomes a feasible method for quickly covering a large area. The major impasse is the presence of vegetation, which either must be sparse or removed so that cracks are visible. For instance, Velde (1999) took images of cracks from a cultivated field where cracks were clearly visible. Vegetation may enhance water loss, so removing vegetation may modify the real feature of crack dynamics and our ability to non-invasively monitor cracking over time.

Electrical resistivity tomography in soils is used to look at temporal dynamics of wetness and indirectly understand the crack depth and volume (Amidu and Dunbar, 2007), apart from using it to measure cracks in a laboratory (Samouëlian et al., 2003 and 2004). Amidu and Dunbar (2007) used this technique to quantify the effect of gilgai and cracks on soil water variability of Texas Vertisols and found different soil water regimes with depth that occurred due to preferential flow of water and microrelief topography. The field application of the technique is easy because it is noninvasive. However, interpretation of resistivity requires separation of changes in water content and crack development, which both affect resistivity of the soil; therefore, a good instrument calibration is necessary. Moreover, the technique is not sensitive to crack orientation and the isotropic shrinkage property of soils.

Filling a crack with a known volume of fine sand might also be applied to estimate a crack volume in a field though we have not seen any reported results of this field application, however, this technique could be labor and resource intensive and hence cannot be applied on large area and addition of sand may modify the soil environment.

Experimental design

Experimental design in a field can be challenging for a study of shrink-swell and crack dynamics. For instance, selection of representative soil depth and site(s) to measure cracks and soil shrinkage requires a thorough investigation of the spatial variability of the area. While the study of the dynamics at several depths provides more fundamental information, availability of resources limits its field application. Studies also suggest that measurement of soil shrinkage at 0.15 m soil depth would be enough to obtain total crack volume of a soil (Bandyopadhyay et al., 2003; Arnold et al., 2005). However, we have observed cracks that are up to 1.0 m deep on a grazed pasture in central Texas, and cracks up to 1.40 m deep were observed in the Gulf Coast Prairie of Texas (Miller et al., 2010). The decision to what depth to measure soil shrinkage needs to be based on, but not limited to, the depth of soils, the degree of soil water fluctuation in the soil layer and through the soil profile, the amount of inorganic C, and depth and pattern of plant roots.

Because of a spatial variation in clay, soil water content and inorganic C across a catena, soil shrinkage and crack formation can exhibit a similar degree of spatial variability. The variability in degree of changes of water content in space affects the size and depth of cracks. Usually, cracks become narrower in the subsoil than in the surface because there is less drying in the subsoil. Inorganic carbon reduces soil shrinkage by dilution and/or by cementing aggregates together (Deshpande et al., 1964; Rimmer and Greenland, 1976) and hence its variability with depth (generally inorganic carbon content increases with depth) and across a landscape affects the choice of measurement depth and location. Depth and pattern of roots also govern the spatial distribution of soil water lost through transpiration and hence affect soil shrinking so must be considered in experimental design.

The presence of gilgai (surface microrelief) and associated subsurface features make the experimental design and measurement of soil vertical shrinkage more complex (Miller et al., 2010). Shape, size, depth and length of gilgai modify the shrink-swell dynamics of soils across as a space and complicate placement of measurements (Kishné et al., 2009). Similarly, we observed two types of gilgai in Central Texas: circular and linear. Absence of clear understanding on the relationship between microhighs/microlows and cracks are also an additional challenge. For instance, there are studies that indicate as microhighs have a greater crack density than microlows (Amidu and Dunbar, 2007; Kishné et al., 2009), while others reported greater crack density on microlows (Thompson and Beckmann, 1982). Presence of gilgai in a field may affect the soil layer continuity, which also limits comparison of soil subsidence layer by layer across a field.

We observed a relatively greater soil water content in the circular microlows than microhighs in the Vertisols of Central Texas, which makes soils in the microlows wetter than microhighs, and hence less cracks in microlows (Knight, 1980; Kishné et al., 2009). Nonetheless, because of the wetness, more vegetation is common in microlows than in the microhighs. The presence of vegetation could increase cracking by enhancing loss of water through transpiration (Thompson and Beckmann, 1982) and at the same time retard soil cracking by keeping soils together with their roots (Mitchell and Van Genuchten, 1992). Therefore, the crack variability associated with microhighs and microlows must be considered at that scale.

In addition to the measurement techniques, the type of study (whether it is in a laboratory or field) affects the result and interpretation of the shrinkage properties of soils. Bronswijk (1991) developed equations that relate vertical soil subsidence and crack volume to change in soil water storage based on the assumption of isotropic shrinkage. These equations have been used in hydrology models (e.g., SWAT model, Arnold et al., 2005). However, there is evidence suggesting that soils do not always shrink equally in the three dimensions. Peng et al.(2006) found that vertical and horizontal soil shrinkages are anisotropic, and Cabidoche and Ozier-Lafontaine (1995) found a vertical soil movement slightly greater than horizontal movement, claiming that soils slide along slickensides during shrinking that limits the opening of the cracks. However, in small cores where slickensides are less observed, shrinkage of small soil cores was found to be isotropic (Yule and Ritchie, 1980b; Bronswijk, 1990). This lack of consensus on shrinkage property of soils could be due to difference in measurement scale in addition to the measuring techniques.

Measuring soil water in Vertisols

Since changes in soil water content is the main governing factor for shrinking and swelling of soils and formation of cracking, measuring soil water is equally important as measuring cracking. Usually, a neutron meter is used to measure soil water in cracking soils (Baer and Anderson, 1997; Kirby et al., 2003) because it minimizes soil disturbances, is non-destructive (Corbeels et al., 1999), and quicker than gravimetric sampling. Use of other soil water measuring instruments, such as time domain reflectometry and other electromagnetic sensors is limited in Vertisols because cracks separate the soil from the sensors and/or a limited sphere of measurement by the sensors and hence our discussion focuses on a neutron meter. The large sphere of influence of a neutron meter reduces the effect of cracking on the soil water measurement and does not require the sensor to be in direct contact with the soil. A neutron meter can sense from 900 cm^3 to 4.2 m^3 (~a diameter of 97 mm to 1.6 m) of soils at a very wet and dry conditions, respectively (Evett et al., 2009). A relationship between soil water and soil subsidence measurements, therefore, can be developed with confidence, given a good calibration.

Calibration of a neutron meter in a Vertisol is critical and can be different from calibrations in other soils because Vertisols change volume upon drying. Literature on calibration of neutron meters is abundant (Greacen and Schrale, 1976; Greacen and Hignett, 1979; Hodgson and Chan, 1987; Evett and Steiner, 1995; Corbeels et al., 1999; Evett et al., 2006; Mazahrih et al., 2008). Usually the calibration of the neutron meter is performed in the field, but if it is made on a packed barrel, a subsequent adjustment of the calibration based on soil volume change is suggested (Kirby et al., 2003), though the technique is tedious. Because of its simplicity, we prefer a field calibration for Vertisols at dry and wet soil conditions. A field calibration in dry conditions automatically accounts for volumetric changes. More than one calibration site may be needed depending on the objective of the research. If the objective is a long-term measurement over a wide area, the calibration model needs to address the spatial variability of soil properties such as clay content and inorganic C (Evett, 2008) that could affect the reading of soil water content.

Soil water content at different depth can be measured using a neutron meter. While collecting soil water measurement over time with a neutron meter, the distance between the soil surface and the top of the neutron access tube varies because the elevation of the soil surface changes. During soil drying or wetting, measurements taken at a constant distance from the top of the access tube will be at different depths in the soil, depending on the magnitude of the soil vertical movement (Kirby et al., 2003). Based on our field observations, the distance can vary up to 50 mm from its origin. Placing a neutron meter on a stand with a constant height above soil surface avoids this problem (Kirby et al., 2003; Evett, 2008). Presence of cracks near and around the access tube can affect soil water measurement. If rain falls when cracks are open, runoff may accumulate between the outer side of the neutron access tube and the soil wall, which can result in overestimation of soil water content in the soil profile. Moreover, since we observed an access tube with free water inside, the access tubes have to be checked for wetness before taking a measurement or have to be sealed at the bottom during installation. Assessing free water inside and around the access tube before measurement is, therefore, important to reduce measurement error.

Laboratory measurement techniques

In hydrology models, soil shrink-swell potential along with water content measurements is a common way to estimate the magnitude of soil cracks. The relationship between soil shrink-swell potential and soil physical and chemical properties has been studied (Anderson et al., 1973; McCormack and Wilding, 1975; Ross, 1978; Reeve et al., 1980; Yule and Ritchie, 1980b; Smith et al., 1985; Wilding and Tessier, 1998; Gray and Allbrook, 2002). Major soil properties correlated with soil shrink-swell potential are fine and total clay content, water holding capacity, dry and wet bulk density, inorganic and organic C content, specific surface area, and exchangeable cations. Researchers have reported similar and contradicting results about shrink-swell potential and soil properties as discussed below.

Clays in Vertisols have high surface area and minerals (mainly smectitic minerals) that make them have high shrink-swell potential and most studies show a positive and strong correlation between soil shrink-swell potential and total clay content (Anderson et al., 1973; Ross, 1978; Reeve et al., 1980; Smith et al., 1985). In contrast, Yule and Ritchie (1980b) and Gray and Allbrook (2002) found no relationship between clay content and soil shrinking potential in their studies. However, Gray and Allbrook (2002) had allophane in the clay-size fraction and once allophane was removed, a better relationship between clay content and shrink-swell potential were found. The soils studied by Yule and Ritchie (1980b) ranged in clay content from 45 to 70%. At this range, other soil properties dominate the variability in shrink-swell potential. Regardless, McCormack and Wilding (1975) concluded that clay content is a reliable source to calculate shrink-swell potential.

Coefficient of linear extensibility is used to describe the shrink-swell potential of natural soil clods and gives the relative potential of soils to shrink and swell within a water potential range of -33.3 kPa and oven dry (Grossman, 1968; Bronswijk, 1990). The COLE is typically calculated using the volume of a soil clod measured at -33.3 kPa (V_m) and measured after oven dried (V_d),

$$COLE = \frac{V_m^{1/3} - V_d^{1/3}}{V_d^{1/3}}$$

The water contents used to produce V_d does not occur under field conditions. Therefore, measuring the shrinkage limit of soil clods at oven dry may over estimate the soil shrinkage expected to occur in the field. During estimation of COLE, swelling of soils at potentials greater than -33.3 kPa is also ignored. Because Vertisols are high in clay content (≥ 30 %), the field capacity of the soil may go beyond the commonly assumed soil water potential of -33.3 kPa; therefore, we might expect the soil to swell at soil water contents wetter than -33.3 kPa water potential. Researchers have used -10 kPa instead of -33.3 kPa water potential for clayey materials to represent soil water at field capacity (Messing and Jarvis, 1990).

In most studies, the volume of soil clods is measured based on Archimedes's principle, i.e. the clod is immersed in water, and the volume of water displaced by the clod is the same as the volume of the clod. To avoid penetration of water into clods during immersion, clods are usually coated with Saran or a paraffin wax. The advantages of Saran coating clods is that soil samples are intact (natural fabric) and the measurement error is low (Tunny, 1970; Sander and Gerke, 2007). It has been reported that the classical Saran method limits water penetration during immersion, requires a correction for the volume of Saran coatings, may limit swelling, and may not properly shrink with the clod (Cornelis et al., 2006; Sander and Gerke, 2007). Moreover, Saran-coated clods may not be reused for other analysis, like chemical analysis or volume measurement at multiple water contents. As a result, distinct samples are required for each analysis (Tunny, 1970; Anderson et al., 1973), which makes the method resource demanding. The COLE measurements can also vary depending on the water content a soil clod is coated and studies show that wetting of clods before coating results in greater COLE values (McCormack and Wilding, 1975). As an alternative to Saran-Archimedes's method, use of a 3D image scanner that measures volume of soil clods, allows volume measurement of a single clod at multiple soil water potentials. The disadvantage of the 3D scanner is that it is currently time-consuming (> 1 h/clod), and image processing is prone to subjectivity.

In addition to the Saran coating technique, pedo-transfer functions have been used to estimate COLE. Interpretations of the relationship between soil properties and shrink-swell potential of a soil require a clear mechanistic explanation of how soil properties influence shrink-swell potential. The relationships between COLE and soil properties have been successfully implemented, but results are not consistent. For instance, McCormack and Wilding (1973) computed a multiple regression to relate COLE to soil properties including fine clay, coarse clay, total clay, and water content at 1500 kPa. Surprisingly, none of the variables was significant when total clay was included. Anderson et al. (1985) and Smith et al. (2002) also found a positive correlation between COLE and exchangeable sodium percentage, while Gray and Allbrook (Gray and

Allbrook, 2002) found no significant relationship because the soils had low concentrations of exchangeable cations.

Organic matter improves soil structure and increases soil porosity; therefore, if a soil holds more water, it may shrink more upon drying. On the other hand, if water is held in larger pores, the effect of organic matter on shrink-swell could reduce shrink-swell potential because the water loss is structural (Fig. 2.1). For this reason, the relationship between organic matter and soil shrinkage is not simple (Reeve et al., 1980) and contrary results have been found. For instance, a positive correlation was reported between organic C and shrinkage in both topsoil and subsoil by Reeve et al. (1985), while Smith et al. (1956) reported no significant relationship. Moreover, Davidson and Page (1956) reported that removal of organic matter increases swelling capacity of soils, claiming that adsorption of organic matter on soil clays modifies the swelling property of the clay.

Conclusions

A mechanistic understanding of soil crack formation and geometry for insitu conditions is not well known. Clearly, exploration of soil cracking is very limited by the difficulty in observing the shrink-swell phenomena, particularly observations that are minimally invasive, allowing monitoring of cracking with time. Current techniques of measuring soil cracking and the shrink-swell dynamics of Vertisols are far from providing complete information for understanding their impact on large and small scale hydrological processes. Information needed includes crack area density, depth, orientation and network, opening and closing time, and pattern of formation. No single technique reviewed can provide this information continuously, nondestructively and with reasonable certainty in the field.

While we can currently measure soil subsidence in the field, the relationship between soil subsidence and cracking is poorly developed. Understanding and quantifying the insitu relationship between change in soil water storage and the mechanisms of cracking, which are vertical cracking, surface and subsurface horizontal cracking and diagonal cracking, currently is a challenge to improve our understanding of how water moves through cracks. Improving the accuracy and efficiency of promising technologies such as surface photography, electrical resistivity measurement, and use of magnets provide opportunities to collect more detailed information on soil cracking, particularly when used together with subsidence measurements. Laboratory studies are used to measure and model soil shrink-swell potential so that the information can be transferred to hydrology models and applied on landscape and watershed scales. The COLE helps estimate maximum soil shrinkage in a field, and can be converted to crack volume with certain assumptions. However, COLE does not account for temporal variability of soil water change that mainly governs crack formation. Therefore, to estimate the apparent occurrence and volume of cracks, use of COLE should be supported with the temporal change of soil water storage. A combined use of field and laboratory techniques, assisted by models, may help get all the necessary information for hydrology models. Acquiring crack information will fill the gap in hydrology models that are applied on shrink-swell soils. Developing advanced techniques (both software and hardware) that address the spatial and temporal dynamics of soil shrinkage and crack formation is needed.

CHAPTER III

SHRINK-SWELL BEHAVIOR OF SOILS ACROSS A VERTISOL CATENA

Introduction

Cracks that form as clayey soils dry are known to facilitate rapid infiltration and storage of rainwater, and while the effect of these desiccation cracks has been long recognized as a major reason for poorly defined relationships between the amounts of runoff and rainfall in watersheds with shrink-swell soils (Lindenmaier et al., 2006), few surface hydrology models have modules to accurately track the degree of cracking. Those models that do consider temporal changes in cracking (e.g., SWAT, Arnold et al., 2005) generally do not address the spatial patterns of crack formation and closure within a hydrologic sub-unit having a single soil and land use, and the effect that ignoring that variability has on model estimates of infiltration, runoff, and run-on remains uncertain. Cracks that are large enough to drastically affect partitioning of rainfall most often have been characterized by a calculation of areal density or crack volume derived from vertical movements of soil associated with the shrink-swell process (Bronswijk, 1991) rather than by tedious geometric measurements of the spatial distribution of crack aperture (Cabidoche and Ruy, 2001). We used the same method based on vertical movements of soil to understand the spatial variation of areal density of crack with changes in soil water content in an attempt to characterize soil properties needed to model the development of cracks across an outwardly uniform soil of a Vertisol catena.

In general, the opening and closing of cracks in any given area on a Vertisol catena should depend on the vertical distribution of the potential of the soil to shrink or swell and on the temporal dynamics of soil water content within the soil profile (Baer and Anderson, 1997). The coefficient of linear extensibility (COLE), a routine measure used to characterize shrink-swell potential when soils are mapped (Soil Survey Staff, 2003), expresses the magnitude of change in a length scale of the natural soil matrix between water contents associated with -33.3 kPa matric water potential and the oven dry (105 °C) state, relative to the length scale of the oven dry state (Grossman et al., 1968; Bronswijk, 1990). Variation of COLE has been related to variation in clay content, fine clay content, specific surface area, cation exchange capacity, and saturated water content (Franzmeier and Ross, 1968; Anderson et al., 1973; Thomas et al., 2000a; Vaught et al., 2006). More detailed estimates of shrink-swell potential that account for the interaction of many of these factors exist (e.g., Thomas et al., 2000), but COLE offers a readily available estimate that can be obtained from soil survey data (Soil Survey Staff, 2003). Shrinking or swelling of soil aggregates between the water content limits inherent in COLE is generally accepted to be nearly isotropic (Bronswijk, 1990) and to follow a fairly well-defined relationship with water content, which is illustrated by the soil shrinking characteristic curve (Fig. 2.1) (Olsen and Haugen, 1998; Chertkov, 2007).

It would be expected that COLE could be used to estimate limits of both the vertical movement of soil and the areal density of crack volume at water contents below that associated with -33.3 kPa water potentials. A layer of soil, that exhibits isotropic shrinkage and that collapses vertically on itself during shrinkage, should have a thickness, relative to its thickness at -33.3 kPa matric water potential, that falls between values of 1 and 1/(1+COLE) when wet and oven dry, respectively. The areal density of crack volume that could be generated per unit layer thickness of that same soil as it dries from -33.3 kPa water potential should fall between 0 and $(1/(1+\mathrm{COLE}))(1-(1/(1+\mathrm{COLE}))^2)$. For example, if COLE = 0.1 m m^{-1}, the relative thickness of layer of soil over the range of water contents normally encountered in the field should be between 1 and 0.91 and the areal density of cracks per unit thickness of soil should be between 0 and 0.16. That is to say, a 200 mm layer of soil with COLE = 0.1 m m^{-1} and initially at -33.3 kPa could shrink to a minimum thickness of 182 mm and develop cracks that could hold up to 32 mm of rainfall. Obviously, neither of these limits would be observed under normal field conditions as the soil would not reach an oven dry state, but smaller changes in water content that extend to greater depths in a soil profile can produce cracks with considerably more volume.

For soils having a relatively high COLE, for instance 0.1 m m^{-1}, the maximum ratio change in thickness with depth of water lost by evaporation should be ~ 1/3 m m^{-1}, which indicates isotropic shrinkage (Aitchenson and Holmes, 1953; Yule and Ritchie, 1980b). It is worth noting that Cabidoche and Voltz (1995) found ratios > 1/3 m m^{-1} in a field study on a Vertisol and attributed the higher rate to the soil not only vertically collapsing on itself, but moving diagonally along slickensides. The maximum ratio of production of the areal density of vertical crack volume with depth of water lost should be ~ 2/3 m m^{-1} if the soil shrinks equidimensionally. Obviously, with soil having very low COLE, say 0.01 m m^{-1}, the maximum rate of change in thickness and the maximum rate of production of the areal density of cracks should be appreciably < 1/3 m m^{-1} and 2/3 m m^{-1}, respectively.

How COLE is related to the maximum shrinkage rate with water loss is not readily apparent from information in the literature, as there has not been appreciable work on shrink-swell of soils that have intermediate to low shrink-swell potential. It is worth noting, that even with a high COLE, the observed maximum shrinkage rate of a layer of soil under field conditions with water loss could be considerably less than 1/3 m m^{-1} if the structural units did not fully collapse on themselves due to bridging and/or root support of aggregates that separate as they dry. In this case where vertical shrinkage is < expected from the combination of COLE and the change in water content, appreciable horizontal crack volume would be generated – a crack volume that would not be accounted in the estimates of crack volume by vertical movements of the soil alone.

The temporal dynamics of water in the soil profile at any given location on a catena should be related to the local water storage capacity of the soil, capture of rainfall, rate of evapotranspiration, and subsurface fluxes. The pattern of cracking along topographic positions of a catena may appreciably influence capture of runoff from upslope positions. To improve interpretation of the effect of vertical movements of soil on generation of cracks, temporal measurements of water content within the soil are needed. Our specific objective was to determine whether or not variation in the degree of shrinking and swelling of soil across an outwardly uniform Vertisol, and the inferred large-scale cracking patterns, could be explained by variation in COLE and the temporal distribution of water stored in the pedon.

Materials and Methods

Study area

The research was conducted at the USDA-ARS Grassland, Soil and Water Research Laboratory near Riesel, Texas (96.88° W, 31.47° N). The two soils found in the study area are Houston Black and Heiden clays, both fine, smectitic, thermic Udic Haplusterts (Soil Survey Staff, 2003). The soils are formed from weakly consolidated calcareous clays and marls (Allen et al., 2005). The elevation of the study site ranges from 133 to 145 m above sea level. The climate is warm and sub-humid with a mean annual rainfall of 910 mm. A 7-ha grazed Coastal Bermudagrass (*Cynodon dactylon*) pasture was selected for the study. A survey-quality GPS with 0.25-mm vertical accuracy (R7 base station and R8 Rover Trimble®, Sunnyvale, CA) and an EM38DD (Geonics® Ltd., Mississauga, Ontario, CA) were used to create elevation and apparent soil electrical conductivity (EC_a) maps of the field, respectively.

The study area contained a catena with a 12-m elevation difference within a distance of 330 m. The EC_a map was used to characterize the spatial variability of soil properties across the catena (Corwin and Lesch, 2005) for the purpose of selecting sites to measure soil subsidence and soil water content. Six sites on the Vertisol catena were selected based on landscape position and EC_a values. Measurement sites were selected on the summit, shoulder, backslope and footslope (Fig. 3.1). The backslope and footslope each had two measurement sites because of variability expressed in the EC_a map. On taking soil cores, it was observed that the sites at the backslope differ in soil depth to parent material. One backslope position is mapped in Houston Black clay (very deep, 1.64 m) and found on a softer limestone marl while the other, though still mapped as a Houston Black clay, more closely resembles the Heiden series (moderately deep, 0.75 m) and in this case located on a more weathering-resistant chalk parent material (Soil Survey Staff, 2003). The backslope site on Houston Black was referred to as Backslope-1, while 45-m away and 2.3 m lower in elevation the backslope site mapped as Heiden was referred to as Backslope-2. Two sites were also selected at the footslope. The two sites at the footslope are 85-m apart and 1.5-m elevation difference. The footslope position, which was located at the higher elevation was referred to as Footslope-1 while the one at the lower elevation is referred to as Footslope-2.

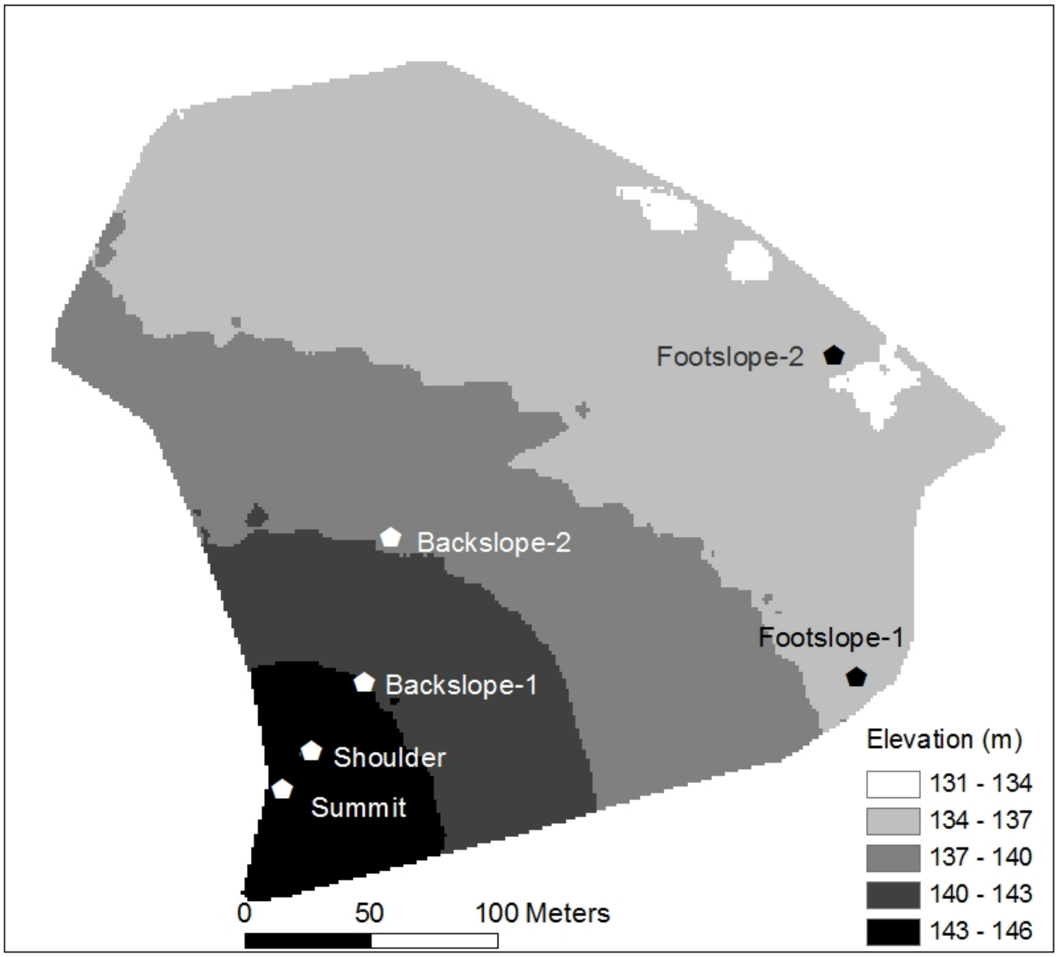

Figure 3.1. Topographic map of the study area located at the USDA-ARS Grassland, Soil and Water Research Laboratory, in Riesel, Texas. The positions in the map show locations of measurement sites.

Field measurements

To measure the vertical shrink-swell movement at each site, 10-mm diameter steel rods (10-mm bars) were anchored at depths of 0.2, 0.8 and 1.2-m at all sites except at the Summit. The site on the Summit was established in 1997 (Arnold et al., 2005). The rods were anchored at 0.3, 0.9, 1.5 and 4.5-m depth. The rod anchored at 4.5 m served as a non-moving reference monument for sites located at the Summit, Shoulder, and Backslope. An additional monument was installed at 3.5-m depth for sites located at the Footslope. The height of each rod with respect to the unmoving monument was measured up to 1.5-mm accuracy and 0.1-mm decimal digits using a level mounted on a tripod and a stadia rod (SDL50, CG Surveying Limited, Elstree Way, Herts, UK). Changes in heights of the rods anchored at different depths in the soil relative to a monument were used to track the temporal trends in thickness of soil layers.

Near each set of rods, a 50-mm diameter aluminum tube was installed to allow measurement of soil water content using a neutron meter (CPN 503DR HYDROPROBE®, CPN International, Inc., CA). Soil water content was measured in 0.2-m intervals to 1.2 m depth, always starting at 0.2 m below the soil surface. The neutron meter was calibrated in the field at dry and wet soil moisture conditions using measurements at two locations in the catena and one nearby. At each calibration site, four soil cores (67-mm diameter) were taken within a radius of 0.08 m from the access tube installed for calibration to a depth of 1.3 m. Each soil core was divided at 0.10 m intervals and used for gravimetric analysis of water content by oven drying at 105 ^{o}C. The average volumetric water content of the four soil cores was used for the calibration (r^2= 0.934; RMSE= 0.025 m^3 m^{-3}). We assumed that calibrating at three locations and down to 1.30-m soil depth would capture the variability in total clay and inorganic C contents across the field. Moreover, changes in soil C contents are minor over short time scales and have little effect on the reading of a neutron meter (Evett, 2008).

Measurements of vertical shrinking and swelling of soils and soil water content were conducted bi-weekly from April 2006 through the end of 2008.

Laboratory measurements

At each measurement site, soil cores were pulled and described in the field. Soil samples from each site and each soil horizon were collected. Soil properties including particle size distribution, dry and wet bulk density, gravimetric water content at field capacity, total C, and organic C were measured. Particle size distribution was measured using the pipette method (Soil Survey Staff, 1996). Three soil clods (diameter 0.05 to 0.06-m and height 0.05 to 0.10-m) were taken from each horizon to determine bulk density, gravimetric water content at field capacity, and COLE (Soil Survey Staff, 1996). Dry and wet bulk densities were measured after coating clods with Saran (Soil Survey Staff, 1996). Total C was measured using dry combustion (Soil Survey Staff, 1996); inorganic C was measured using the modified pressure-calcimeter method (Sherrod et al., 2002); organic C content was calculated as the difference between total and inorganic C contents.

Analysis of soil subsidence and soil water

Soil subsidence data were analyzed in three phases. First, the relationship between thickness of a soil layer, h, with respect to maximum soil layer thickness, h_{fc}, and water content was analyzed for each soil layer and compared against the expected theoretical relationship (Olsen and Haugen, 1998). Volumetric water content at field capacity (θ_{fc})

and saturation (θ_s), and the COLE were used on the Olsen and Haugen model to define the shrinkage curve. In the model, a unit volume of the solid soil was assumed, and the total bulk volume (V_t) at a given time was estimated by, $V_t = 1 + e$ and h= $(V_t)^{1/3}$, where e is the void ratio. The void ratio (e) and water ratio (ϑ) were used to estimate V_t and they were determined as follows, adopting the Olsen and Haugen model (1998). The void ratio was estimated by,

$$e = \frac{1}{2}\left(\lambda_3 * \vartheta + \lambda_2 + \sqrt{(\lambda_3 * \vartheta + \lambda_2)^2 - 4 * \lambda_3 * \lambda_2 (1 - \lambda_1) * \vartheta}\right)$$

where λ_1, λ_2 and λ_3 are coefficients determined from shrinkage characteristics. These coefficients were estimated as follows:

$$\lambda_1 = 1 - \frac{(\lambda_3 * \vartheta_{fc} + \lambda_2)^2 - (2 * e_{fc} - \lambda_3 * \vartheta_{fc} - \lambda_2)^2}{4 * \lambda_2 * \lambda_3 * \vartheta_{fc}};$$

$\lambda_2 = \dfrac{(1 + e_{fc})}{(1 + \mathrm{COLE})^3} - 1$; where e_{fc} is the void ratio at field capacity; and

$\lambda_3 = 1$.

The water ratio ϑ was sequentially assigned values between 0 and ϑ_{fc} to estimate e. Therefore, ϑ_{fc} was estimated first as by $\vartheta_{fc} = \theta_{fc} * (1 + e_{fc})$, where e_{fc} is the void ratio at field capacity. This void ratio was calculated as,

$$e_{fc} = \frac{1}{\frac{1}{\theta_s} - 1}$$

Based on the void ratio (e) and water ratio (ϑ), the volumetric water content of soils (θ) was estimated by,

$$\theta = \frac{\vartheta}{1+\mathrm{e}}$$

Soil subsidence from the top metal rod (0.3 m at Summit and 0.2 m at the rest) with respect to the monument was determined. The maximum height during the study period was taken as a reference to calculate the soil subsidence. The magnitude of soil subsidence from a given soil depth with respect to the monument was calculated as follows;

$$\Delta Z = Z_i - Z_{\max}$$

where, ΔZ is the soil subsidence (m) from the fully swollen state, which is the reduction in soil height due to a change in soil water storage from the saturated state, Z_{max} is the maximum soil height (m) measured during the study period and Z_i is the soil height (m) at a given time, both with respect to the monument. It was assumed that maximum soil swelling occurs when the difference between the monument height and the rod height is very small. Then, the soil subsidence for a given soil layer, denoted as Δz, was quantified by taking the difference between soil subsidences (ΔZ) measured at two different depths.

The relationship between soil subsidence Δz of a given soil layer and the respective change in soil water storage was analyzed using regression analysis. The analysis was made for a soil layer where the soil water content was measured. The soil water content was analyzed for each 0.2-m soil section between 0.2 and 1.2 m soil depth for all positions except at the Summit and Backslope-2. At the Summit, the soil section between 0.3 and 1.5 m depth was used for the analysis. At the Backslope-2, the soil water was analyzed for a soil section between 0.2 and 0.8 m depth. The volumetric soil water content measured at different layers was multiplied by the depth it represents (to get mm of water) and summed to get the soil water content for the whole soil profile section being considered. Since the thickness of each soil layer changes with shrinking and swelling, measurement depths of water content were determined with respect to the soil surface. Estimation of soil water from the volumetric water content (θ) measured at different depth was done as follows,

For the Summit,

$$W = 0.20\text{m} * \theta_{0.4} + 0.20\text{m} * \theta_{0.6} + 0.20\text{m} * \theta_{0.8} + 0.20\text{m} * \theta_{1.0} + (0.40 - \Delta z)\text{m} * \theta_{1.2}$$

For the Backslope-2,

$$W = 0.10\text{m} * \theta_{0.2} + 0.20\text{m} * \theta_{0.4} + 0.20\text{m} * \theta_{0.6} + (0.10\text{m} - \Delta z) * \theta_{0.8}$$

For other locations,

$$W = 0.10\text{m} * \theta_{0.2} + 0.20\text{m} * \theta_{0.4} + 0.20\text{m} * \theta_{0.6} + 0.20\text{m} * \theta_{0.8} + 0.20\text{m} * \theta_{1.0} + (0.10\text{m} - \Delta z) * \theta_{1.20}$$

where, W is the soil water content at given time per unit area (m). The maximum soil water content per unit area (m), W_{max}, was estimated two ways. First, the maximum water content measured in the field at each soil depth was selected. Second, maximum volumetric water content was assumed to be the water content at which all soil pores are filled with water, where porosity was calculated from bulk density of natural soil clods at field capacity (-33.3 kPa) and using a particle density of 2.4 Mg m^{-3}. The values before each θ indicated the soil thickness assigned to the soil water content θ measurement; the subscript of θ indicated the depth below the soil surface where soil water content was measured; and Δz is the soil subsidence (m) of that soil layer.

The maximum soil water content, W_{max}, was taken as a reference to estimate change in soil water storage from the entire soil layer as follows:

$$\Delta W = W - W_{max} ,$$

where ΔW (m) is the change in soil water storage at a given time.

Finally, the change in soil water storage (ΔW) was correlated with the soil subsidence (Δz) using a simple linear regression to determine variability in the relationship between Δz and ΔW. The relationship was analyzed first for the soil layer between 0.2 and 1.20 m and then between 0.2 to 0.8 m and 0.8 to 1.2 m soil layers.

Results and Discussions

Spatial variability of soil shrink-swell potential

The potential of the soil to shrink and swell (COLE) varied both laterally and vertically across the landscape, following the variability in clay and inorganic C content of the soils (Table 3.1). At the top of the catena, COLE varied with depth (CV 17 to 38 %), whereas at the footslope COLE was fairly constant with depth (CV 8 %). The low CV of COLE (with depth) at the Footslope likely indicated deeper weathering and possibly deposition of material with high fine clay and low inorganic C content of the soil at the bottom of the catena.

Simple correlations between COLE and total clay content, fine clay content, and inorganic C ($CaCO_3$) resulted in correlation coefficients of 0.48, 0.48, and -0.91, respectively (Fig. 3.2). Total clays (<2 µm) and fine clays (<0.2 µm) are known to drive the magnitude of COLE and both ranged between 42 to 64 % and 7 to 27 %, respectively, across the catena.

Table 3.1. Soil characterization data by horizon and at six landscape positions along the Vertisol catena, in Riesel, Texas.

Depth	Horizon	Silt	Clay	Fine clay	Texture	Inorganic C	COLE (SD)	$\omega^{\dagger}$ (SD)	ρ_b* (SD)
- - m- -		-------- kg kg^{-1}------				kg kg^{-1}	m m^{-1}	kg kg^{-1}	Mg m^{-3}
					Summit				
0-0.19	Ap	0.35	0.55	0.20	C	0.037	0.18 (0.01)	0.52 (0.07)	0.96 (0.11)
0.19-0.52	Bw	0.35	0.56	0.20	C	0.042	0.15 (0.02)	0.38 (0.06)	1.25 (0.11)
0.52-0.78	Bkss1	0.37	0.55	0.21	C	0.055	0.11 (0.02)	0.36 (0.04)	1.31 (0.06)
0.78-1.18	Bkss2	0.34	0.59	0.27	C	0.051	0.10 (0.01)	0.31 (0.03)	1.40 (0.04)
1.18-1.50	Bkss3	0.34	0.61	0.27	C	0.054	0.09 (0.01)	0.32 (0.03)	1.38 (0.07)
					Shoulder				
0-0.17	A	35.4	0.58	0.18	C	0.040	0.12 (0.01)	0.37 (0.05)	1.26 (0.06)
0.17-0.60	Bw	32.8	0.62	0.23	C	0.045	0.12 (0.00)	0.35 (0.00)	1.34 (0.02)
0.60-0.84	Bkss1	31.5	0.64	0.28	C	0.047	0.11 (0.01)	0.33 (0.02)	1.34 (0.02)
0.84-1.20	Bkss2	36.0	0.60	0.28	C	0.055	0.09 (0.01)	0.32 (0.02)	1.38 (0.03)
1.20-1.64	Bkss3	38.4	0.58	0.21	C	0.065	0.08 (0.00)	0.32 (0.02)	1.37 (0.06)
					Backslope-1				
0-0.20	A	0.40	0.52	0.18	C	0.053	0.13 (0.01)	0.44 (0.04)	1.12 (0.06)
0.20-0.48	Bw	0.46	0.50	0.17	SiC	0.074	0.07 (0.01)	0.31 (0.00)	1.36 (0.03)
0.48-0.91	Bk	0.48	0.47	0.15	SiC	0.082	0.05 (0.00)	0.27 (0.02)	1.42 (0.05)
0.91-1.11	Bkss	0.46	0.48	0.16	SiC	0.080	0.05 (0.00)	0.27 (0.01)	1.45 (0.01)
1.11-1.37	BCk1	0.43	0.51	0.13	SiC	0.081	0.07 (0.01)	0.29 (0.02)	1.41 (0.06)
1.37-1.64	CBk2	0.40	0.53	0.12	SiC	0.080	0.08 (0.00)	0.34 (0.02)	1.33 (0.03)

Table 3.1 . Continued

Depth	Horizon	Silt	Clay	Fine clay	Texture	Inorganic carbon	COLE (SD)	ω† (SD)	ρb* (SD)
- - m- -		-------- kg kg^{-1}------				kg kg^{-1}	m m^{-1}	kg kg^{-1}	Mg m^{-3}
					Backslope-2				
0-0.22	A	0.44	0.47	0.11	SiC	0.082	0.09 (0.01)	0.39 (0.05)	1.12 (0.07)
0.22-0.48	Bw	0.49	0.44	0.07	SiC	0.087	0.04 (0.00)	0.34 (0.00)	1.34 (0.03)
0.48-0.75	BC	0.52	0.42	0.07	SiC	0.081	0.04 (0.01)	0.28 (0.00)	1.51 (0.01)
					Footslope-1				
0-0.16	A1	0.34	0.51	0.16	C	0.019	0.13 (0.00)	0.42 (0.04)	1.16 (0.06)
0.16-0.37	A2	0.32	0.54	0.21	C	0.024	0.14 (0.01)	0.40 (0.02)	1.23 (0.03)
0.37-0.56	Bss	0.33	0.53	0.23	C	0.024	0.15 (0.01)	0.42 (0.02)	1.20 (0.03)
0.56-0.90	Bkss1	0.33	0.54	0.20	C	0.025	0.16 (0.01)	0.43 (0.01)	1.20 (0.01)
0.90-1.29	Bkss2	0.36	0.52	0.18	C	0.023	0.15 (0.02)	0.44 (0.00)	1.20 (0.01)
1.29-1.95	Bkss3	0.36	0.54	0.22	C	0.037	0.14 (0.00)	0.40 (0.02)	1.26 (0.03)
					Footslope-2				
0-0.25	A1	0.36	0.53	0.16	C	0.025	0.14 (0.01)	0.44 (0.04)	1.14 (0.06)
0.25-0.50	A2	0.33	0.58	0.21	C	0.027	0.14 (0.01)	0.39 (0.02)	1.26 (0.02)
0.50-0.94	Bkss1	0.39	0.53	0.16	C	0.028	0.17 (0.02)	0.45 (0.02)	1.17 (0.03)
0.94-1.40	Bkss2	0.37	0.54	0.22	C	0.028	0.16 0.00)	0.46 (0.02)	1.16 (0.01)
1.40-1.90	Bkss3	0.37	0.53	0.15	C	0.030	0.17 (0.02)	0.45 (0.02)	1.16 (0.03)
1.90+	Bkss4	0.32	0.57	0.23	C	0.030	0.16 (0.01)	0.44 (0.02)	1.17 (0.03)

† Gravimetric water content at -33 kPa water potential.
* Bulk density at -33.3 kPa water potential.

The highest clay and fine clay contents were found toward the top of the catena (Summit and Shoulder). Just like COLE, fine clay varied the most within the soil profile at the top of the catena (CV 14 to 17 %), and was most uniform at the bottom (CV 4 to 6 %). The highest inorganic C content was measured at Backslope-2, followed by Backslope-1, Shoulder, Summit and the Footslope positions. The magnitudes of COLE were highest at the Footslope and lowest at Backslope-2, following the variation in soil inorganic C. At all positions, inorganic C increased with depth as weathering of the soil dissolves calcium carbonates from the soil surface. The majority of the catena is weathered from calcareous marls; whereas around Backslope-2, a stratum of less weatherable chalk is exposed on the mid to lower Backslope (Allen et al., 2005; Soil Survey Staff, 2003). The Footslope position likely receives more water (from surface and subsurface lateral flow) than the rest of the positions and, therefore, has more leaching of carbonates (Suarez, 2006).

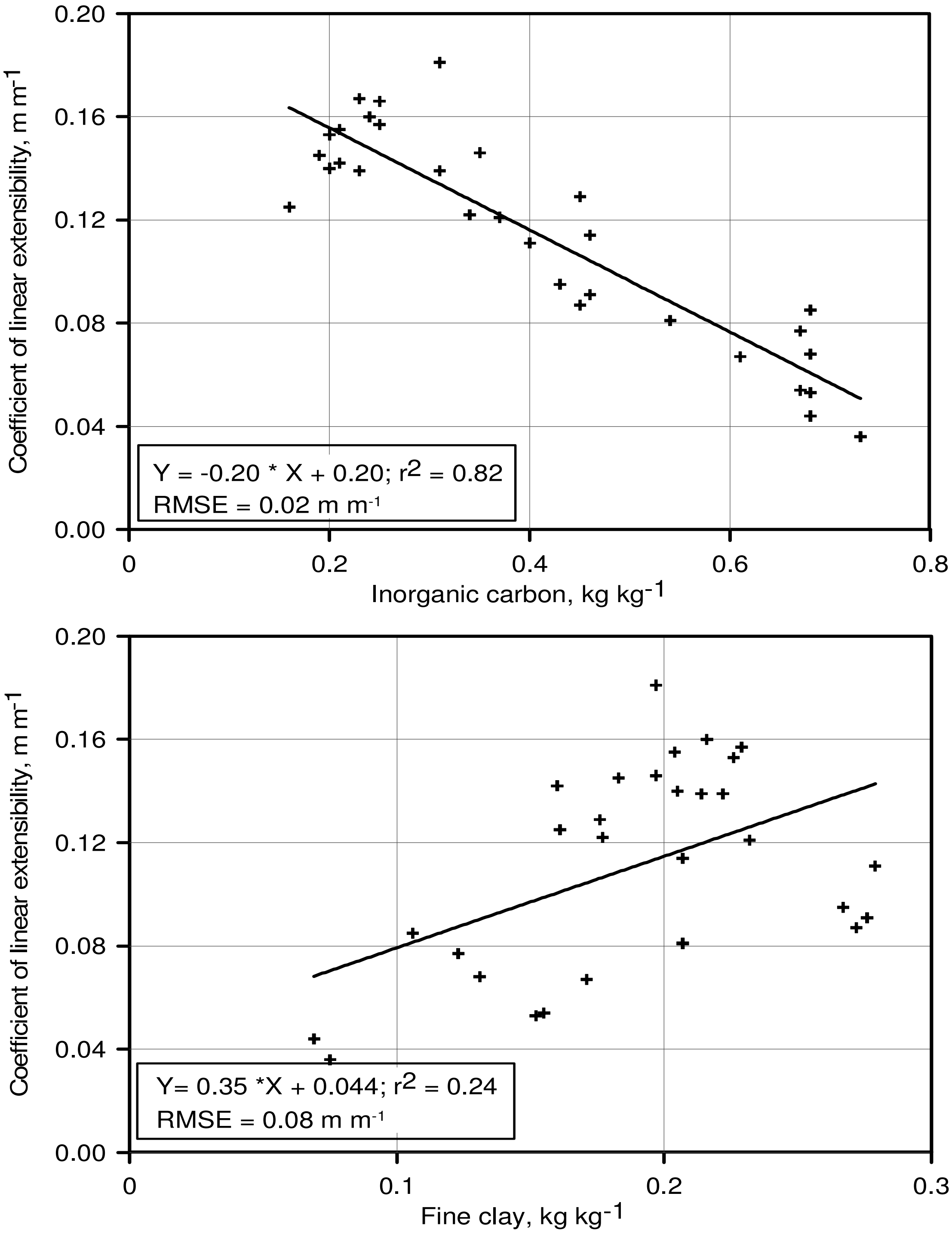

Figure 3.2. The relationship between COLE with $CaCO_3$ and fine clay content of soils.

Generally, because of the spatial variability of clay and inorganic C (calcium carbonate) content of soils and their effect on shrink-swell potential (Deshpande et al., 1964; McCormack and Wilding, 1975; Rimmer and Greenland, 1976), we expected that the spatial variability in soil subsidence on the catena to vary congruently with the magnitude of COLE. However, soils with the highest COLE did not always shrink the most in the field because the variability of change in soil water storage also affected soil shrinkage.

Spatial variability of soil subsidence

The magnitude of soil subsidence varied across the Vertisol catena, both temporarily and spatially (Fig. 3.3). Generally, during the three-year study period, the overall maximum soil subsidence occurred in 2006 because of less rainfall in 2006 and the year prior. Because of high rainfall in the previous three consecutive months, the maximum soil thickness was observed in August 2007 when subsidence is usually greatest. The maximum soil subsidence measured at the Summit between 0.3 m and the monument depth was 79 mm, which was comparable to a 82-mm maximum soil subsidence measured at the same site by Arnold et al. (2005). On the Shoulder, Backslope-1, Backslope-2, Footslope-1 and Footslope-2, the maximum soil subsidence measured between 0.2-m deep and the monument was 78, 72, 19, 57, and 64-mm, respectively. With the exception of Backslope-2, maximum soil subsidence decreased from the Summit to the Footslope. For instance on 26 September 2006, the soil subsidence at the Footslope-1 (43 mm) was < at the Summit and Shoulder (77 mm), almost by half. The difference in soil subsidence across the landscape illustrates the variability of shrink-swell dynamics and the associated crack formation in the Vertisol catena.

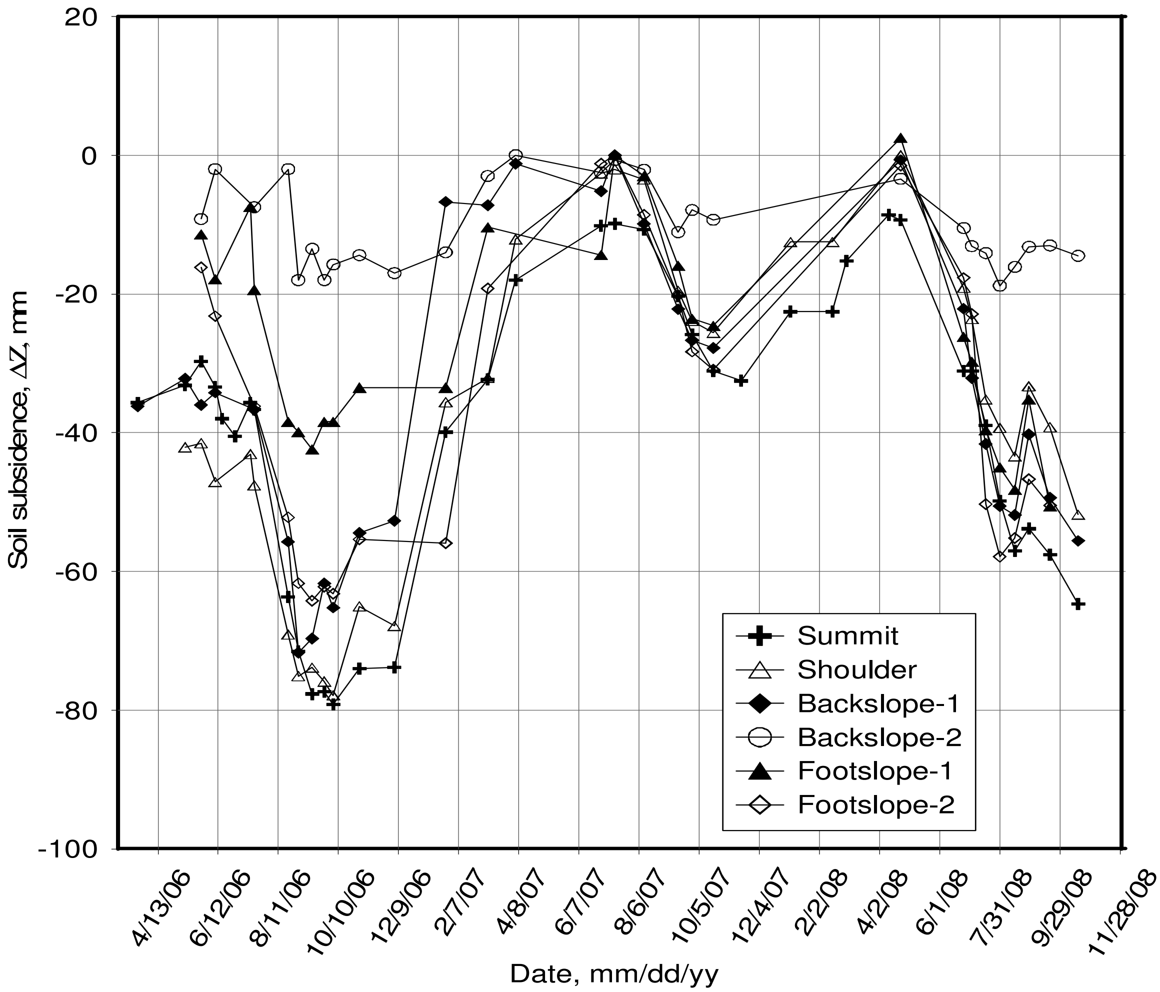

Figure 3.3. The soil subsidence (ΔZ) between a monument and rod installed at 0.3-m deep for the Summit and at 0.2-m deep for other locations in the Vertisol catena, in Riesel, Texas.

The high soil subsidence at Backslope-1 compared to the Footslopes positions illustrates the interaction between a shrink-swell potential and soil water loss. The Footslope positions have higher COLE (Table 3.1), but did not have the most subsidence. In all positions excluding Backslope-2, maximum subsidence appeared to be primarily driven by water loss. Our observed locations of maximum soil subsidence across the Vertisol catena varied from those reported for an Alfisol catena (Baer and Anderson, 1997). Results from the Alfisol catena, indicated that shrink-swell potential, not overall water loss drove soil subsidence (cracking). Soil subsidence in the Alfisol catena was most likely from spatial variation of clay content in the topsoil, which was found to be greater on the Backslope (25.1 %) than the Summit (19.1 %), even though the Backslope had less change in soil water storage than at the Summit. In our Vertisol catena, soil clay is more uniform therefore inorganic C content drives variability in COLE, and COLE is relatively high everywhere but one location, Backslope-2. Water loss seems to be the more important part driving variability in cracking.

Our study also showed a considerable difference in soil subsidence among the landscape positions prior to a rainfall event that further reinforces the importance of incorporating the spatial variability of cracks extent in hydrology models. For example, on 5 October 2006, the soil subsidence at the Summit, Shoulder, Backslope-1, Backslope-2, Footslope-1 and Footslope-2 was 79, 78, 65, 16, 63 and 42-mm, respectively. Five days later, on 10 October 2006, it rained 30 mm and there was no runoff. On 25 June 2008, the soil subsidence measured at the Summit, Shoulder, Backslope-1, Backslope-2, Footslope-1 and Footslope-2 was 31, 19, 22, 11, 29 and 18-mm, respectively, and after a 15-mm rainfall two days later, there was no runoff. In both cases, the spatial variability of soil subsidence in the catena, mainly between Summit, Backslope-2 and Footslope-2 were considerably high. This variability in soil subsidence could affect the amount of runoff captured by the associated cracks at each position and affect the distribution of water in the soil profile at each site. For instance, assuming equidimensional shrinkage (Bronswijk, 1991), the maximum crack volume per unit area in year 2006 is 32 mm at the Shoulder, estimating the capacity of the cracks to capture 32 mm (1.3 inch) of rain. Similar statements can made for the crack volume estimated at other positions and at different times.

Soil subsidence and soil water

A ten-year study of crack area density reported ten-fold differences in crack area density measured in different years, but at similar water contents (Kishné et al., 2010). Evidence in Kishne et al. (2010) suggested that the water content at which the soil starts drying influences the magnitude of cracking. In other words, more surface cracks were measured when the soil dried from wet conditions compared to drier conditions. Maximum water loss vs. the associated subsidence in this study is shown in Fig. 3.4. At

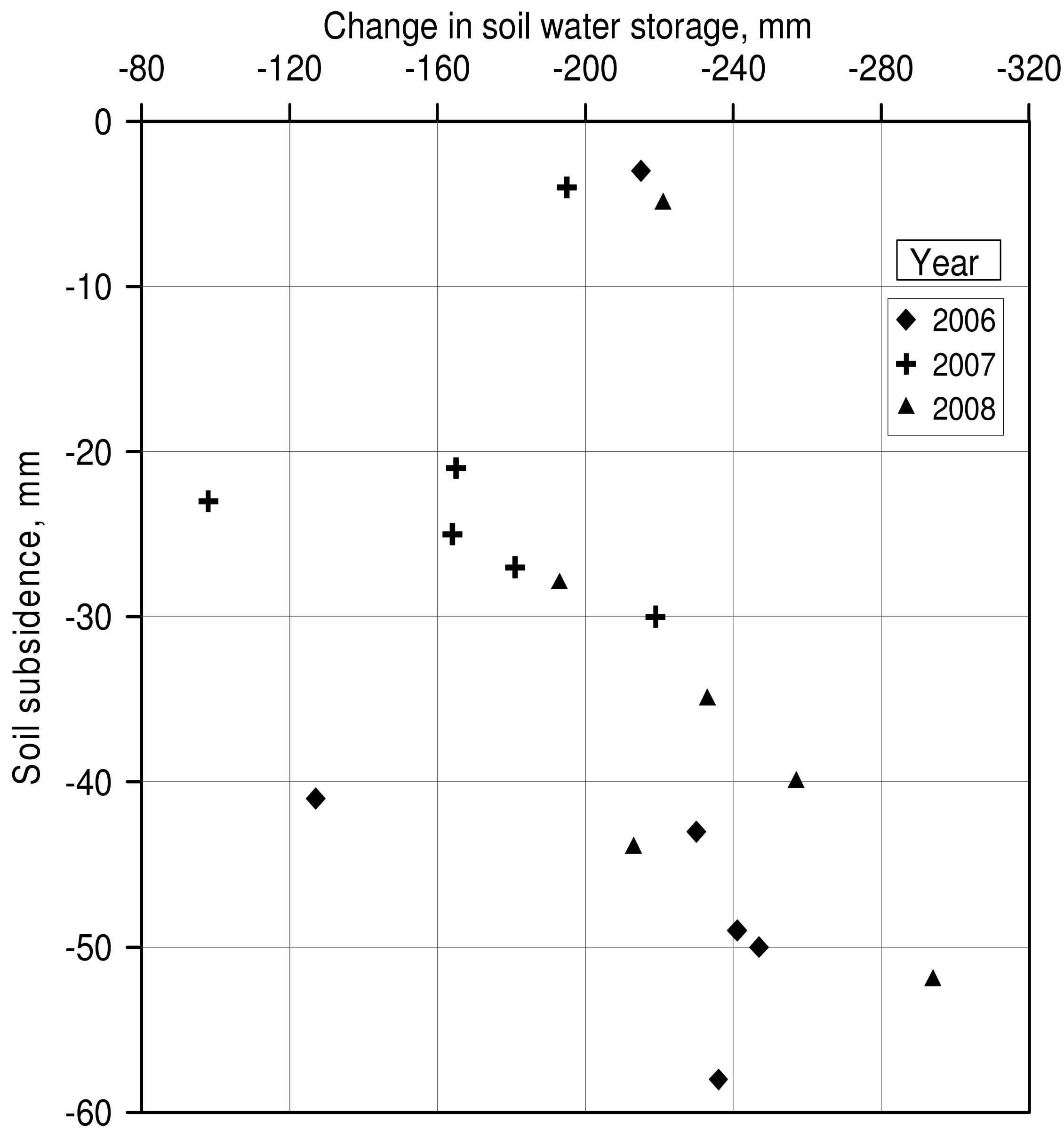

Figure 3.4. The maximum water loss vs. the associated subsidence measured at different landscape positions for each year of the study. Soil subsidence and change in soil water storage were calculated between 0.30 and 1.5 m for the Summit; 0.2 and 0.8 m for the Backslope-2, and 0.2 and 1.2 m for all other positions.

~ 240 mm of water loss, subsidence was higher in 2006 than the other two years. Though these are not measures of soil cracking, but soil subsidence, this three-year data set suggests that there might be temporal instability in the relationship between soil cracking and water loss.

Change in soil water storage in the soils layer of each position in the catena was heterogeneous as well, i.e., the soils in the catena did not dry homogenously with depth. The soil water content in the soil layers of Summit to Backslope changed frequently with time, to 1.2 m deep, while the soil water content at the Footslope dried less frequently below 0.8 m (Fig. 3.5). Therefore, the soil subsidence measured at Footslope was usually due to soil water loss in the upper 0.8-m soil layer, whereas at other landscape positions, it was due to a change in soil water storage from the whole soil layer. This spatial variability of change in soil water storage with soil depth shows the importance of analyzing soil subsidence layer by layer, especially if COLE changes with depth.

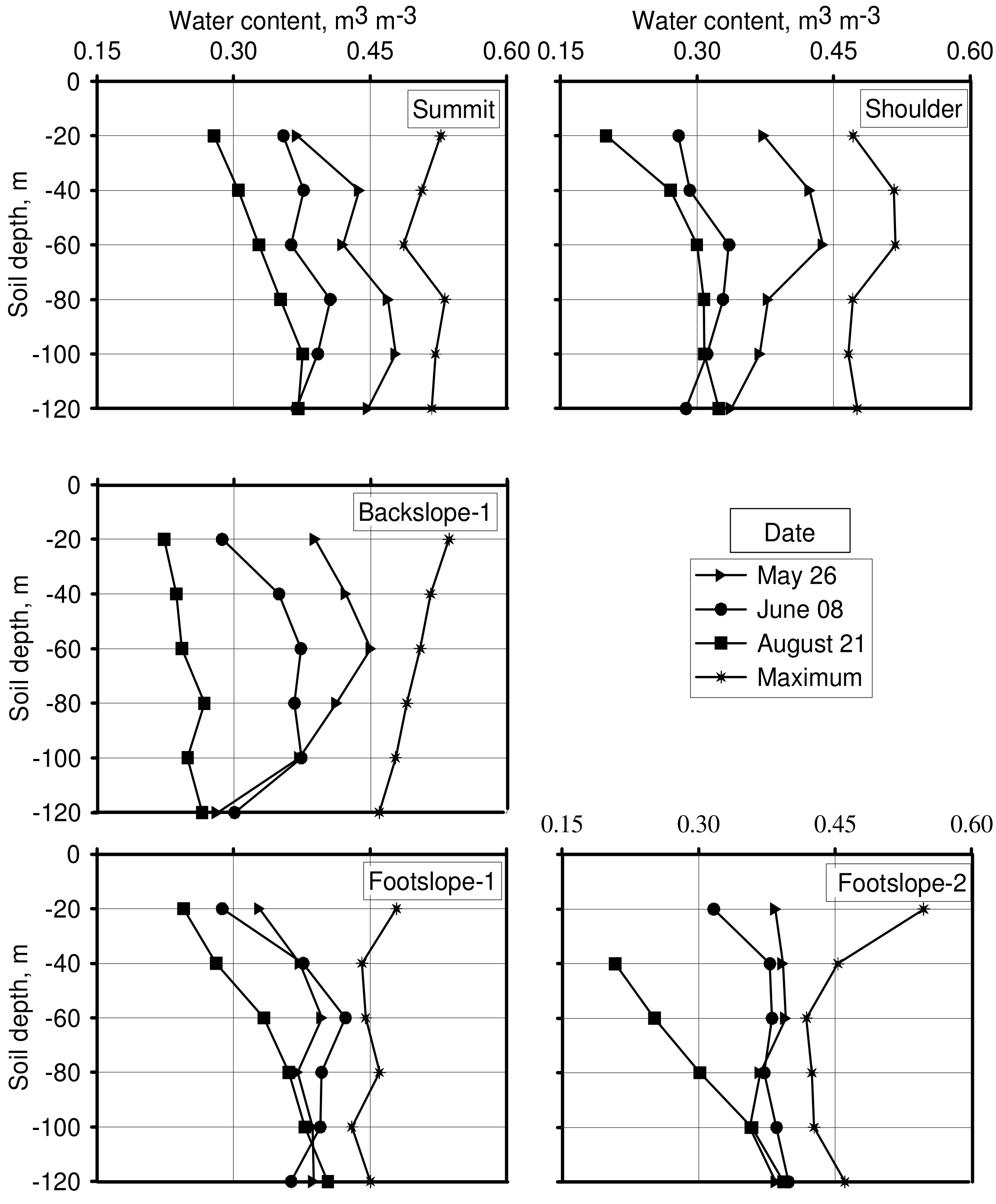

Figure 3.5. The difference in variation of volumetric water content with depth at the landscape positions, all measured in 2006. The maximum soil water content represents the maximum water content measured in the field at each soil layer (at different times of the year).

Expected vs. measured soil subsidence

The relationship between the relative thickness of a soil layer (h/h_{fc}) and its respective water content at each landscape position was analyzed (Figs. 3.6-3.8). The theoretical relationship between the thickness and water content was also developed based on the model developed by Olsen and Haugen (1998) and using COLE estimated in the laboratory (Table 3.1). The general trend of the relationship between the field-measured soil thickness and soil water content agreed with the theoretical relationship at most soil layers. However, the soil thickness did not shrink to the expected level for the corresponding water content. Moreover, at the Summit and Shoulder, the relationship between soil thickness and water content at the soil surface was not as expected, i.e. compared to at the subsurface, there was less subsidence at the surface although COLE was high. Yule and Ritchie (1980a) also found that the relationship between soil shrinkage and soil water loss varies with depth, with a greater shrinkage at the subsurface (0.7-0.8-m) than at the surface (0.1-0.2-m). Low soil subsidence at the surface, for a given change in water content, could be attributed to several factors. Firstly, soil units may not fully collapse onto themselves due to roots acting to support the units. Secondly, water loss at the surface may contribute to the formation of horizontal cracks rather than vertical shrinkage. Since roots usually develop near the surface, the role of roots on supporting aggregates and limiting soil subsidence is minimal in the subsurface. Additionally, soils aggregates are smaller and usually formed at the surface because of frequent drying and wetting cycles, as a result, larger and structural pores are usually expected on the soil surface. This means that water loss from large and structural pores do not result in appreciable soil shrinkage, which is usually described as structural shrinkage phase (Fig. 2.1).

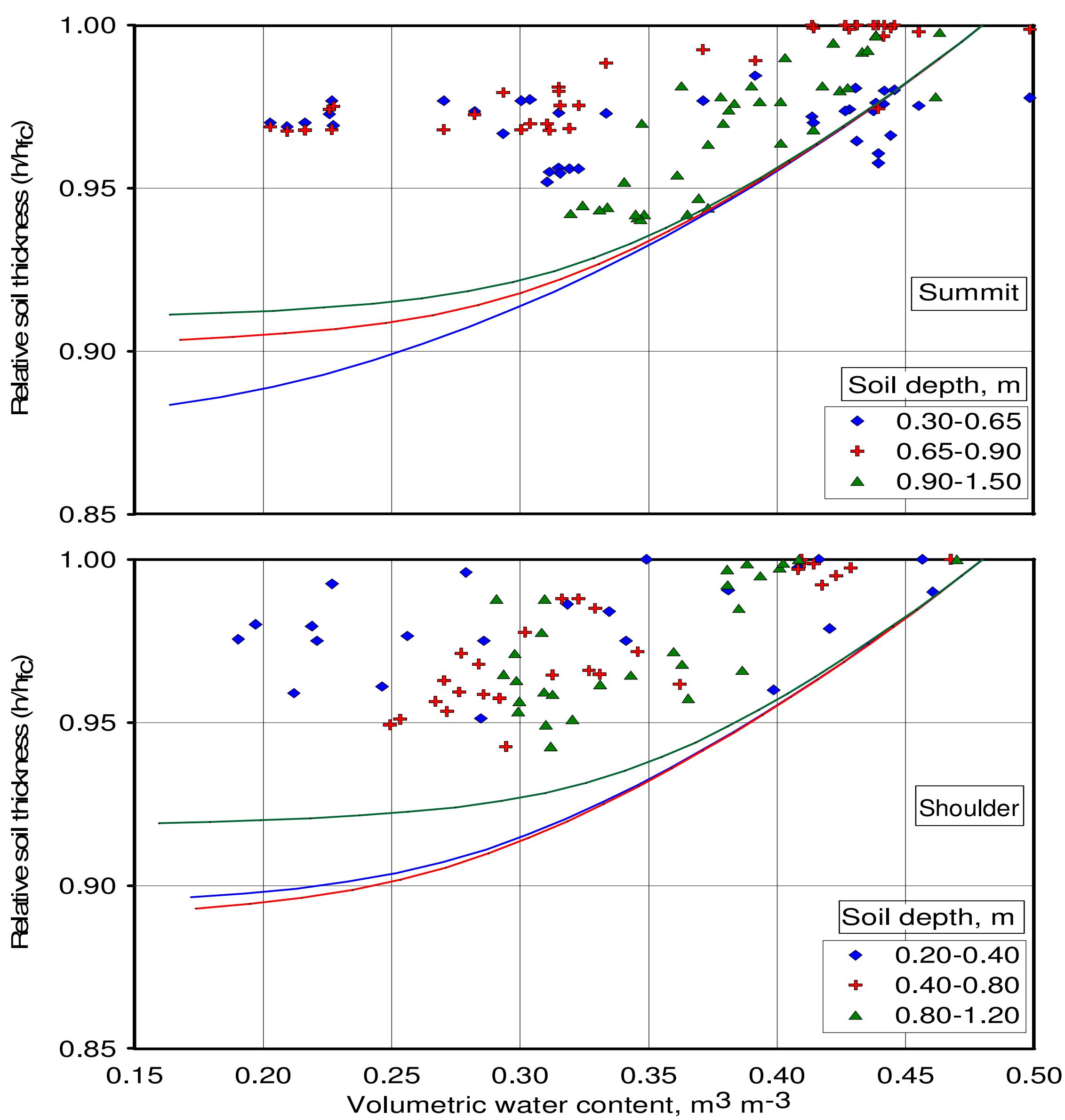

Figure 3.6. The measured and theoretical relationship between the relative soil thickness and water content at different soil layers of the Summit and Shoulder positions in the Vertisol catena. The measured relationship is plotted while the theoretical relationship is shown as lines in the same color corresponding with the plotted data.

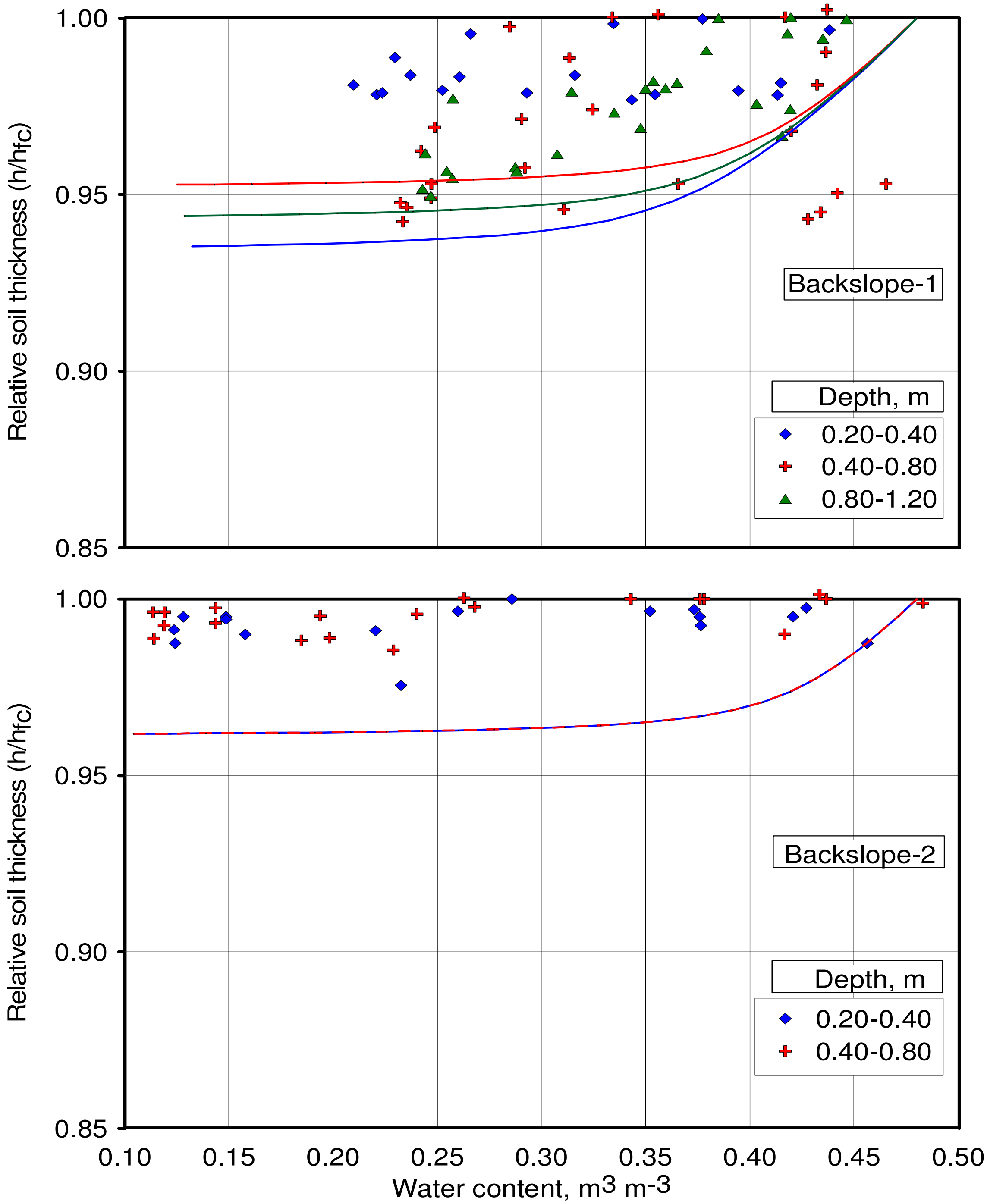

Figure 3.7. The measured and theoretical relationship between the relative soil thickness and water content at different soil layers of the Backslope-1 and -2 positions in the Vertisol catena. The measured relationship is plotted while the theoretical relationship is shown as lines in the same color corresponding with the plotted data.

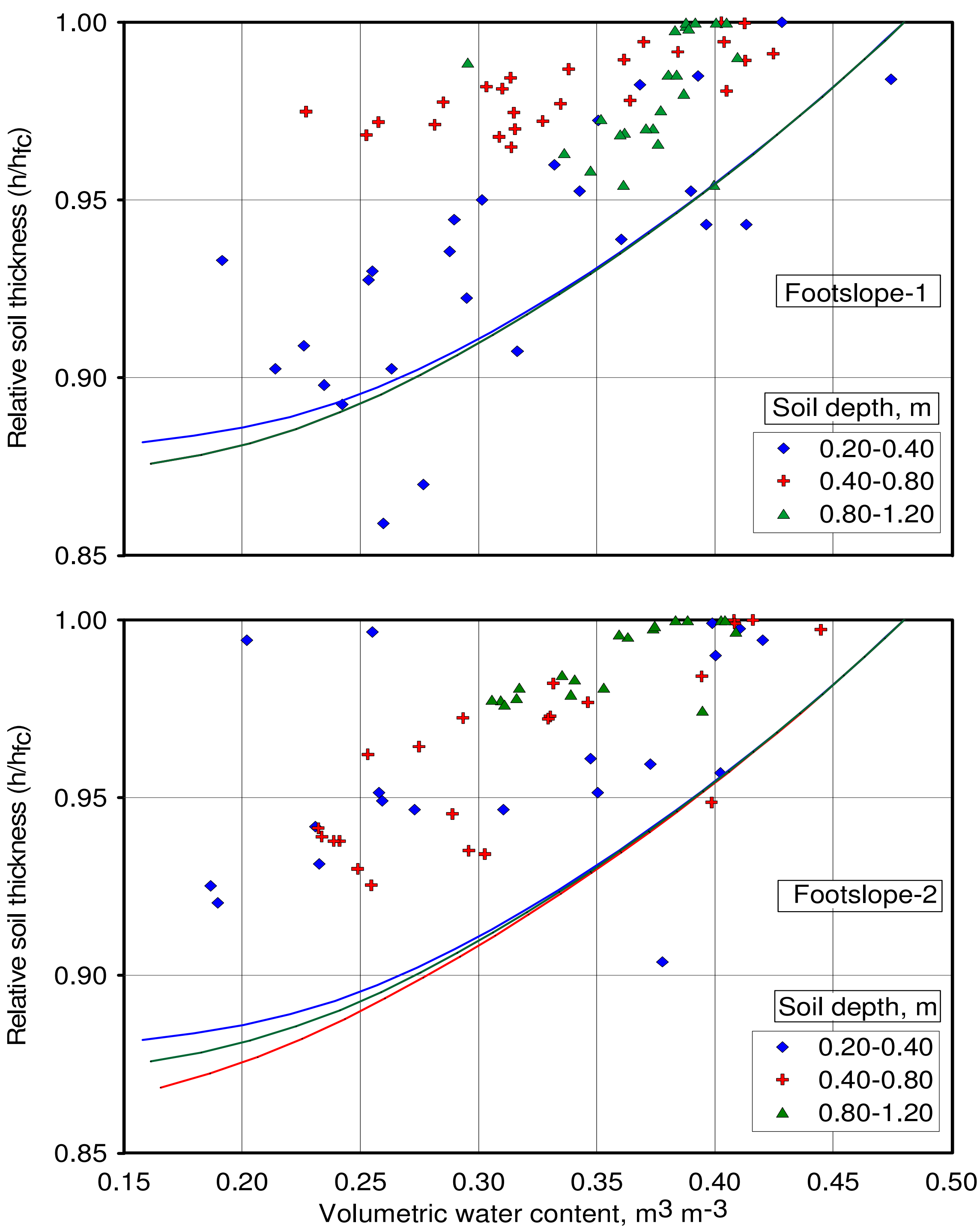

Figure 3.8. The measured and theoretical relationship between the relative soil thickness and water content at different soil layers of Footslope-1 and -2 positions in the Vertisol catena. The measured relationship is plotted while the theoretical relationship is shown as lines in the same color corresponding with the plotted data.

To model soil cracking in the field, it is useful to know the water content at which soils begin to shrink and then if the shrinkage is isotropic. When using subsidence measurements, this information should appear by evaluating the slope and intercept of a graph of soil subsidence vs. water loss. The maximum water holding capacity of a soil was estimated by using measured porosity at -33.3 kPa and field measurements of maximum water content for each soil layer. Estimates for water holding capacity using porosity were lower than field measurements changing the intercept of the line (Fig. 3.9). Using porosity as an estimate created results where soil subsidence began before appreciable water loss occurred (no structural shrinkage). While field estimates of maximum water content created a more realistic graph, estimating maximum soil water for field conditions is always difficult. For simulating soil shrinkage, there will be additional disadvantages to not having field measurements of wet field conditions. Regression results of subsidence and change in soil water storage from the whole soil layer resulted in slight variability in magnitude of slope across the different landscape positions (Fig. 3.9).

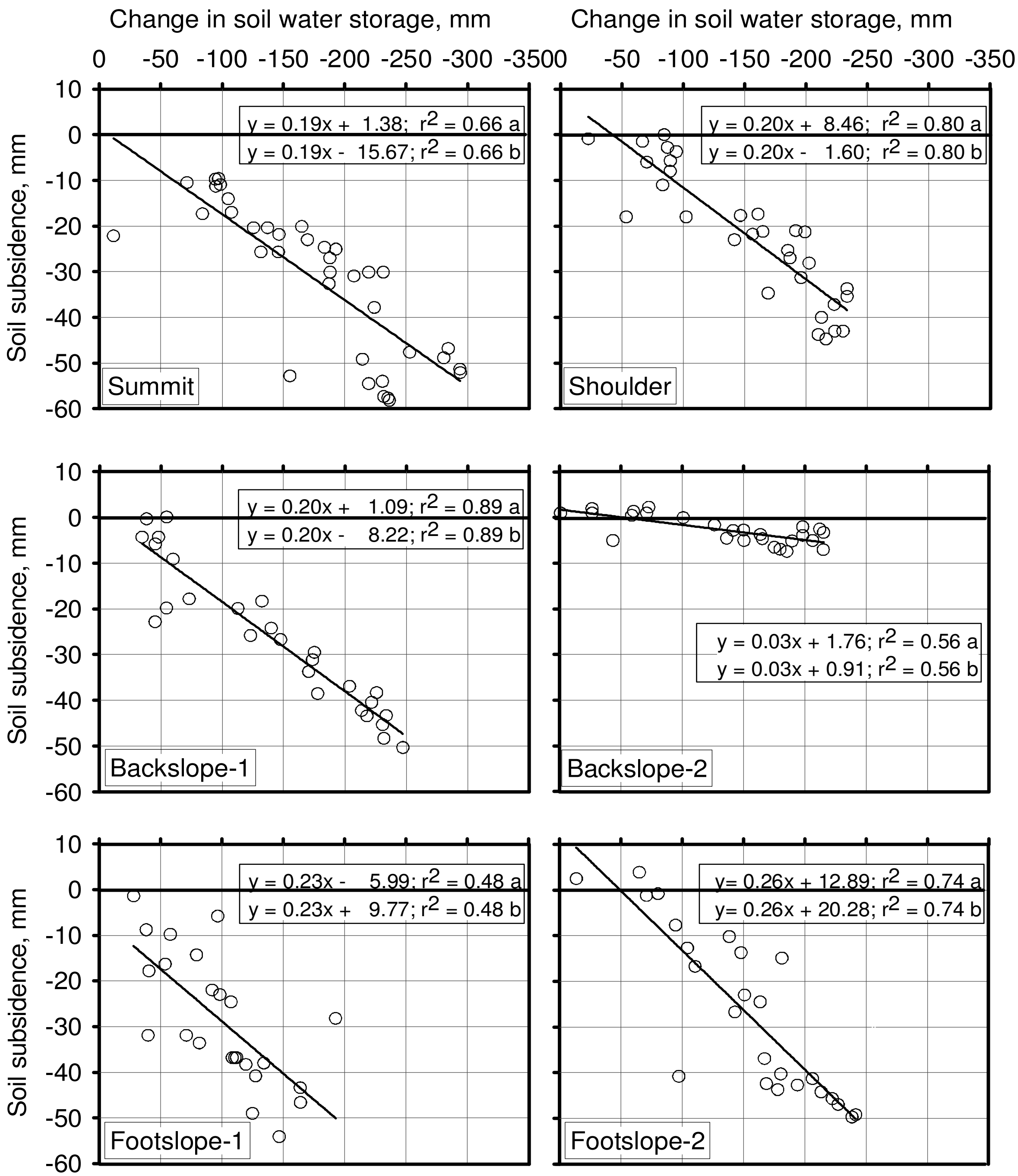

Figure 3.9. Soil subsidence and change in soil water storage across the Vertisol catena. Soil subsidence and change in soil water storage were calculated between 0.3 and 1.5 m for the Summit; 0.2 and 0.8 m for the Backslope-2, and 0.2 and 1.2 m for all other positions. The symbols next to each regression equation indicate maximum water content in the soil was "a" measured in the field and "b" estimated using soil porosity.

Because of the evidence that variation of volumetric water content with depth (Fig. 3.5) and some surface layers did not shrink (Fig. 3.6), analysis of soil subsidence and change in soil water storage was done by dividing a soil layer into an upper (0.2 - 0.8-m) and a lower (0.8 - 1.2-m) set of soil layers at all sites except at the Summit. At the Summit, the layer was divided into 0.3 - 0.9-m and 0.9 – 1.5-m soil layer. Results showed a considerable spatial variability in slope of the regression line at the top layer (0.2 - 0.8-m) (Fig. 3.10). Slopes from the upper layers ranked similarly with the coefficient of linear extensibility, COLE, values of those same soil layers. Though the reason is not clear, the slopes from the subsoil subsidence were greater on the upper layers at the Summit, Shoulder and Backslope-1, and the ratio of soil subsidence to change in soil water storage was uniform with depth for the Footslopes. Dividing the layers did result in evidence that structural shrinkage was measured at these sites. In general, structural shrinkage appeared to end at 12 to 25-mm of water loss.

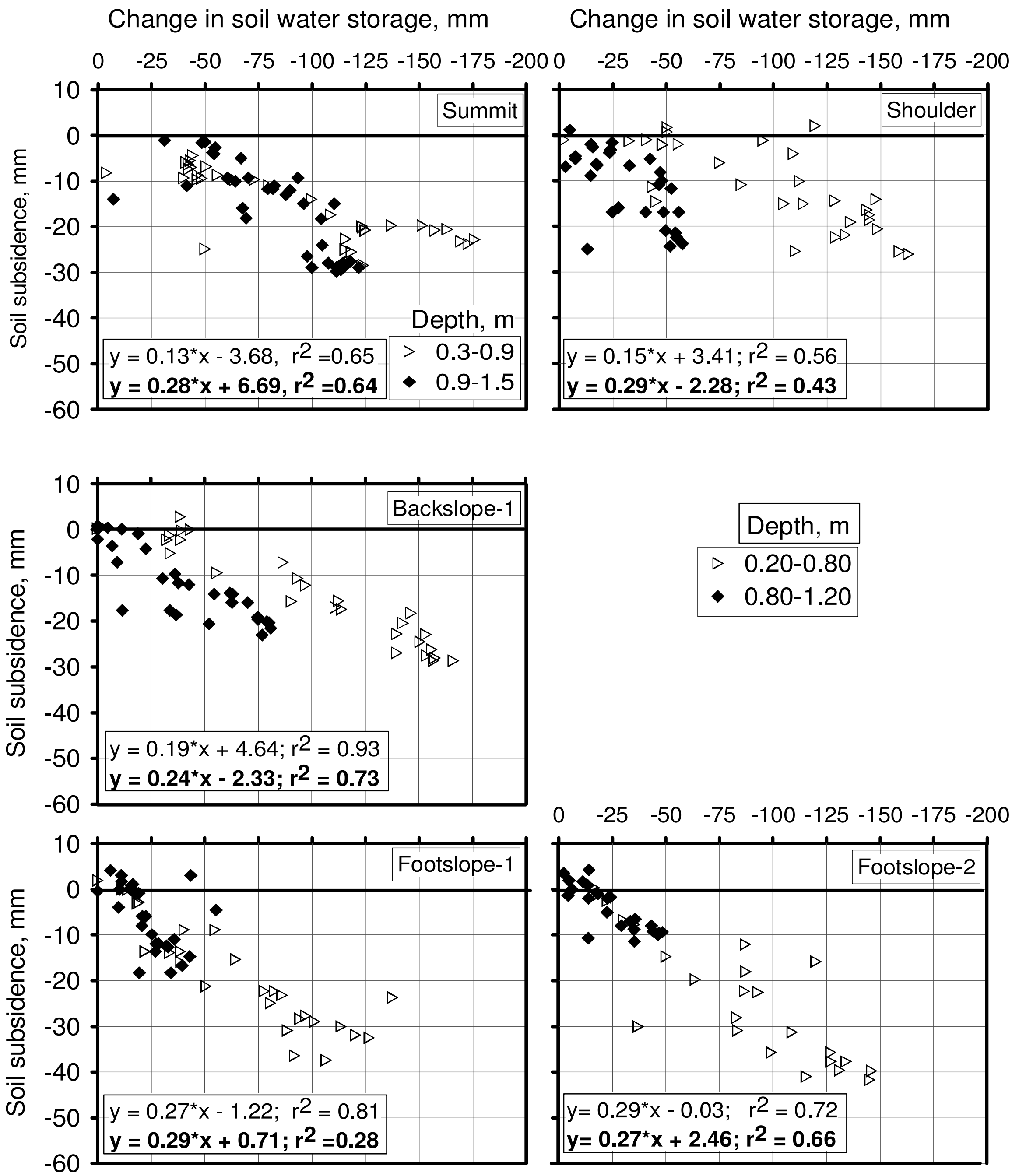

Figure 3.10. The Soil subsidence is plotted with change in soil water storage for an upper soil layer (0.3 to 0.9-m at the Summit and 0.2 to 0.8-m on other sites) and lower soil layer (0.9 to 1.5-m at the Summit and 0.8 to 1.2-m on other sites). The regression equation in bold is for the sub soil layer and the other is for the top soil layer.

Conclusions

Shrink-swell potential is inversely correlated with inorganic C (calcium carbonate) in this Vertisol. The Houston Black and Heiden clay, both Vertisols, have weathered from calcareous marls and chalks. Though COLE values were variable on this outwardly uniform Vertisol catena, the COLE values were high (primarily ≥ 0.1 m m^{-1}) except in one backslope position where soils were relatively shallow and weathered from a more resistant chalk parent material. To map COLE variability in this catena, it is necessary to map inorganic C.

Because COLE values at all other locations were high, soil water content was the primary driver in the spatial and temporal variability in vertical shrinking and swelling. For example, the soils at the footslope position had higher shrink swell potential, but dried primarily at the top 0.8 m, resulting in the same amount of subsidence as the upper area of the catena that was drying to 1.2-m deep. In this catena, we would expect the cracks to be much deeper at the top of the catena, have few to no shallow cracks at the lower backslope where the chalk occurs, and have significant but shallower (0.5-m deep) cracks at the footslope. This variability in crack capacity and depth affects how water will redistribute into the soil profile during rainfall and runoff.

Vertical subsidence measurements suggest that the soil is not shrinking isotropically. Most evident of non-isotropic shrinkage was found in the surface layers at some site positions. Models that use soil shrinkage characteristics usually assume isotropic shrinkage to estimate crack volume and capacity to hold and infiltrate water. The lack of vertical subsidence during drying suggests that there are more large horizontal voids in these soil layers than the current literature assumes. Additionally, models of soil subsidence using COLE measurement overestimated soil subsidence. Soil subsidence is reasonable easy to quantify in the field; however, coupling this measurement with crack imaging (2D or 3D) or crack capacitance measurement would further clarify soil cracking behavior, in situ.

CHAPTER IV

SHRINK-SWELL DYNAMICS OF VERTISOL UNDER DIFFERENT LAND USES

Introduction

Measurements of shrink-swell potential and knowledge of soil water content have been used to provide temporal estimates of the capacity of cracks to facilitate rapid infiltration and storage of water in clayey soils (Bronswijk, 1991; Baer and Anderson, 1997; Arnold et al., 2005). These estimates of crack capacity that have been used to improve simulations of surface hydrology on lands with shrink-swell soils generally contain the assumptions that both soil aggregates and pedons equidimensionally shrink or swell with changes in water content (e.g., SWAT, Arnold et al., 2005). There is considerable evidence, though, that soils express unequidimensional shrinkage – sometimes greater in the vertical than horizontal directions (Cabidoche and Voltz, 1995) and sometimes less (Mitchell, 1991; Mitchell and Van Genuchten, 1992).

There are various conceptual reasons for observed unequidimensional shrinkage, and these reasons vary with the type of soil and local environmental conditions. In Vertisols, it is possible that soil structural units in the subsoil slide along diagonal slickensides and fill cracks formed by horizontal shrinkage thereby producing greater apparent vertical shrinkage than horizontal (Cabidoche and Voltz, 1995). In the case where vertical shrinkage is observed to be < horizontal shrinkage, plant roots may prevent the soil from vertically subsiding as it shrinks (Mitchell and Van Genuchten, 1992). In either case, estimations of the capacity of cracks to hold water and to redistribute that water into the soil matrix would be different than with equidimensional shrinkage, and the consequences of unequidimensional shrinkage should be considered in hydrologic models attempting to partition rainfall into infiltration and runoff.

From simultaneous measurements of the vertical movement and water content of field soil, a surface shrinkage ratio $b = \Delta z / \Delta W$ can be calculated (Mitchell 1991), where Δz is the change in thickness of a given layer of soil (vertical subsidence) and ΔW is the volume of water loss from that layer per unit area of land surface. When the change in volume aggregates in the soil is equal to the change in volume of water they contain (i.e., isotropic shrinkage during basic or normal shrinkage) (Bronswijk, 1991) and when the shrinkage of both the aggregates and pedon are equidimensional, the value of b should be very near 0.33. If shrinkage of aggregates was isotropic but they did not vertically collapse on themselves, b would be less than 0.33. The shrinkage ratio could also be <0.33 if the shrinkage of aggregates were not isotropic. Obviously, soils with very low COLE do not shrink appreciably with loss of water so b would be near 0 for these soils. The shrinkage ratio could be >0.33 if the shrinkage of the aggregates were not isotropic and/or equidimensional (more vertical than horizontal) or if aggregates were to slide diagonally downward, as might be expected in the bowl of a gilgai, and fill some of the vertical cracks formed by the horizontal shrinkage.

Since it is generally accepted that aggregates shrink isotropically (Yule and Ritchie, 1980a; Bronswijk, 1991), the value of b should be an indicator of the magnitude of subsurface cracking when the aggregates are undergoing basic shrinkage. Values of $b<0.33$ in soils with high shrink-swell potential should be an indicator of the void spaces developed by horizontal cracks. The purpose of discussion and measurement of b in Mitchell (1991) was to express its importance in calculating soil water from subsidence measurements. Knowing b in surface hydrology modeling provides a better understanding of how to estimate volume and geometry of cracks from water loss. Volume and geometry of cracks influence the portioning of rainfall into infiltration and runoff, and the spatial distribution, absorption and redistribution of water.

Field observations suggest that the geometry of cracks in dry soil is strongly influenced by land use and vegetation. Johnston and Hill (1944) recorded the effect of land use by observations of surface and subsurface cracking in Austin and Houston Black clays of Central Texas. Under row cropping, the soil cracked parallel and between the rows of sorghum while in other vegetation, the cracking was more randomly oriented and uniform. Johnston and Hill (1944) suggested the cracking occurred where the soil was most moist as the soil dried out due to root uptake of water. Kishne et al. (2009) reported higher crack area density on microhighs on a 10×10 meter plot of a Central Texas Vertisol with circular gilgai, and under native prairie vegetation.

Measurements of subsidence could explain the influence of vegetation and management on soil shrinkage if soil were cracking. Mitchell (1991) found isotropic soil shrinkage on a field of alfalfa after treating the land with five machinery traffic regimes. Upon further investigation, Mitchell and Van Genuchten (1992) found unequidimensional shrinkage, i.e. differences in vertical subsidence with change in soil water between soil under fallow, wheat, and alfalfa. They suggested that their observations supported the idea of Johnston and Hill (1944) that the perennial roots supported the soil profile and reduced vertical subsidence. A field study by Cabidoche and Voltz (1995) on a gilgai grassland showed highly variable anisotropic and/or unequidimensional soil shrinkage. In multiple subsidence measurement along a Vertisol catena with a high shrink-swell potential, we found evidence of unequidimensional shrinkage, particularly in the upper soil layers between 0.2 and 0.8 m deep (See Chapter III). In contrary, Kirby et al. (2003) consistently found a shrinkage ratio of 1/3 at different soil depths under three types of cultivation.

During isotropic shrinkage, if soil shrinks unequidimensionally in soil profiles, it would be useful to know whether or not the soil consistently subsides to the same magnitude for a given water loss under a particular management practice, or with a particular vegetation type. However, limited measurements of soil shrinkage are available for soils of high shrink-swell potential under different vegetation types. Field observations indicate that whole-soil shrinkage is not equidimensional but spatial variability (Johnston and Hill, 1944; Cabidoche and Voltz, 1995) and limited observations of vegetation differences (Mitchell and Van Genuchten, 1992) does not provide conclusive evidence of equidimensional shrinkage. The objective of the study was to quantify the spatial and temporal consistence of subsidence with water loss under three land use types. Specifically, this study includes measurements of subsidence and water content over three years, on three land uses, and multiple landscape positions. Information from this study can be used to support estimates of soil cracking for a mechanistic hydrology modeling in watersheds with vertic soils.

Materials and Methods

Materials

The research was conducted at the USDA-ARS Grassland, Soil and Water Research Laboratory near Riesel, Texas. The dominant soils in the study area are Houston Black and Heiden clays, both fine, smectitic, thermic Udic Haplusterts (Soil Survey Staff, 2003). Three land use types, each on its own subwatershed, were selected to measure soil subsidence and soil water content for two years (2008 - 2010). These land uses are row crop (8.7 ha), native prairie (1.4 ha) and grazed pasture (1.5 ha).

In the row crop, corn *(Zea mays. L.*) was grown in 2008-09 study year and haygrazer in 2009-10. The crops were planted in the spring and harvested by August. Before planting, multiple passes were made with a field cultivator, and after harvest the field was disked, chisel plowed (sweep chisel), and field cultivated. The average slope of the row crop subwatershed is ~ 3 % and it contains contour terraces and grassed waterways. The native prairie watershed has had consistent management since 1948, and it cut for hay once to twice a year (Harmel et al., 2006). Little bluestem (*Schizachyrium scoparium*) is the dominant vegetation, and other plants include side oats gramma (*Bouteloua curtipendula*), big bluestem (*Andropogon gerardii*), Indian Grass (*Sorghastrum nutans*), and a few forbs. The average slope of the native prairie is ~ 5 % and the subwatershed contains linear gilgai (width of up to 1 m) perpendicular to the contour. The dominant grass in the grazed pasture is coastal bermudagrass (*Cynodon dactylon*), and the average slope of the land is ~ 2 %. Cattle are rotated into the pasture, year around, as need, for grazing. Circular gilgai (1 to 2-m diameter and 0.15 to 0.25-m deep) are common in the grazed pasture.

Four measurement sites each on the row crop and native prairie and five measurement sites on the grazed pasture were selected by stratifying site locations by landscape position and apparent soil electrical conductivity. Elevation was measured using a survey quality GPS, with a vertical error of 20 mm (R7 base station and R8 Rover Trimble®, Sunnyvale, CA), and apparent soil electrical conductivity was measured over each field using electromagnetic induction (EM38, Geonics® Ltd., Mississauga, Ontario, CA). In the row crop field, sites were located at the summit, shoulder, backslope and footslope landscape positions, hereafter referred to as RC1, RC2, RC3 and RC4, respectively. In the native prairie, the measurement site located at the upper slope is referred to as N1; sites located in the middle slope are referred to as N2, and N3 and the site located at the footslope is referred to as N4. Out of the five measurement sites in the grazed pasture, two of them were located at the upper part of the backslope, referred to as G1 and G2; two were located at the middle of the backslope, G3 and G4; and one was located at the lower part of the backslope, G5.

Because soil texture and inorganic C are the primary soil properties that affect shrink-swell dynamics in Vertisols formed from calcareous residuum (Chapter III), soil samples from each site and each soil horizon were collected for analysis of inorganic C content and particle size distribution. Inorganic C content was measured using a modified pressure-calcimeter method (Sherrod et al., 2002). Calcium carbonate equivalent was calculated from inorganic C. Particle size distribution was analyzed using the pipette method (Soil Survey Staff, 1996). The coefficient of linear extensibility (COLE) of soils was estimated from inorganic C using the pedotransfer function, COLE= $-0.20 \times IC + 0.20$, where IC is inorganic carbon in kg kg^{-1} (Fig. 2.2). The root mean squared error (RMSE) of pedotransfer function is 0.02 m m^{-1}.

Plastic discs were used to measure surface subsidence and metal rods were used for subsurface subsidence measurements; all were installed in July 2008 at the grazed pasture and native prairie and August 2008 at the row crop after harvesting the crop. A 0.2-m diameter and 10-mm thick plastic disks were attached using metal pins to the soil surfaces at all sites to measure the vertical movement of soils from the surface. Metal rods (10-mm diameter concrete reinforcing bar) were anchored at 0.9-m depth at all four sites. Two monuments each were anchored at 3 m depth at the rowcrop and grazed pasture, and three were anchored at the native prairie – all within line of sight of all shrink-swell measurement locations. The change in height of the rods relative to the unmoving monuments were measured using a laser level and stadia rod (SDL50, CG Surveying Limited®, Elstree Way, Herts, UK) with greater than 1.5 mm accuracy and 0.1 mm decimal digits. Changes in elevation of tops of plastic disks and metal rods anchored to the soil, relative to a monument anchored at 3 m, were used to track the temporal trends in soil subsidence and thickness of soil layers. Near each set of rods, a neutron access tube was installed to measure soil water content using a neutron meter (503DR Hydropobe®, Campbell Pacific International, Inc., CA). The soil water content was measured from 0.2 to 1.2 m depth in 0.2-m intervals. Calibration of the neutron meter was made in the field at moist and dry soil water conditions, and at multiple locations (see Chapter III). The r^2 and RMSE of the calibration are 0.934 and 0.025 m^3 m^{-3}, respectively. Measurements of soil vertical movement and soil water content were made bi-weekly from June 2008 to September 2010.

Methods

Maximum soil swelling and soil water content recorded during the study period were used as references to calculate the soil subsidence and change in soil water storage, respectively. The subsidence of a given layer of soil was calculated as

$$\Delta Z = Z_i - Z_{max}$$

where, ΔZ is the soil subsidence (m) from the fully swollen state (the reduction in soil height due to a soil water loss from the saturated state), Z_{max} is the maximum height of soil layer (m) and Z_i is the height of soil layer (m) at a given time, both measured relative to the height of the monument. The ΔZ value was calculated for two depth intervals, between the surface and the monument anchor (3 m) and between the metal rod at 0.9 m and the monument. Subsidence between the soil surface and the 0.9-m metal rod is referred to as Δz, which was calculated by taking the difference of ΔZ measured at the surface and at the 0.9-m soil deep.

Because the thickness of soil layer changes with shrinking and swelling, estimation of water contents for the upper 0.9-m soil layer from the field-measured volumetric water content (θ) was done as follows,

$$W = 0.30m*\theta_{0.2}+0.20m*\theta_{0.4}+0.20m*\theta_{0.6}+(0.20m- \Delta z)*\theta_{0.8},$$

where W is the volumetric water content per unit area at given time (m). The coefficients before each θ show the thickness (m) of the soil layer represented byθ; the subscripts of each θ show the soil depth below the surface where the soil water content was measured. The maximum soil water content per unit area (m), W_{max} , was estimated by taking the maximum θ measured at each soil depth and assuming no subsidence (Δz = 0).

The maximum soil water content measured at each depth was used as a reference to estimate change in soil water storage from the entire soil layer. The change in soil water storage from a given layer of soil was calculated as;

$$\Delta W = W - W_{\max} ,$$

where ΔW (m) is the change in soil water storage (volume per unit area) at given time.

Finally, the relationship between soil subsidence and change in soil water storage was analyzed for a soil layer between the soil surface and 0.90 m deep. The ratio of a soil subsidence to a change in soil water storage (Δz/ΔW) was used to characterize the temporal and spatial variability of the shrinking and swelling property of soils under the three land uses. Moreover, the maximum soil subsidence measured form a soil surface at the sites of grazed pasture, row crop and native prairie were taken to test whether or not the difference in maximum soil subsidence among the three land uses was significant.

Results and Discussions

Because of the spatial variability in total clays and amount of $CaCO_3$ among the three land uses (Table 4.1), some variability in soil shrink-swell potential is expected (Anderson et al., 1973; Reeve et al., 1980; Baer and Anderson, 1997), though there was no considerable difference in amount of rainfall between the three sites. During the study period, the annual rainfall for 2008, 2009 and 2010 was 642, 1178 and 748-mm, respectively, and the 47-year mean annual rainfall is 898 mm.

Table 4.1. Properties of soils at each site in the row crop, native prairie and grazed pasture subwatershed, located at the USDA-ARS Grassland, Soil and Water Research Laboratory, Riesel, Texas.

Depth m	Horizon	Sand	Clay	Fine clay	Texture	Inorganic C kg kg^{-1}	COLE m m^{-1}
		- --	- kg kg^{-1}- -	- - - - -			
				CR1			
0 - 0.65	Ap	0.06	0.55	0.12	C	0.048	0.119
0.65-1.15	Bw	0.05	0.60	0.29	C	0.048	0.118
1.15-1.60	Bk1	0.06	0.56	0.22	C	0.050	0.115
1.60-1.80	Bk2	0.06	0.51	0.18	SiC	0.062	0.096
				CR2			
0-0.30	Ap	0.09	0.50	0.09	SiC	0.046	0.122
0.30-0.80	Bss	0.08	0.53	0.11	C	0.047	0.120
0.80-1.10	Bk1	0.07	0.54	0.15	C	0.050	0.115
1.10-1.50	Bk2	0.05	0.54	0.17	SiC	0.059	0.102
				CR3			
0-0.25	Ap	0.10	0.49	0.11	SiC	0.047	0.120
0.25-0.62	Bk1	0.07	0.45	0.19	SiC	0.067	0.089
0.62-1.16	Bk2	0.06	0.42	0.13	SiC	0.071	0.083
1.16+	BCk	0.10	0.44	0.09	SiC	0.073	0.078
				CR4			
0-0.80	Ap	0.15	0.52	0.13	C	0.004	0.188
0.80-1.35	Bkss	0.10	0.51	0.20	C	0.018	0.166

Table 4.1. Continued

Depth m	Horizon	Sand - --	Clay - kg kg^{-1}- -	Fine clay - - - - -	Texture	Inorganic C kg kg^{-1}	COLE m m^{-1}
				N1			
0-0.35	Ap	0.14	0.48	0.22	C	0.010	0.179
0.35-0.71	Bw	0.12	0.51	0.20	C	0.017	0.168
0.71-1.00	Bk1	0.12	0.52	0.19	C	0.025	0.155
1.00-1.35	Bk2	0.12	0.52	0.26	C	0.024	0.156
1.35-1.50	BCk	0.09	0.50	0.28	SiC	0.039	0.133
				N2			
0-0.30	Ap	0.13	0.44	0.19	SiC	0.025	0.154
0.30-0.60	Bw	0.12	0.47	0.17	SiC	0.032	0.143
0.60-0.90	Bk1	0.10	0.52	0.21	C	0.036	0.138
0.60-1.20	Bk2	0.10	0.54	0.27	C	0.037	0.136
				N3			
0-0.30	Ap	0.17	0.42	0.14	SiC	0.021	0.161
0.30-0.60	Bw	0.07	0.49	0.26	SiC	0.036	0.138
0.60-0.90	Bk1	0.06	0.49	0.21	SiC	0.041	0.129
0.90-1.10	Bk2	0.07	0.50	0.21	SiC	0.042	0.128
1.10+	Bk3	0.06	0.50	0.22	SiC	0.041	0.129
				N4			
0-0.40	Ap	0.17	0.46	0.14	C	0.008	0.182
0.40-0.72	Bw	0.13	0.50	0.25	C	0.022	0.159
0.72-1.20	Bk	0.12	0.50	0.18	C	0.028	0.150
				G1			
0-0.30	Ap	0.11	0.50	0.28	C	0.027	0.152
0.30-1.15	Bss	0.15	0.51	0.20	C	0.031	0.145
1.15-1.70	Bk1	0.05	0.54	0.16	SiC	0.055	0.107
1.70-2.80	Bk2	0.09	0.55	0.21	C	0.031	0.145
				G2			
0-0.18	Ap	0.16	0.46	0.11	C	0.009	0.180
0.18-1.10	Bkss	0.13	0.52	0.12	C	0.012	0.175
1.10-1.50	Bk	0.12	0.52	0.14	C	0.010	0.178
				G3			
0-0.20	Ap	0.16	0.47	0.12	C	0.013	0.174
0.20-0.85	Bkss1	0.15	0.50	0.11	C	0.015	0.171
0.85-1.15	Bkss2	0.15	0.50	0.13	C	0.016	0.169
1.15-1.45	Bk	0.15	0.46	0.17	C	0.026	0.154
				G4			
0-0.20	Ap	0.16	0.44	0.12	C	0.022	0.160
0.20-1.20	Bkss	0.12	0.49	0.13	C	0.027	0.152
1.20-1.60	Bk1	0.09	0.50	0.14	SiC	0.035	0.139
1.60-2.50	Bk2	0.06	0.49	0.14	SiC	0.060	0.100
				G5			
0-0.42	Ap	0.15	0.48	0.24	C	0.034	0.141
0.42-0.67	Bss	0.13	0.48	0.14	C	0.038	0.135
0.67-1.20	Bk1	0.11	0.51	0.15	C	0.037	0.135
120+	Bk2	0.06	0.52	0.27	SiC	0.047	0.120

Soil swelling and soil subsidence corresponded with the rainfall pattern because the rainfall amount affects the change in soil water storage (Fig. 4.1). Maximum soil subsidence at all three land uses occurred during or a month after the driest month of the year. However, the overall soil subsidence and the period of maximum soil subsidence varied between sub-watersheds likely because of difference in vegetation, variation in total clay and inorganic C content (Wilding and Tessier, 1998), soil structure (Srivastava et al., 1989) and presence of gilgai in the field (Thompson and Beckmann, 1982; Kishné et al., 2009).

The maximum soil subsidence measured from the soil surface at the sites of grazed pasture, row crop, and native prairie ranged from 91 to 120 mm, 67 to 76 mm and 54 to 75 mm, respectively, and the maximum soil subsidence in the grazed pasture was significantly (α =0.01) greater than what measured on the other lands.

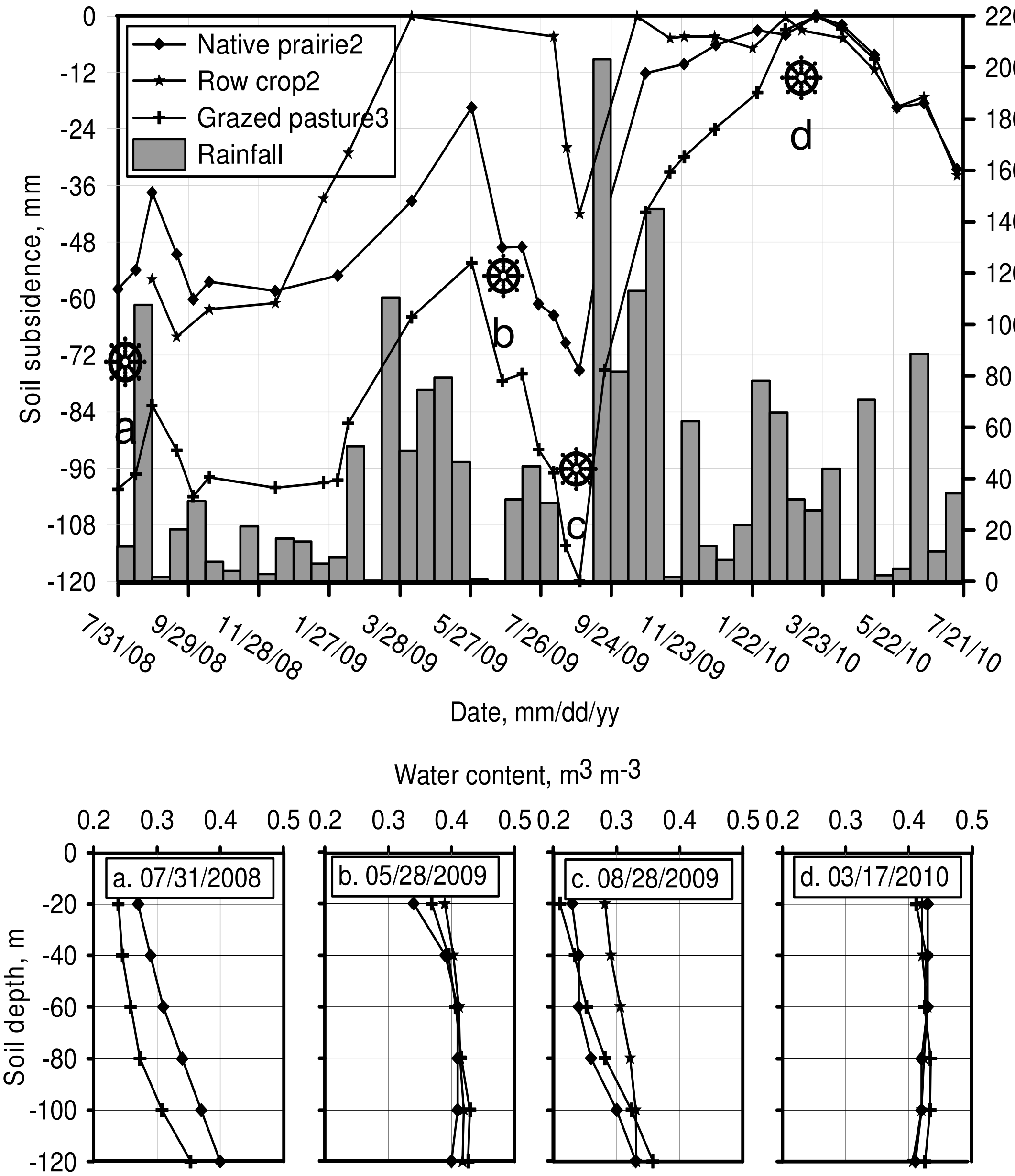

Figure 4.1. The 14 d cummulative rainfall and soil subsidance at the Native prairie, Grazed pasture and Row crop. The arrows indicate selected days corresponding to the maximum soil subsidence and swelling time and their respective soil water content with depth.

Soil subsidence in the grazed pasture was highest likely due to several reasons. First, the shape of gilgai is circular with a radius of 1 to 2-m and a depth down to 0.25 m. Since gilgai are plentiful in the area (~ every 2 to 3 m), they hold more water and helped soils capture and infiltrate more water during wet seasons and shrunk proportionally in dry seasons, resulting greatest soil subsidence and change in soil water storage. Studies also show that wide and frequent cracks occur in microlows (Thompson and Beckmann, 1982; Wilding and Tessier, 1998; Kishné et al., 2009). Because of compaction on the grazed pasture by cattle and on the row crop by heavy machinery, the soils at the virgin native prairie may have better structure, and hence less soil subsidence (Lauritzen and Stoltenberg, 1940). The elongated shape of gilgai in the native prairie, which is parallel to the flow direction of runoff, cannot capture runoff to aide in wetting the soil profile and hence lesser shrink-swell dynamics compared to the grazed pasture.

The measured soil subsidence and soil water content at each land use showed the spatial and temporal variability of soil shrinking and swelling (Fig. 4.1). The relationship between soil subsidence and change in soil water storage was investigated for all sites. Generally, at all sites, the 0 to 0.9-m soil layer started subsiding considerably after losing 60 mm of water. Given the high COLE values (Table 4.1), if the soils were shrinking isotropically and equidimensionally, $\Delta z/\Delta W$ is expected to be 0.33 (Bronswijk, 1991); however, the three-year average of the ratio was well below 0.33 at all sites. The three-year averages of $\Delta z/\Delta W$ were 0.21, 0.20, and 0.24, for the native prairie, grazed pasture, and row crop land uses, respectively. The three-average ratios for the three land uses is quite consistent and suggest that overall, soils shrink more horizontally than vertically. Mitchell and Van Genuchten (1992) also found a ratio that ranged from 0.13 on wheat crop land to 0.23 on a bare soil. Cabidoche and Voltz (1995) also found a ratio that ranged from 0.11 to 0.82 from a three year study on a grassland that has a gilgai. However, Kirby et al. (2003) reported that the $\Delta z/\Delta W$ is consistently 1/3, which is contrary to our results that did not support this constant ratio in any of the three land use.

A ratio of < 0.33 suggests that the soil profiles are not completely collapsing, vertically, as they shrink. The intriguing finding from this two year measurement is the temporal instability in the subsidence:water loss ratio (Figs. 4.2 - 4.4). The CV's for the three-year average of the ratios were 27, 28, and 45% for the native prairie, grazed pasture, and row crop land uses, respectively. Even though the coefficient of variability at the crop land was greater, the variability in ratio within sites was lower at the crop land. It ranged from 17 - 31, 24 - 35 and 42 – 47 % at the native prairie, grazed pasture, and row crop land uses, respectively. Any time during basic shrinkage phase, the $\Delta z/\Delta W$ ratio should be close to 0.33 when soils shrink isotropically and equidimensionally, or 0.22 in this case, however, during times when the soil was wetting, the ratio decreased that might be due to the loss of water from macro pores, which might not induce a considerable soil subsidence.

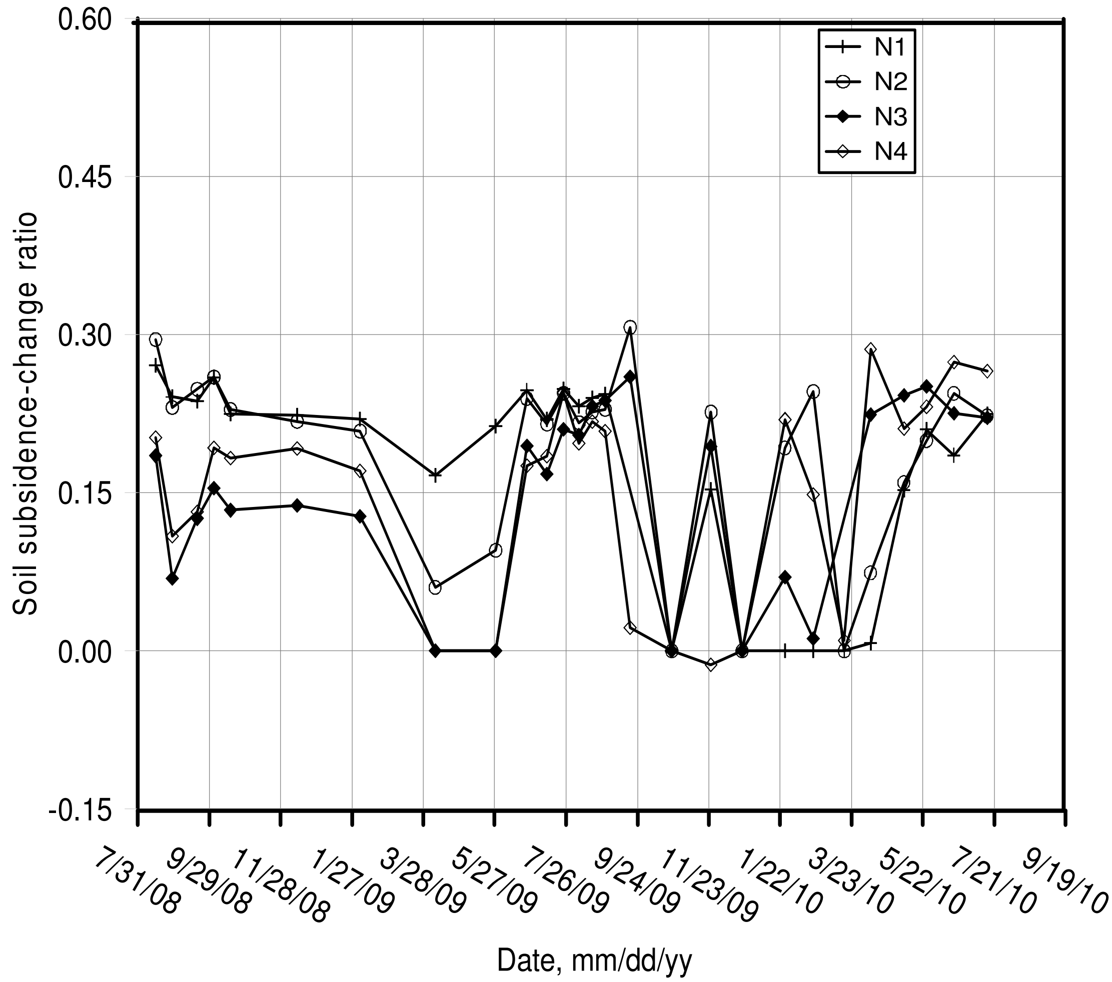

Figure 4.2. The ratio of the soil subsidence to the change in soil water storage ($\Delta z/\Delta W$) at four measurement sites on the Native prairie watershed, located at the USDA-ARS Grassland, Soil and Water Research Laboratory, in Riesel, Texas.

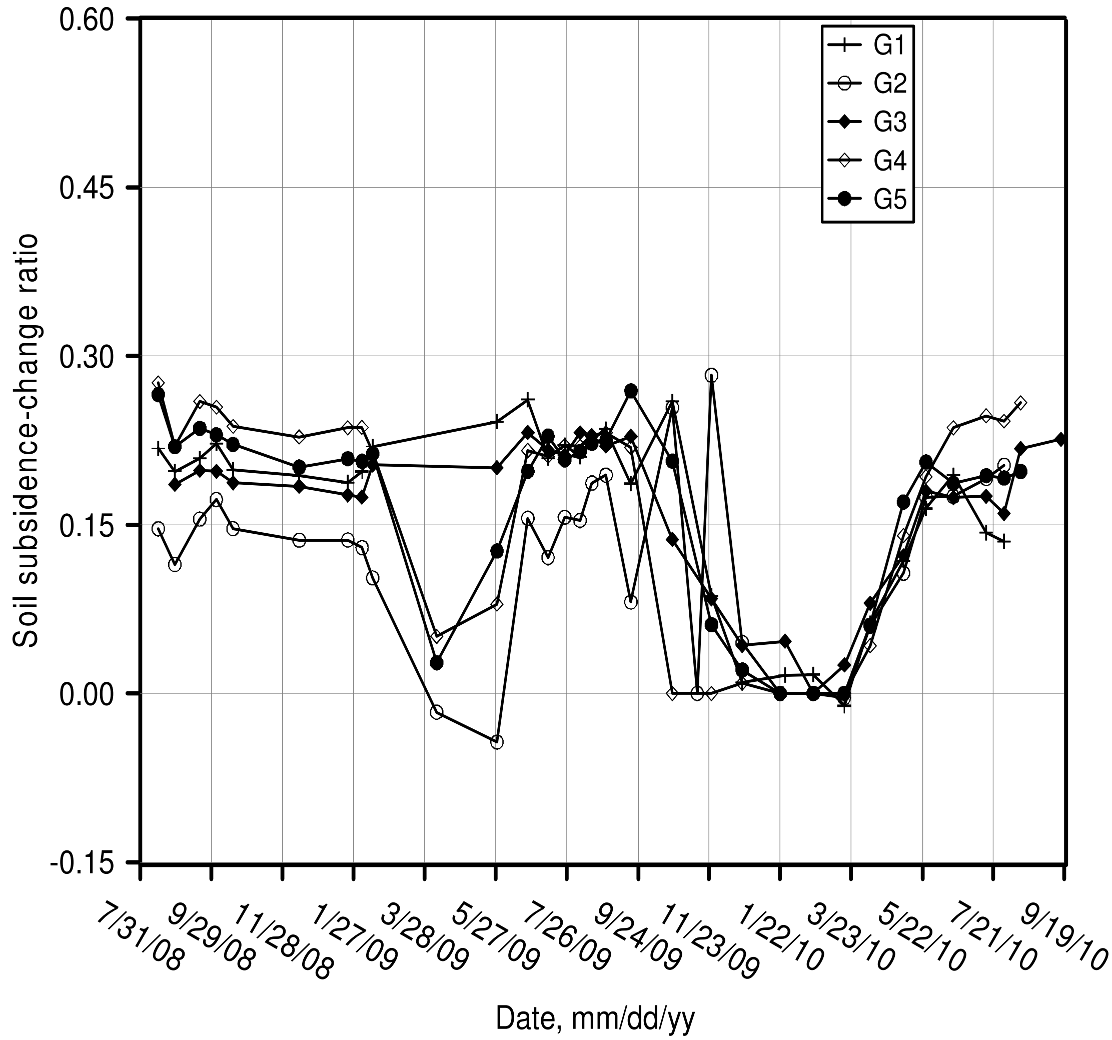

Figure 4.3. The ratio of the soil subsidence to the change in soil water storage ($\Delta z/\Delta W$) at five measurement sites on the Grazed pasture watershed, located at the USDA-ARS Grassland, Soil and Water Research Laboratory, in Riesel, Texas.

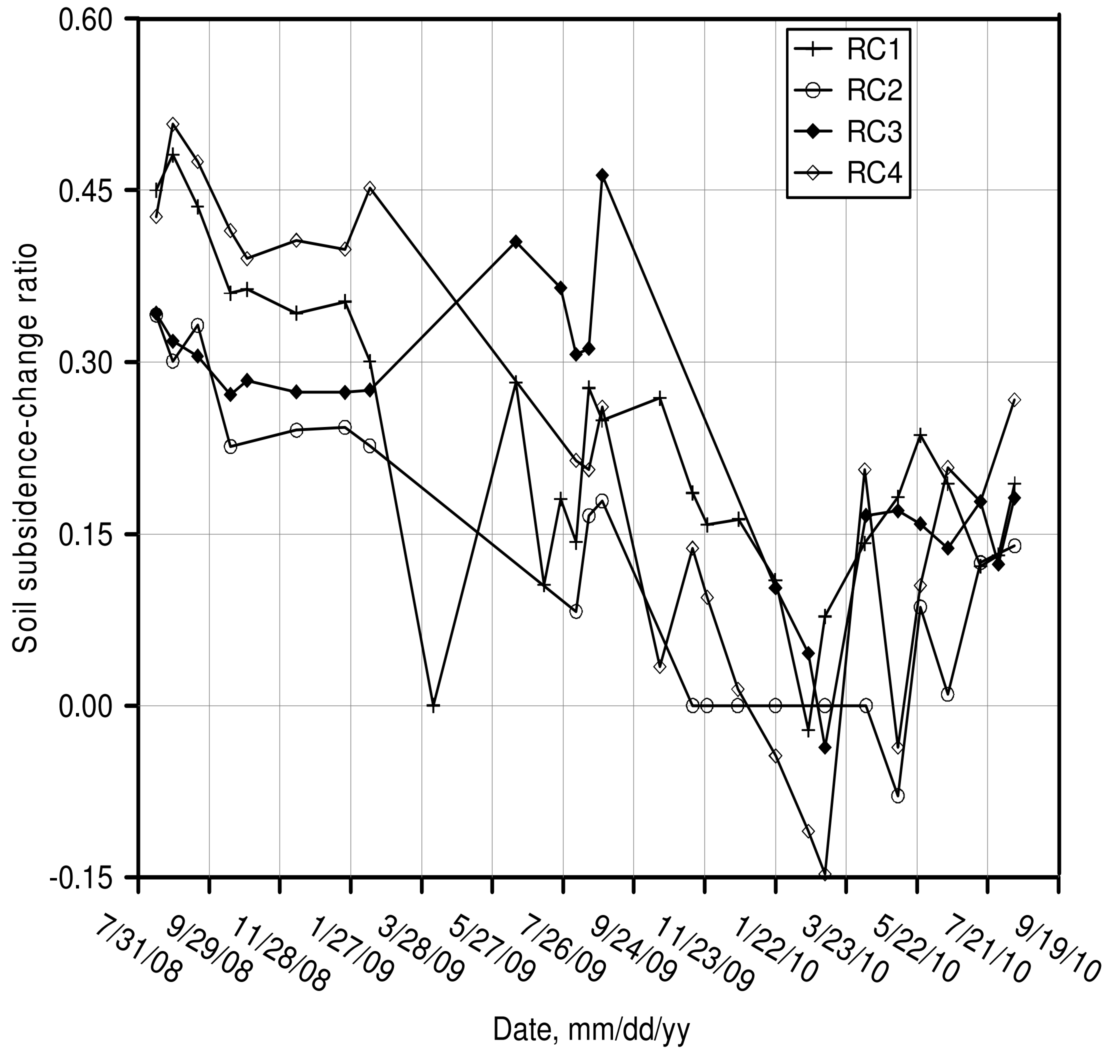

Figure 4.4. The ratio of the soil subsidence to the change in soil water storage (Δz/ΔW) at four measurement sites on the Row crop watershed, located at the USDA-ARS Grassland, Soil and Water Research Laboratory, in Riesel, Texas.

During a wetting cycle, the ratio was quite unstable and seldom became negative (Figs. 4.2-4.4). The values of ΔZ and ΔW are always negative, based on Eqs. 1 and 3. Consequently, Δz is expected to be negative, making Δz/ΔW positive. In some instances, however, Δz/ΔW is negative (Fig. 4.4, e.g., R2), which might not necessarily be due to a measurement error. A Δz value could be positive when the soil layer (0-0.9 m) becomes wet and could swell while the subsurface soil layer (0.9 m to the monument) shrinks or stays at its original height. During this period, Δz of the 0.0 - 0.90-m soil layer would be positive and thus the $\Delta z/\Delta W$ would be negative. Moreover, there were also situations where the ratio was very high (>1), which did not necessarily mean the soils shrunk greater than the amount of soil water lost from the soil layer. Other than possible measurement errors, such situation could occur during wet seasons and a structural soil subsidence phase, when the amount of change in soil water storage (ΔW) is close to zero and simultaneously smaller than the soil subsidence (Δz) and hence the ratio, $\Delta z/\Delta W$, would be highly exaggerated (> 1).

The ratio of the soil subsidence to the change in soil water storage in the row crop sub-watershed had a different pattern compared to the grazed pasture and native prairie sub-watersheds. During the first summer (the dry season), $\Delta z/\Delta W$ was greater than 0.33 at the row crop and < 0.33 at the grazed pasture and native prairie. Assuming all water lost results in soil shrinkage (which is expected for soils of high COLE), a ratio > 0.33 at the row crop indicates that there was more vertical shrinkage in the row crop. In contrary, a $\Delta z/\Delta W < 0.33$ indicates that either 1) the soil is not shrinking with equal proportion to loss of water, which is the case during a structural shrinkage phase, but could be an equidimensional shrinkage or 2) basic and isotropic shrinkage but no/less subsidence, creating more surface cracks (crack area density) and more macropore void space below the soil surface. Given the high shrink swell-potential in the study area, as witnessed from the COLE value, we would expect an equidimensional and isotropic shrinkage in all lands but we found a different shrinkage property. If the scenario were isotropic but unequidimensional with a ratio < 0.33, there would be more crack area to capture runoff and more void space to hold the water within the soil. Moreover, if the shrinkage were not proportional to the change in soil water storage or the ratio was > 0.33, there would be less crack area to capture runoff. Our physical observations also showed that cracks were wider and more frequent on the grazed pasture than on the row crop and native prairie. Under the isotropic shrinkage scenario, we expect the soil aggregation and perennial plant roots to limit soil subsidence during some water loss (Mitchell and Van Genuchten, 1992), and this difference may have an implication on preferential flow of water in each land and on runoff. Even though the overall soil subsidence at the row crop and native prairie were not considerably different, their ratios were not the same. Therefore, the assumption of equidimensional shrinkage is not always true, and the ratio of soil subsidence to soil water loss may vary in space and time (Fig. 4.2).

Conclusions

The results from this study demonstrated the temporal and spatial variability in shrinkage property of soils as explained by the ratio of the soil subsidence to the change in soil water storage. This variation indicated that observations do not always follow the mechanics of equidimensional soil shrinkage and showed the variability in the property of soil shrinkage in time and space. Soil structure and vegetation associated with land use, gilgai presence and shape and inorganic C were found to be an important factor for variation in soil subsidence and possibly in the relationship between the soil subsidence and change in soil water storage. Despite the differences in soil subsidence for a change in soil water storage, and the possible soil properties that affect the soil subsidence, the ratio of soil subsidence to change in soil water storage varied with time at all land uses. The variation in the ratio of soil subsidence to change in soil water storage indicated the possible variability in horizontal shrinkage (crack size) with time in a space, which in turn, affects distribution of water in a soil layer and surface flow of water. The knowledge gained from this study, therefore, would help revise hydrology models applied on vertic lands.

CHAPTER V

CHANGE IN VOLUME OF SOILS ABOVE FIELD CAPACITY

Introduction

The coefficient of linear extensibility (COLE) determined from measurements of the change in volume of soil from a change in water content is a common measure used to characterize the relative shrinkage or swelling potential of a clayey soil as it dries or wets (Franzmeier and Ross, 1968; Grossman et al., 1968; Reeve et al., 1980; Bronswijk, 1991; Thomas et al., 2000b). The magnitude of COLE expresses the change in a length scale derived from the specific volume of an aggregate between water contents associated with -33.3 kPa soil water potential and the oven dry (105 °C) state, relative to the length scale at the oven dry state (Reeve et al., 1980; Soil Survey Staff, 1996; Thomas et al., 2000a). Data used to determine COLE defined two points on the curve relating specific volume to gravimetric water content, a curve that has information that can be used in simulating the magnitude of crack development in a drying soil. The two points from COLE, the specific volumes at the water contents associated with -33.3 kPa water potential and the oven dry state, along with one of numerous empirical models (e.g., McGarry and Malafant, 1987; Olsen and Haugen, 1998; Chertkov, 2007) can be used to define the mathematical relationship when the soil water potential is < -33.3 kPa. The shape and slope of the relationship at water contents above that associated with -33.3 kPa water potential is not as well understood because it is strongly influenced by the nature of soil macroporosity, which is highly variable.

Our field studies showed periods where soil water contents were greater than those measured on core samples equilibrated at -33.3 kPa water potential, and surprisingly we found changes in soil height on the field at that greater water content. Therefore, understanding the dynamics of change in volume of soil at water content between saturation and -33.3 kPa water potential is necessary. The objective of this study was to characterize the relationship between specific volume and gravimetric water content for soil as a function of soil depth at two landscape positions.

Materials and Methods

Soil samples were collected from an improved grazed pasture the USDA-ARS Grassland, Soil and Water Research Laboratory near Riesel, Texas. A truck-mounted probe (Giddings Machine Company, Windsor, CO) was used to collect soil core segments (a radius of 33.5 mm and length of 20 - 60 mm) from the surface to 1.0-m deep at two landscape positions: summit and footslope. The soil at the both positions is fine, smectitic, thermic Udic Haplusterts (Soil Survey Staff, 2003). The core segments collected from both sites were returned to a laboratory and dipped once in Saran to maintain their integrity.

The volume of core segments were measured using a 3D Laser scanner (NextEngine Desktop 3D Scanner Model 2020i, NextEngine, Inc., Santa Monica, CA) at 0 (saturation), -3.3, -6.7, -16.7 -33.3-kPa water potential and after being oven dried at 105 °C. To accomplish this sequence of measurements, the soil core segments were first soaked in water for two weeks to allow them to saturate. The volumes of the core segments were then measured using the scanner. Next, the saturated core segments were sequentially placed on columns of fine sand producing soil water potentials of -3.3 and -6.7 kPa and then in a pressure plate apparatus producing soil water potentials of -16.7 and -33.3 kPa. At each water potential, the core segments were allowed to equilibrate for 7 to 10 d. After equilibration at each water potential, the volumes of the core segments were measured using the scanner. During the volume measurements, the weights of the soil core segments were measured using an electronic balance (0.01 g). The volume estimated from the 3D scanner was verified by comparison to volume determined using the traditional Archimedes' principle (Rossi et al., 2008) (Fig. 5.1).

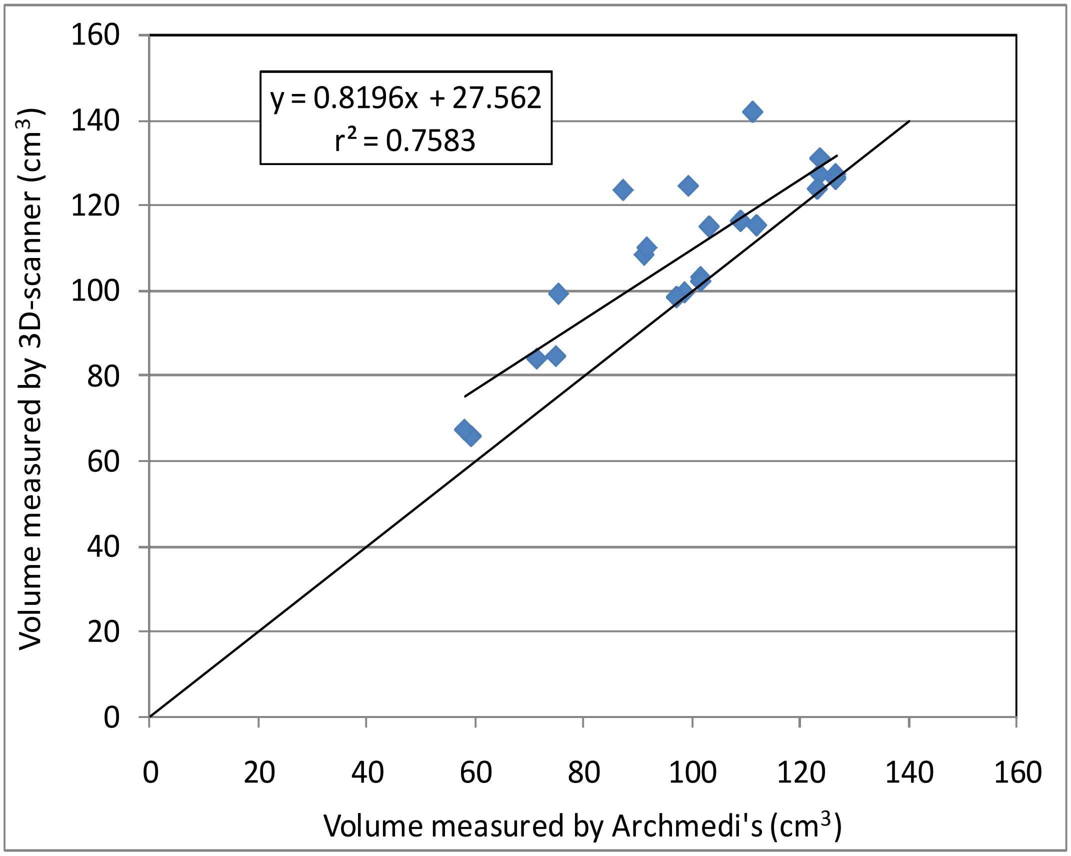

Figure 5.1. Volume estimated from the 3D scanner as related to volume measured by Archimedes' principle.

Volumes, masses, water contents, densities, and specific volumes were determined from the laboratory data as follows:

$$V_{v,sat} = m_{w,sat} = (m_{t,sat} - m_d) * \rho_w$$
$$V_s = V_{t,sat} - V_{v,sat}$$
$$m_{w,i} = m_{t,i} - m_d$$
$$V_{v,i} = V_{t,i} - V_s$$
$$\omega_i = m_{w,i} / m_d$$
$$\rho_p = m_d / V_s$$
$$\rho_{b,t} = m_d / V_{t,i}$$
$$\nu_{s,t} = 1 / \rho_{b,t} = V_{t,i} / m_d$$

where

$V_{v,sat}$	is the volume of void at saturation (m^{-3}).
$m_{w,,sat}$	is the weight of water at saturation (kg).
$m_{t,sat}$	is the total weight of soil at saturation (kg).
m_d	is the weight of solid soil (kg).
ρ_w	is the density of water and taken as 1 Mg m^{-3}.
V_s	is the volume of solid soil (m^{-3}).
$V_{t,sat}$	is the volume of bulk soil at saturation (m^{-3}).

$m_{w,i}$ is the weight of water at a given water potential (kg).

$m_{t,i}$ is the total mass of soil at a given water potential (kg).

$V_{v,i}$ is the volume of void at a given water potential (m^{-3}).

$V_{t,i}$ is the total volume of soil at a given water potential (m^{-3}).

$\omega_{w,i}$ is the gravimetric water content of soil at a given water potential.

ρ_p is the particle density of soil ($Mg\ m^{-3}$).

$\rho_{b,t}$ is the wet bulk density of soil at a given water potential ($Mg\ m^{-3}$).

and,

$\nu_{s,t}$ is the specific volume of soil at a given water potential ($m^3\ Mg^{-1}$).

The COLE of a core segment was calculated using the difference in volume of a segment measured at -33.3 kPa (V_m) and measured at oven dry state (V_d) (Grossman et al., 1968) as follows,

$$COLE = \frac{V_m^{1/3} - V_d^{1/3}}{V_d^{1/3}}$$

Results and Discussions

From saturation to the water content at -33.3 kPa water potential, the relationships between the change in specific volume of the clods and change in water content was most often linear with slopes < that of the load line, the line where the soil is considered to consists of only solids and water (Fig. 5.2). With respect to the volume of soil at saturation, the soil samples shrank between 1 and 4 % when dried to their -33.3 kPa water contents. When this change in soil volume is related to COLE, if the COLE was measured from saturation (instead of -33.3 kPa), it would increase by 4 to 16 %. If shrinkage in the field were isotropic, this would represent between 7 and 25 mm of soil subsidence per a meter of soil layer.

The gravimetric water contents and wet bulk densities of the soil core segments were used to make soil shrinkage characteristic curves (Figs. 5.3 and 5.4). The reference line in the figures represents a linear change in volume of bulk soils for a unit change in soil water. The slope of the relationship between the change in bulk density of soils and change in water content curve was theoretically expected to be close to zero during structural shrinkage phase. However, our result showed a slope that is considerably different from zero at different depths of the two locations, which indicated the existence of change in volume of soils between the field capacity (-33.3 kPa) and the saturated water content.

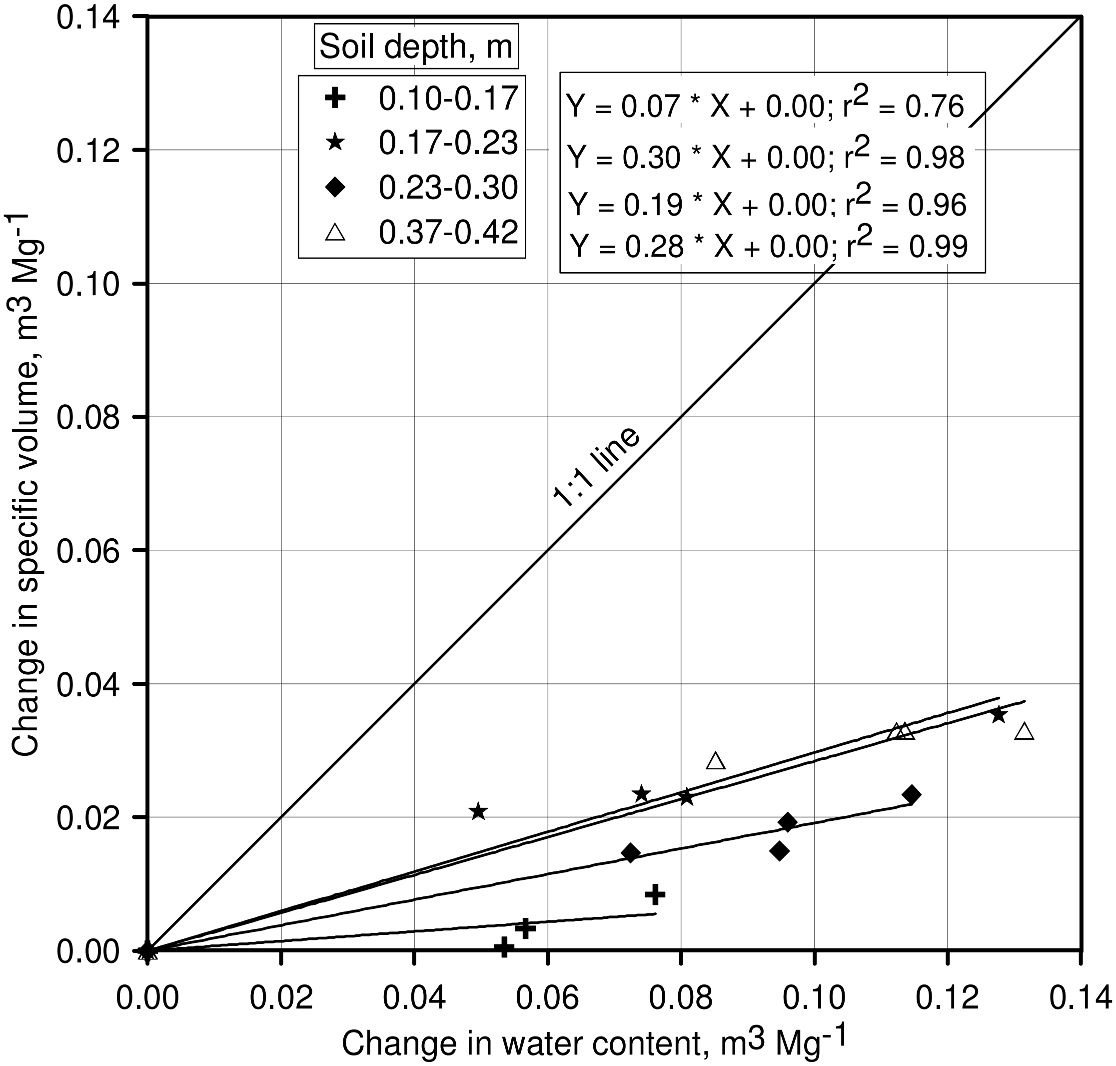

Figure 5.2. The relationship between changes in specific volume of soil with change in soil water content, both with respect to the saturated state. Zero on the axis represents the saturated state. The 1:1 line represents the relationship if no air were to enter a soil sample on drying.

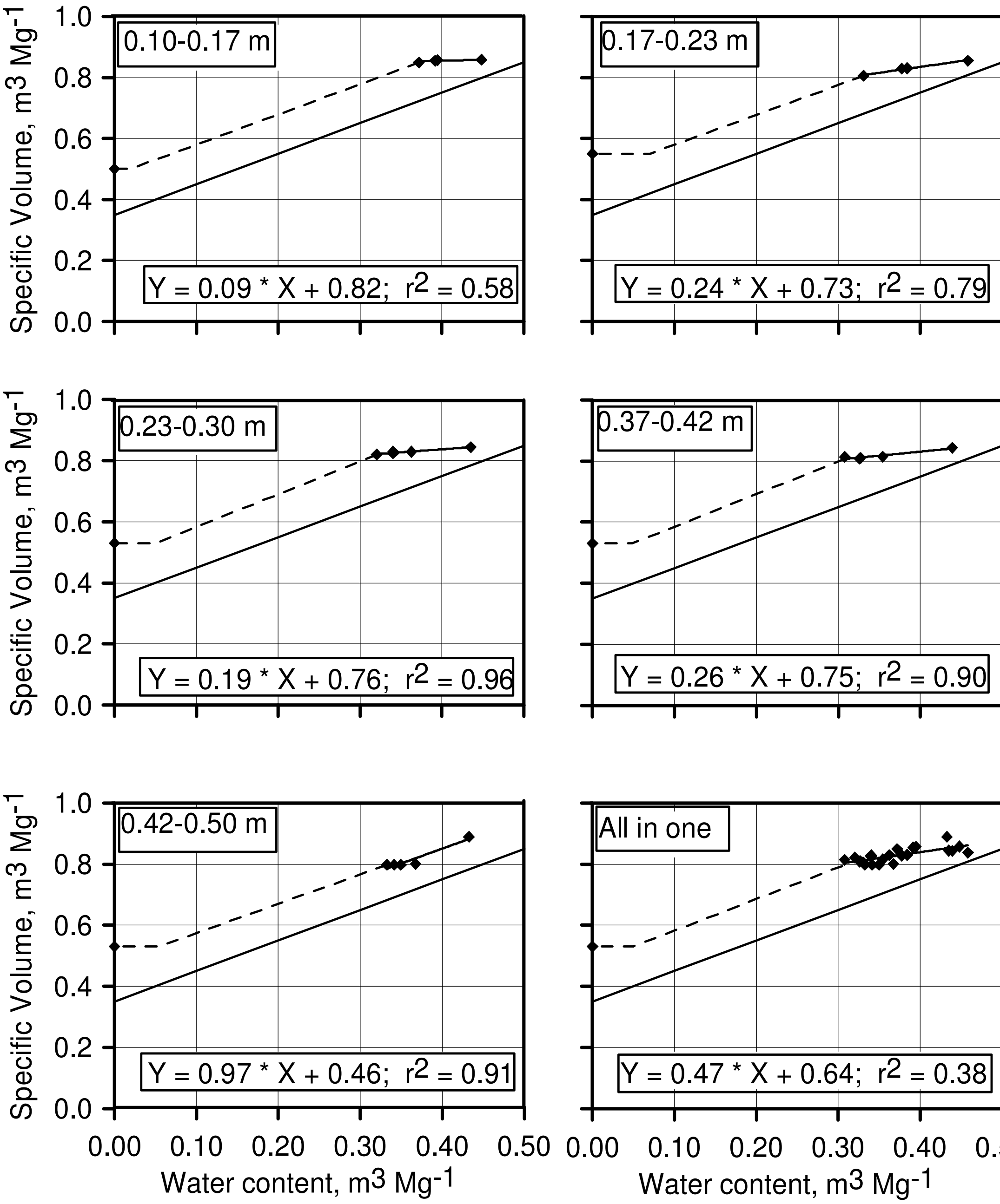

Figure 5.3. Soil shrinkage characteristics curve of soil core segments collected at different depth from the footslope position. The solid lines through the data points represent lines of linear regression. The dashed lines represent rough expectations of the shape of the relationships between the water contents associated with the -33.3 kPa water potential and oven dry. The solid line below the data points is the theoretical load line where the soil would consist only of solids and water, no air.

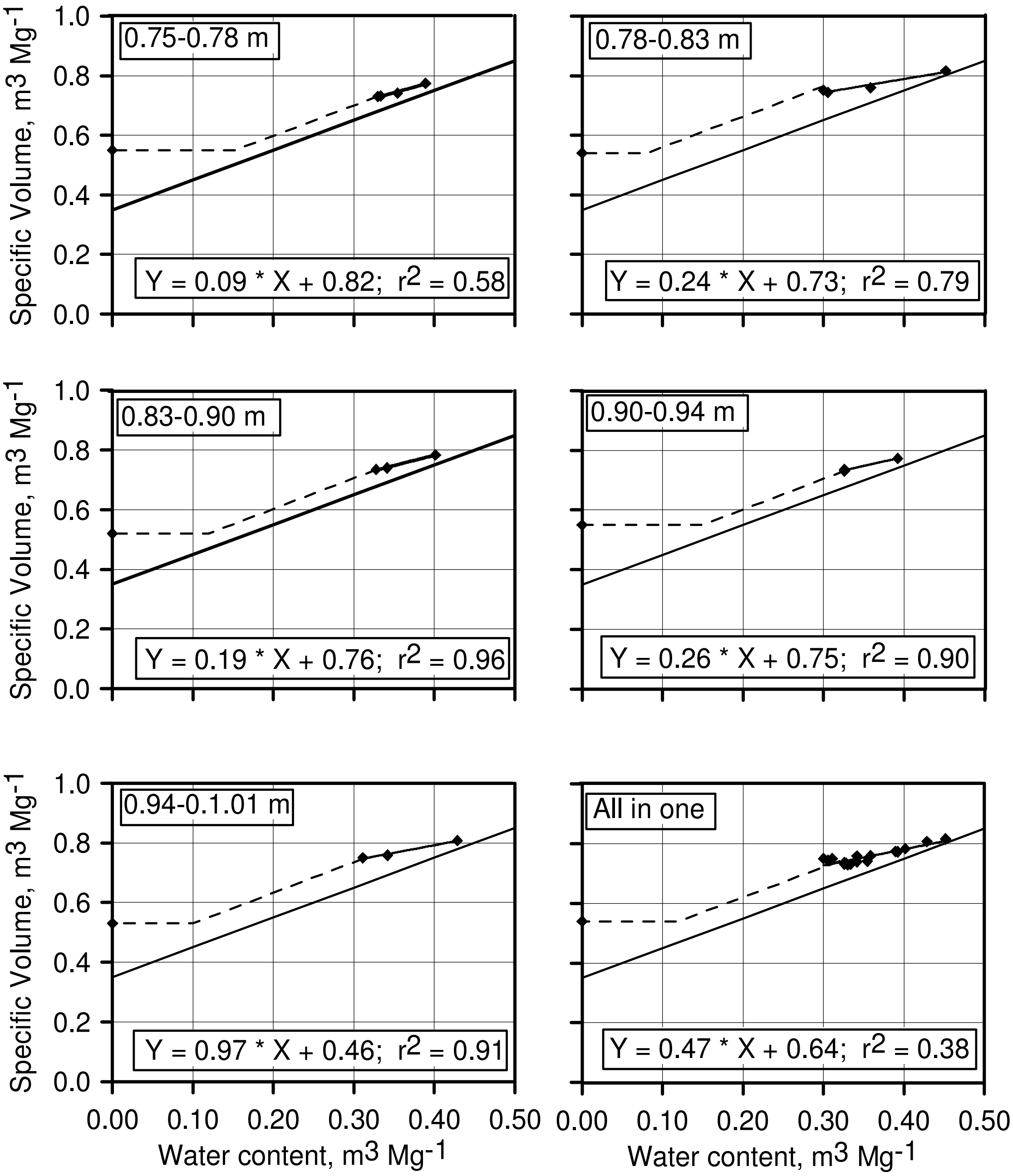

Figure 5.4. Soil shrinkage characteristics curve of soil core segments collected at different depth from the summit position. The solid lines through the data points represent lines of linear regression. The dashed lines represent rough expectations of the shape of the relationships between the water contents associated with the -33.3 kPa water potential and oven dry. The solid line below the data points is the theoretical load line where the soil would consist only of solids and water, no air.

The variability in slope with depth at the footslope may be associated with the structure of the soil and the increase in fine clay content with depth. The fine clay content of soils (0.10 - 0.50-m deep) at the footslope was between 0.16 to 0.23 kg kg^{-1} (Table 5.1). At this location, soil at the surface is expected to have less structure than the subsurface soils because of frequent drying and wetting, and trampling by cattle. Surprisingly, the rate of change in bulk density of soils with change in water content was also high at the subsurface soils of the summit location and the variability with depth was less, which further supports our argument of the influence of soil texture and fine clay content. The fine clay content of soils (0.77 - 1.01-m deep) at the summit was 0.27 kg kg^{-1} and the structure of the soil is little affected by shrinking and swelling of soils as compared to surface soils.

If the data from each soil layer were combined, the slope of the relationship at the summit and footslope locations would be close to 0.54 and 0.47, respectively (Figs. 5.3 and 4.4). This slope shows that from a given volume of water loss between saturation and field capacity, the volume of the bulk soils changes by > half of the volume of the water lost. To further elaborate, for a slope of 0.5, a m^3 of soil block with a porosity of 0.50 at saturation and volumetric water content of 0.46 m^3 m^{-3} at field capacity would subside about 20 mm between field capacity and saturation. This result implied that if the soils shrink isotropically and equidimensionally, there could be about 20-mm wide crack in the field when the soil loses water from saturation to the traditionally assumed field capacity (-33.3 kPa) and formation of such wide cracks, in turn, could potentially affect runoff and water distribution in the soils. Our field measurement of soil subsidence and soil water also indicated a vertical movement of soils at water content above what measured in the laboratory at the field capacity. In this field measurement, 17 mm of soil subsidence was measured at the summit between the soil depth of 0.3 and 1.5-m when the soil water content was 0.45 $m^3\ m^{-3}$. Therefore, it is important to address the change in volume of soils between saturation and field capacity in shrink-swell studies.

Table 5.1. The coefficient of linear extensibility (COLE), total clay and fine clay content at the study locations.

Depth	$COLE^{+}$	$COLE^{*}$	Clay	Fine clay
m	- - m m^{-1}- -		- - kg kg^{-1}- -	
		Footslope		
0.10-0.17	0.079	0.083	0.51	0.16
0.17-0.23	0.087	0.102	0.54	0.21
0.23-0.30	0.059	0.069	0.54	0.21
0.37-0.42	0.064	0.076	0.53	0.23
0.42-0.50	0.068	0.107	0.53	0.23
		Summit		
0.75-0.78	0.073	0.093	0.59	0.27
0.78-0.83	0.080	0.110	0.59	0.27
0.83-0.90	0.069	0.092	0.59	0.27
0.90-0.94	0.063	0.082	0.59	0.27
0.94-1.01	0.064	0.092	0.59	0.27

$^{+}$ measured from -33.3 kPa, *from saturation

The measured COLE of all core segments were lower than samples taken from the same site in our previous study. Prior COLE measurements from these two positions showed that COLE ranges from 0.09 to 0.18 m m^{-1} and from 0.13 to 0.17 m m^{-1} at the summit and footslope, respectively (Table 3.1). The current study, however, showed that COLE ranged from 0.06 to 0.08 m m^{-1} and 0.06 to 0.09 m m^{-1} at summit and footslope position, respectively (Table 5.1). The reason for the considerable difference in volume of soils, which affected the COLE value, was not clear. The results from bulk higher soil volume estimates by the scanner were compared to Archimedes' principle estimates at oven dry. In a comparison of bulk density estimates at field capacity and at oven dry, the major difference in volume was primarily at oven dry (Table 5.2). The CV of bulk density of clods measured at field capacity using the Archimedes' principle and the 3D scanner was less than the CV of bulk density of multiple clods measured at field capacity using the Archimedes' principle. However, at the oven dry state, the CV of bulk density of clods using the Archimedes' principle and the 3D scanner was greater than the CV of bulk density of multiple clods measured at field capacity using the Archimedes' principle. Therefore, to calculate the specific volume of soils at the oven dry state, the volume measured by the Archimedes' principle was used.

Table 5.2. Comparisons of bulk density of clods measured using the Archimedes' principle and the 3D scanner.

Soil depth	$FC\rho_b{}^1$	$OD\rho_b{}^1$	$FC\rho_b{}^2$	$OD\rho_b{}^2$	FC CV[3]	OD CV[3]	FC CV[4]	OD CV[4]
m	- -- - - - - - - - - - -Mg m^{-3}- - - -- - - - - - -				- - - - - -- - - - - - -CV % - - - - - - - - - - - -			
				footslope				
0.10-0.17	1.16	1.65	1.18	1.49	5.38	5.39	1.07	7.12
0.17-0.23	1.23	1.82	1.24	1.61	2.44	1.15	0.70	8.73
0.23-0.30	1.23	1.82	1.22	1.45	2.44	1.15	0.58	15.97
0.37-0.42	1.20	1.84	1.24	1.48	2.20	1.44	2.28	15.17
0.42-0.50	1.20	1.84	1.25	1.53	2.20	1.44	3.10	12.85
				Summit				
0.75-0.78	1.40	1.84	1.37	1.70	2.89	1.44	1.53	5.57
0.78-0.83	1.40	1.84	1.31	1.66	2.89	1.44	4.81	7.47
0.83-0.90	1.40	1.84	1.36	1.67	2.89	1.44	1.99	6.93
0.90-0.94	1.40	1.84	1.37	1.65	2.89	1.44	1.68	7.86
0.94-1.01	1.40	1.84	1.34	1.62	2.89	1.44	3.17	9.20

$FC\rho_b{}^1$ and $OB\rho_b{}^1$ is bulk density measured at field capacity and at oven dry, respectively, using Archimedes' principle.

$FC\rho_b{}^2$ and $OB\rho_b{}^2$ is bulk density measured at field capacity and at oven dry, respectively, using 3D scanner.

FC CV[3] and OB CV[3] is the coefficient of variability of bulk densities of three clods measured at field capacity and at oven dry, respectively, using Archimedes' principle.

FC CV[4] and OB CV[4] is the coefficient of variability between bulk densities measured using Archimedes' principle and 3D scanner at field capacity and at oven dry, respectively.

Conclusions

There was an appreciable change in volume of soils between saturation and field capacity. The result showed that COLE measurement based on the commonly assumed soil water potential (-33.3 kPa) did not capture the complete shrink-swell potential of soils.

Use of the 3D image scanner proved to have several advantages over the traditionally used Archimedes's principle. These include: the same sample could be reused for multiple soil water potential studies, the shrinking and swelling of core segments are less limited because of few coating with Saran, and the problem of water penetration into the core segment during the traditional method is avoided. However, the process of clod scanning is very time consuming (> 1 h per image of a single core segment).

CHAPTER VI

A TECHNICAL PAPER: ORIENTATION OF CRACKS AND HYDROLOGY IN SHRINK-SWELL SOILS

Introduction

Most studies of shrinkage and cracking of Vertisols have focused on the size and areal density of cracks, not on the orientation of cracks. The orientation of cracks can have tremendous effect on the surface flow and capture of water. Cracks that are parallel to the direction of overland flow of water might capture less water than cracks that are perpendicular. The objective of this technical paper is to demonstrate the potential importance of crack orientation from a field survey.

Methodology of the Survey

The survey was conducted at the USDA-ARS Grassland, Soil and Water Research Laboratory near Riesel, Texas. The climate is warm and sub-humid with a mean annual rainfall of 910 mm. Two watersheds with different land use systems were selected for the investigation of cracks orientation. The land use types were native prairie and grazed pasture. The dominant soil in the area is Houston Black (fine, smectitic, thermic Udic Haplusterts) that consists of very deep, moderately well drained, very slowly permeable soils formed from weakly consolidated calcareous clays and marls of Cretaceous age (USDA-NRCS, 1997). The dominant vegetation in the native prairie is little bluestem (*Schizachyrium scoparium*) and in the grazed pasture is coastal bermudagrass (*Cynodon* *dactylon*). The average slope of the native prairie and grazed pasture is ~ 5 and 2 %, respectively (Figs. 6.1 and 6.2).

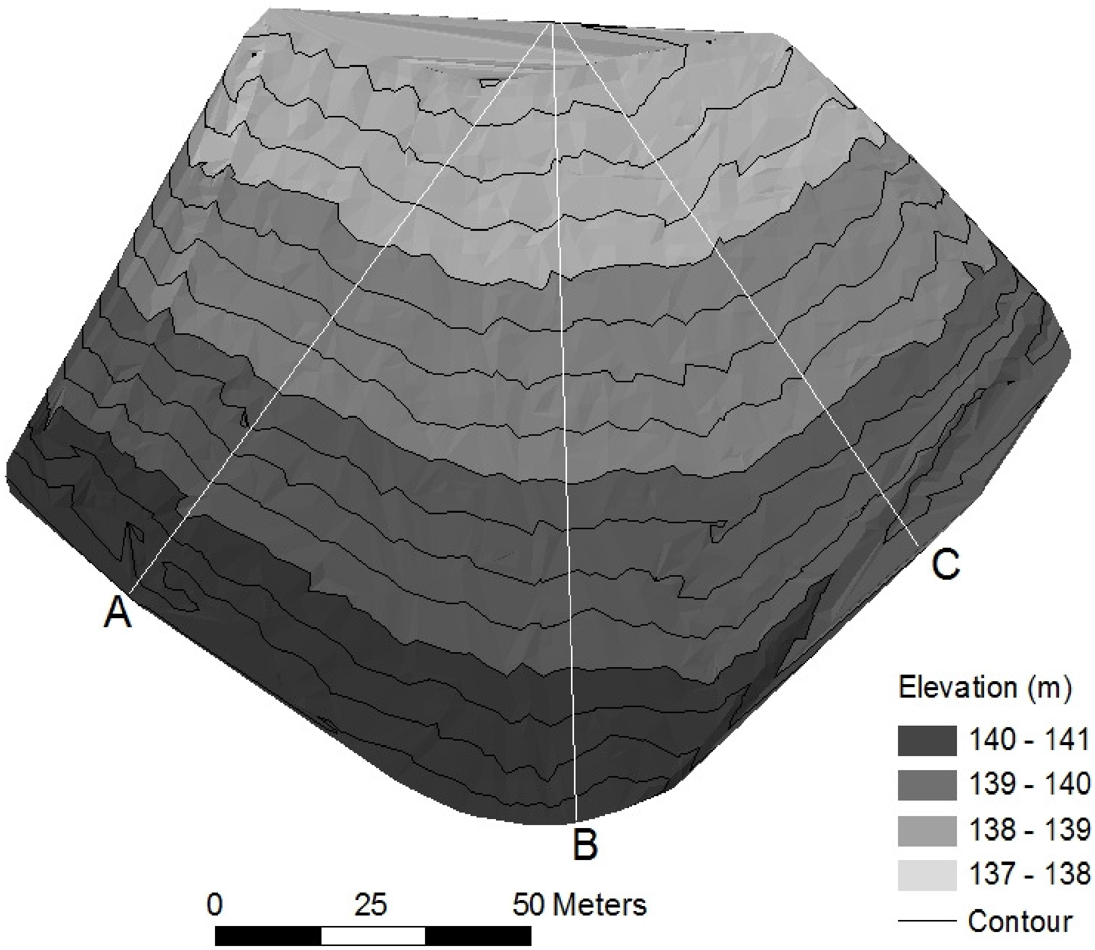

Figure 6.1. Topographic map of the Native prairie with a contour (0.25 m), located at the USDA-ARS Grassland, Soil and Water Research Laboratory, in Riesel, Texas. The symbols A, B and C indicate the locations where the surveys started and the lines indicate the paths of the surveys.

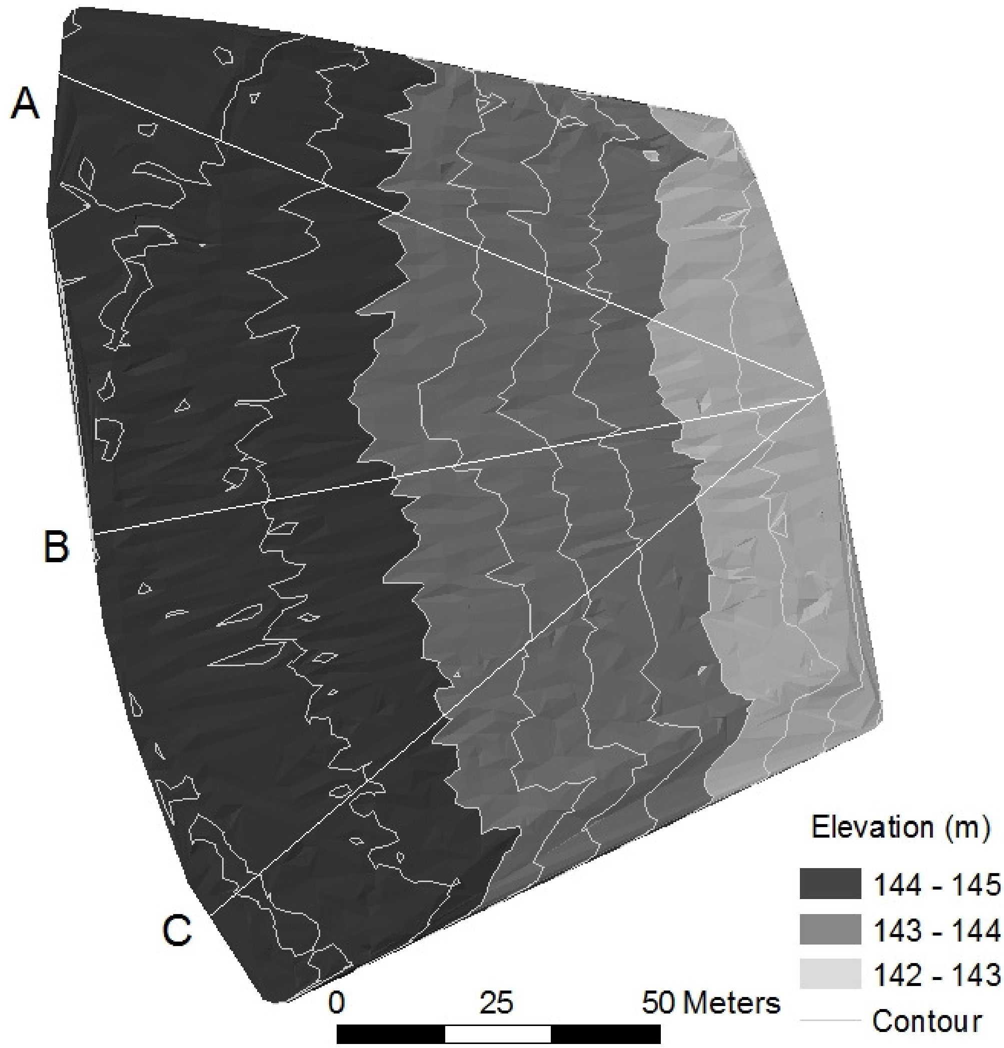

Figure 6.2. Topographic map of the Grazed pasture with a contour (0.25 m), located at the USDA-ARS Grassland, Soil and Water Research Laboratory, Riesel, Texas. The symbols A, B and C indicate the locations where the survey started and the lines indicate the paths of the surveys.

A survey was conducted on 11 August 2009 when there were many large cracks in the soil. Three slopewise transects were selected for the survey in each watershed (Figs. 6.1 and 6.2). The final destination of the transect survey was the watershed outlet. The length of the transect lines ranged from 100 - 120 and 100 - 125 m in the grazed pasture (1.5 ha) and native prairie (1.4 ha), respectively.

The orientations of the cracks were categorized as parallel, perpendicular, or irregular (neither parallel nor perpendicular) with respect to the slope of the land and flow direction of runoff. A crack (>= 10 mm) was considered parallel when it followed the direction of runoff flow; and perpendicular when it was parallel to the contour, both ~ within ± 30° of tolerance; and irregular when it was neither parallel nor perpendicular. Finally, the difference and similarities in cracks orientations among and within the land use types were compared.

Field Observations

The number of large cracks observed on the native prairie and grazed pasture from the three lines of transects were 53 and 58, respectively. Among the cracks observed, 61 % and 48 % were oriented parallel to the runoff direction in the native prairie and grazed pasture, respectively (Fig. 6.3). While 28 % and 45 % of cracks observed were oriented perpendicular to the flow direction of a runoff, in the native prairie and grazed, respectively.

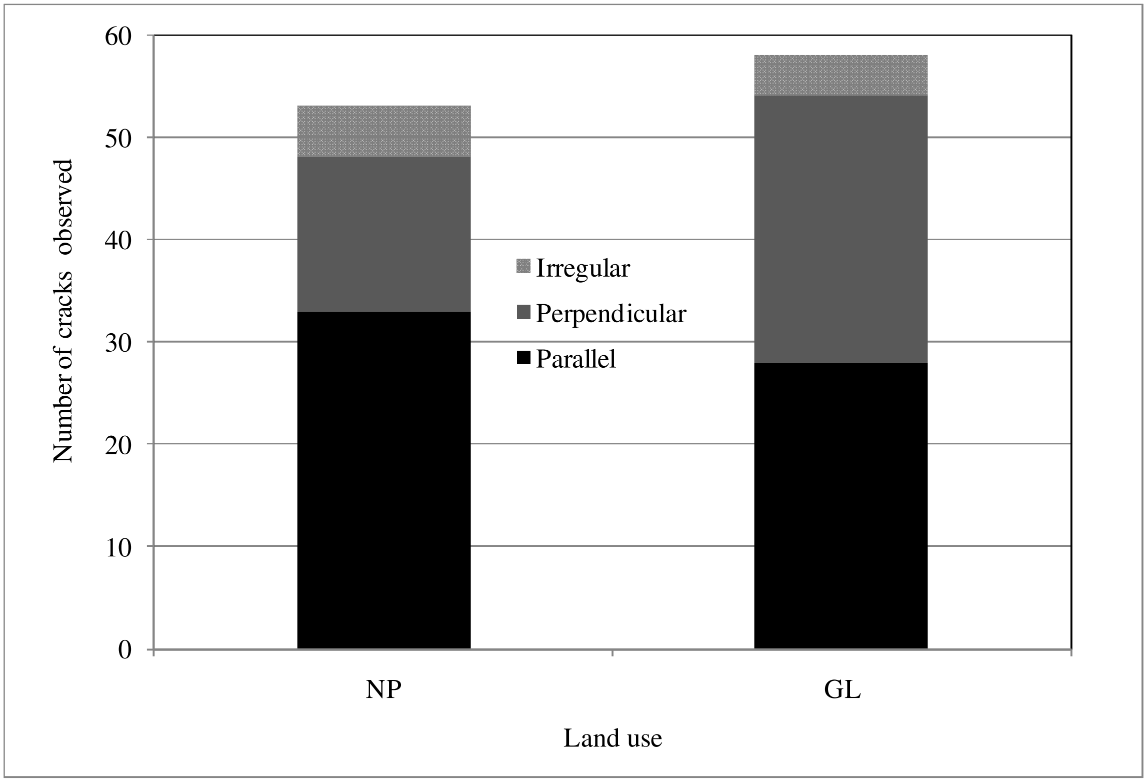

Figure 6.3. Distribution of cracks orientation on the native prairie (NP) and grazed pasture (GL) based on a transect walk made on 11 August 2009.

The survey showed that most cracks were oriented parallel to the direction of a runoff in the native prairie. However, the numbers of parallel and perpendicular cracks were not considerably different at the grazed pasture. In both lands, the frequency of occurrence of irregular cracks was not high compared to parallel and perpendicular cracks. The difference in orientations of cracks among the land use types could be due to not only the differences in vegetation cover, but also to the inherent size and shape of gilgai microhigh and microlow topographic and subsurface features. In both lands, cracks that oriented parallel were mostly observed on the ‘lower points’ of the gilgai microtopography where runoff would flow.

The gilgais in the native prairie were very elongated (up to 1 m length and 0.5 to 1 m width) in the direction of a slope that formed a natural channel for flow of runoff. The shape of gilgais in the grazed pasture was circular with a diameter of up to 3 m and a depth of up to 0.1-0.2 m. The existence of parallel cracks in slopewise elongated microlows, where runoff would flow, shows the possible influence of cracks orientation on flow and distribution of water in a vertic watershed. In contrast, a crack orientation in a circular microlow may not considerably affect the amount of runoff generated from a vertic watershed because the circular gilgai, regardless of the orientation of cracks formed inside, would capture water. The influence of crack orientation on runoff and water distribution depends on the existence and type of microlows. Cracks that oriented parallel to the runoff direction would likely enhance more surface runoff as compared to cracks oriented horizontally. However, since parallel cracks likely trap greater volume of surface runoff, the volume of subsurface runoff and soil water distribution around the horizontally oriented cracks could be high and need to be addressed in a study of hydrology of shrink-swell soils.

Challenges in Quantifying Cracks Orientation

Attempts have been made to study crack geometry using photography in a laboratory (Peng et al., 2006) and in a field (Velde, 1999). This technique has the advantage of taking data easily, continuously and nondestructively. However, the technique does not provide other crack information such as depth of cracks and difficult to get a quality data in a vegetative land. The direct measurement of crack orientation in a field is another technique to measure crack geometry, but it is very challenging, especially on a wide area. First, categorizing the direction of a crack could be subjective, especially when it is neither clearly parallel nor perpendicular. Second, apart from the presence of gilgai, the existence of any other microtopography on the land has to be considered to classify the direction of the crack orientation and whether this microtopography is considerably important or not. If it is important, categorizing the direction of cracks should not be based on the general slope direction of the entire land but the classification has to follow the slope of the microtopography as long as our interest is for hydrology (their impact on a runoff). This shows that the decision has to be site specific and based on the flow direction of a runoff on that particular site. Several minor cracks that are a branch to the major crack would also be a challenge for categorizing the orientation of the cracks. Use of a survey quality GPS to measure crack location may help reduce these problems.

Conclusions

Since the crack orientation has an impact on the amount of runoff, hydrological models should incorporate not only the size, depth, and density of cracks but also their orientation. Because of the challenges associated with studying crack orientations, simple and practical guidelines are needed, or other techniques that capture all the necessary crack information (the size, depth, density and orientation of cracks) need to be used. Further study is necessary to understand whether there is a spatial pattern to cracks orientations and whether there is a trend on the distance between wide cracks.

CHAPTER VII

SUMMARY

Measurements of the vertical movements of Vertisols with changes in soil water contents showed that shrinking and swelling of soils spatially and temporally varied across the landscape. Because COLE at most locations was high (>0.1 m m^{-1}), except where inorganic C was very high, change in soil water storage was the primary driver in the spatial and temporal variability of vertical shrinking and swelling of soils on outwardly uniform Vertisol catena. The trend of the relationships between the measured soil thickness and water content loosely agreed with the theoretical model; however, the relationship at the surface soil layers of the Summit and Shoulder were not well calculated because these soils with high shrink-swell potential did not subside. The low of vertical subsidence during drying suggests that there are more large horizontal cracks in these soil layers, which is useful information for hydrologic modeling. The magnitude of soil subsidence at the Footslope was lower than at the Summit and Shoulder because the change in soil water storage at the Footslope was less and subsoils dried less frequently. Shrink-swell potential was found to be inversely correlated with inorganic C (calcium carbonate) and directly correlated with fine clay in this Vertisol catena. When inorganic C content was high (> 0.08 kg kg^{-1}), COLE was low (<0.05), and little shrinking and swelling was measured.

The magnitude of soil subsidence varied with land use, likely because of variation in soil structure and nature of the vegetation associated with land use. Gilgai presence and shape and inorganic C contents were also found to be important factors for variation in soil subsidence and possibly in the relationship between the soil subsidence and change in soil water storage. The ratio of soil subsidence to change in soil water storage varied with time under all land uses. The ratio of soil subsidence to change in soil water content under these high shrink-swell potential soils also proved variability in equidimensional property of soil shrinkage in space that shows the variability of cracks, which is an important factor in affecting the hydrology of soils.

The change in volume of soils between saturation and -33.3 kPa water potential was also studied in the laboratory. Results showed considerable difference in soil volume, which is contrary to the previous assumption that there is a negligible change in volume of soils between saturation and -33.3 kPa water potential.

Generally, despite the fact that this study provided information about the spatial and temporal variability of shrink-swell dynamics on vertic watersheds based on long-term field measurements of soil subsidence and soil water, estimate of soil subsidence may not be enough to improve hydrology models because crack orientation and geometry are also an important factor to govern flow and distribution of water in a vertic watershed. Lack of adequate technology to measure crack orientation and geometry, both efficiently and non-destructively, is a major challenge in a current study of crack dynamics. Current techniques of measuring soil cracking and the shrink-swell dynamics of Vertisols are far from providing complete information of cracks such as crack area density, depth, orientation and network, opening and closing time, and pattern of formation. Soil subsidence is reasonably easy to quantify in the field; however, coupling this measurement with crack imaging (2D or 3D) or crack capacitance measurement would further clarify soil cracking behavior, in situ. Therefore, a combined use of field and laboratory techniques, assisted by models, may help obtain and process all the necessary information.

REFERENCES

Aitchenson, G.D., Holmes, J.W., 1953. Aspects of swelling in the soil profile. Aust. J. Appl. Sci. 4, 244-259.

Allen, P.M., Harmel, R.D., Arnold, J., Plant, B., Yelderman, J., King, K., 2005. Field data and flow system response in clay (Vertisol) shale terrain, north central Texas, USA. Hydrol. Processes, 19, 2719-2736.

Amidu, S.A., Dunbar, J.A., 2007. Geoelectric studies of seasonal wetting and drying of a Texas Vertisol. Vadose Zone J., 6, 511-523.

Anderson, J.U., Fadul, K.E., O'Connor, G.A., 1973. Factors affecting the coefficient of linear extensibility in Vertisols. Soil Sci. Soc. Am. J., 37, 296-299.

Arnold, J.G., Allen, P.M., Muttiah, R., Bernhardt, G., 1995. Automated base flow separation and recession analysis techniques. Ground Water, 33, 1010-1018.

Arnold, J.G., Potter, K.N., King, K.W., Allen, P.M., 2005. Estimation of soil cracking and the effect on surface runoff in a Texas Blackland Prairie watershed. Hydrol. Processes, 19, 589-603.

Azam, S., Abduljauwad, S., Al-Shayea, N., Al-Amoudi., O.S.B., 2000. Effects of calcium sulfate on swelling potential of expansive clay. In: Vaught, R., K.R. Brye, and D.M. Miller (Eds.), Relationships among Coefficient of Linear Extensibility and Clay Fractions in Expansive, Stoney Soils: Soil Sci. Soc. Am. J. 70, 1983-1990.

Baer, J.U., Anderson, S.H., 1997. Landscape effects on desiccation cracking in an Aqualf. Soil Sci. Soc. Am. J., 61, 1497-1502.

Bandyopadhyay, K.K., Mohanty, M., Painuli, D.K., Misra, A.K., Hati, K.M., Mandal, K.G., Ghosh, P.K., Chaudhary, R.S., Acharya, C.L., 2003. Influence of tillage practices and nutrient management on crack parameters in a Vertisol of central India. Soil Tillage Res., 71, 133-142.

Blokhuis, W.A., 2006. Vertisols. In: Rattan Lal (Ed.), Encyclopedia of Soil Science: Second Edition. Taylor and Francis, Boca Raton, pp.1830 - 1840.

Bronswijk, J.J.B., 1990. Shrinkage geometry of a heavy clay soil at various stresses. Soil Sci. Soc. Am. J., 54, 1500-1502.

Bronswijk, J.J.B., 1991. Relation between vertical soil movements and water-content changes in cracking clays. Soil Sci. Soc. Am. J., 55, 1220-1226.

Cabidoche, Y.-M., Ozier-Lafontaine, H., 1995. THERESA: I. Matric water content measurements through thickness variations in vertisols. Agr. Water Manage., 28, 133-147.

Cabidoche, Y.-M., Ruy, S., 2001. Field shrinkage curves of a swelling clay soil: analysis of multiple structural swelling and shrinkage phases in the prisms of a Vertisol. Aust. J. Soil Res., 39, 143-160.

Cabidoche, Y.-M., Voltz, M., 1995. Non-uniform volume and water content changes in swelling clay soil: II. A field study on a Vertisol. Euro. J. Soil Sci., 46: 345-355.

Chertkov, V.Y., 2007. The reference shrinkage curve of clay soil. Theor. Appl. Frac. Mec., 48, 50-67.

Corbeels, M., Hartmann, R., Hofman, G., Van Cleemput, O., 1999. Field calibration of a neutron moisture meter in Vertisols. Soil Sci. Soc. Am. J., 63, 11-18.

Cornelis, W.M., Corluy, J., Medina, H., Díaz, J., Hartmann, R., Van Meirvenne, M., Ruiz, M.E., 2006. Measuring and modelling the soil shrinkage characteristic curve. Geoderma, 137, 179-191.

Corwin, D.L., Lesch, S.M., 2005. Characterizing soil spatial variability with apparent soil electrical conductivity: I. Survey protocols. Comput. Electron. Agri., 46, 103-133.

Coulombe, C.E., Wilding, L.P., Dixon, J.B., 1996. Overview of Vertisols: characteristics and impacts on society. Advan. Agron., 57, 289–375.

Daniells, I., 1989. Degradation and restoration of soil structure in a cracking grey clay used for cotton production. Aust. J. Soil Res., 27, 455-469.

Davidson, S.E., Page, J.B., 1956. Factors influencing swelling and shrinking in soils. Soil. Sci. Soc. Am. J., 20, 320-324.

Deshpande, T.L., Greenland, D.J., Quirk, J.P., 1964. Role of iron oxide in the bonding of soil particles. Nature 201, 107 - 108.

Dudal, R., Eswaran, H., 1988. Distribution, properties, and classification of vertisols. In: Arnold, J.G., Potter, K.N., King, K.W., Allen, P.M. (Eds.), Estimation of soil cracking and the effect on surface runoff in a Texas Blackland Prairie watershed. Hydro. Process, 19, 589-603.

Evett, S.R., 2008. Neutron moisture meters. In Evett, S.R., Heng, L.K., Moutonnet, P., Nguyen, M.L. (eds.) Field Estimation of Soil Water Content: A Practical Guide to Methods, Instrumentation and Sensor Technology. IAEA-TCS-30. International Atomic Energy Agency, Vienna, Austria, pp. 39-54.

Evett, S.R., Schwartz, R.C., Tolk, J.A., Howell, T.A., 2009. Soil profile water content determination: spatiotemporal variability of electromagnetic and neutron probe sensors in access tubes. Vadose Zone J., 8, 926-941.

Evett, S.R., Steiner, J.L., 1995. Precision of neutron scattering and capacitance type soil water content gauges from field calibration. Soil Sci. Soc. Am. J., 59: 961-968.

Evett, S.R., Tolk, J.A., Howell, T.A., 2006. Soil profile water content determination: sensor accuracy, axial response, calibration, temperature dependence, and precision. Vadose Zone J., 5, 894-907.

Franzmeier, D.P., Ross, S.J., Jr., 1968. Soil swelling: laboratory measurement and relation to other soil properties. Soil. Sci. Soc. Am. J., 32, 573-577.

Gray, C.W., Allbrook, R., 2002. Relationships between shrinkage indices and soil properties in some New Zealand soils. Geoderma, 108, 287-299.

Greacen, E., Hignett, C., 1979. Sources of bias in the field calibration of a neutron meter. Soil Research, 17, 405-415.

Greacen, E., Schrale, G., 1976. The effect of bulk density on neutron meter calibration. Soil Research, 14, 159-169.

Grossman, R.B., Brasher, B.R., Franzmeier, D.P., Walker, J.L., 1968. Linear extensibility as calculated from natural-clod bulk density measurements. Soil Sci. Soc. Am. J., 32, 570-573.

Haines, W.B., 1923. The volume-changes associated with variations of water content in soil. Jour. Agri. Sci., 13, 296-310.

Harmel, R.D., Richardson, C.W., King, K.W., Allen, P.M., 2006. Runoff and soil loss relationships for the Texas Blackland Prairies ecoregion. J. Hydro., 331, 471-483.

Hodgson, A.S., Chan, K.Y., 1987. Field calibration of a neutron moisture meter in a cracking grey clay. Irri. Sci., 8, 233-244.

Johnston, J.R., Hill, H.O., 1944. A study of the shrinking and swelling properties of Rendzina soils. Soil Sci. Soc. Am. J., 9, 24-29.

Júnior, R.P.S., Boesten, J.J., 2005. Simulation of pesticide leaching in a cracking clay soil with the PEARL model. Pest Manag. Sci., 61, 432-448.

Keen, B.A., 1931. The physical properties of the soil. Q. J. Roy. Meteor. Soc., 58, 490-491.

Kirby, J.M., Bernardi, A.L., Ringrose-Voase, A.J., Young, R., Rose, H., 2003. Field swelling, shrinking, and water content change in a heavy clay soil. Aust. J. Soil Res., 41, 963-978.

Kishné, A.S., Morgan, C.L.S., Ge, Y., Miller, W.L., 2010. Antecedent soil moisture affecting surface cracking of a Vertisol in field conditions. Geoderma, 157, 109-117.

Kishné, A.S., Morgan, C.L.S., Miller, W.L., 2009. Vertisol crack extent associated with gilgai and soil moisture in the Texas Gulf Coast Prairie. Soil Sci. Soc. Am. J., 73, 1221-1230.

Knight, M.J., 1980. Structural analysis and mechanical origins of gilgai at Boorook, Victoria, Australia. Geoderma, 23, 245-283.

Komornik, A., 1969. Proceedings of the second international research and engineering conference on expansive clay soils. In: Vaught, R., Brye, K.R., and Miller, D.M. (Eds.), Relationships among coefficient of linear extensibility and clay fractions in expansive, Stoney Soils. Soil Sci. Soc. Am. J. 70, 1983-1990.

Lauritzen, C.W., Stoltenberg, N.L., 1940. Some factors which influence infiltration and its measurement in Houston Black clay. J. Am. Soc. Agron., 32, 853-866.

Lin, H.S., Mclnnes, K.J., Wilding, L.P., Hallmark, C.T., 1998. Macroporosity and initial moisture effects on infiltration rates in Vertisols and Vertic intergrades. Soil Sci., 163, 2-8.

Lindenmaier, F., Zehe, E., Helms, M., Evdakov, O., Ihringer, J., 2006. Effect of soil shrinkage on runoff generation in micro and mesoscale catchments. In: Sivapalan, M., Wagener, T., Uhlenbrook, S., Zehe, E., Lakshmi, V., Liang, X., Tachiawa, Y. and Kumar, P. (Eds), Predictions in ungauged basins: promise and progress, Wallingford: International Association of Hydrological Sciences Publ., pp. 305 – 317.

Mazahrih, N.T., Katbeh-Bader, N., Evett, S.R., Ayars, J.E., Trout, T.J., 2008. Field calibration accuracy and utility of four down-hole water content sensors. Vadose Zone J., 7, 992-1000.

McCormack, D.E., Wilding, L.P., 1975. Soil properties influencing swelling in Canfield and Geeburg soils. Soil. Sci. Soc. Am. J., 39, 496-502.

Messing, I., Jarvis, N.J., 1990. Seasonal variation in field-saturated hydraulic conductivity in two swelling clay soils in Sweden. Euro. J. Soil Sci., 41, 229-237.

Miller, W.L., Kishné, A.S., Morgan, C.L.S., 2010. Vertisol morphology, classification and seasonal cracking patterns in the Texas Gulf Coast Prairie. Soil Surv. Horiz., 51, 10-16.

Mitchell, A.R., 1991. Soil surface shrinkage to estimate profile soil water. Irri. Sci., 12, 1-6.

Mitchell, A.R., van Genuchten, M.T., 1992. Shrinkage of bare and cultivated soil. Soil. Sci. Soc. Am. J., 56, 1036-1042.

Olsen, P.A., Haugen, L.E., 1998. A new model of the shrinkage characteristic applied to some Norwegian soils. Geoderma, 83, 67-81.

Peng, X., Horn, R., Peth, S., Smucker, A., 2006. Quantification of soil shrinkage in 2D by digital image processing of soil surface. Soil Tillage Res., 91, 173-180.

Reeve, M.J., Hall, D.G.M., Bullock, P., 1980. The effect of soil composition and environmental factors on the shrinkage of some clayey British soils. Euro. J. Soil Sci., 31, 429-442.

Rimmer, D.L., Greenland, D.J., 1976. Effects of calcium carbonate on the swelling behaviour of a soil clay. Euro.J. Soil Sci., 27, 129-139.

Rivera, L., 2008. Comparing methods of estimating crack volume in shrink-swell soils. A Senior Scholars Thesis. Texas A&M University, College Station, TX.

Ross, G.J., 1978. Relationships of specific surface area and clay content to shrink-swell potential of soils having different clay mineralogical compositions. Can. J. Soil Sci., 58, 159-166.

Rossi, A.M., Hirmas, D.R., Graham, R.C., Sternberg, P.D., 2008. Bulk density determination by automated three-dimensional laser scanning. Soil. Sci. Soc. Am. J., 72, 1591-1593.

Samouëlian, A., Cousin, I., Richard, G., Tabbagh, A., Bruand, A., 2003. Electrical resistivity imaging for detecting soil cracking at the centimetric scale. Soil Sci. Soc. Am. J., 67, 1319-1326.

Samouëlian, A., Richard, G., Cousin, I., Guerin, R., Bruand, A., Tabbagh, A., 2004. 3D crack monitoring by electrical resistivity tomography. Euro. J. Soil Sci., 55 (4), 751-762.

Sander, T., Gerke, H.H., 2007. Noncontact shrinkage curve determination for soil clods and aggregates by three-dimensional optical scanning. Soil Sci. Soc. Am. J., 71, 1448-1454.

Sherrod, L.A., Dunn, G., Peterson, G.A., Kolberg, R.L., 2002. Inorganic carbon analysis by modified pressure-calcimeter method. Soil Sci. Soc. Am. J., 66, 299-305.

Smith, C.W., Hadas, A., Dan, J., Koyumdjisky, H., 1985. Shrinkage and Atterberg limits in relation to other properties of principal soil types in Israel. Geoderma, 35, 47-65.

Soil Survey Staff, 1996. Soil survey laboratory methods and procedures for collecting soil samples. Soil Survey Investigations Report No. 42. United States Government Printing Office, Washington, DC.

Soil Survey Staff, 1999. Soil Taxonomy, A basic system of soil classification for making and interpreting soil surveys. U.S. Gov. Print. Office, Washington, DC. soils.usda.gov/technical/classification/taxonomy/ Accessed on 05/17/ 2010.

Soil Survey Staff, 2003. Natural Resources Conservation Service, United States Department of Agriculture. Web Soil Survey. Available online at websoilsurvey.nrcs.usda.gov/ accessed 04/20/2011.

Srivastava, K.L., Smith, G.D., Jangawad, L.S., 1989. Compaction and shading effects on surface cracking in a vertisol. Soil and Tillage Research, 13, 151-161.

Stirk, G., 1954. Some aspects of soil shrinkage and the effect of cracking upon water entry into the soil. Aust. J. Agri. Res., 5, 279-296.

Suarez, D.L., 2006. Inorganic Carbon: Land Use Impacts. In: Rattan Lal (Ed.), Encyclopedia of Soil Science: Second Edition. Taylor and Francis, Boca Raton, pp. 895 - 897.

Tariq, A.-u.-R., Durnford, D.S., 1993. Analytical volume change model for swelling clay soils. Soil Sci. Soc. Am. J., 57, 1183-1187.

Thomas, P.J., Baker, J.C., Zelazny, L.W., 2000a. An expansive soil index for predicting shrink-swell potential. Soil Sci. Soc. Am. J., 64, 268-274.

Thomas, P.J., Baker, J.C., Zelazny, L.W., Hatch, D.R., 2000b. Relationship of map unit variability to shrink-swell indicators. Soil Sci. Soc. Am. J., 64, 262-268.

Thompson, C.H., Beckmann, G.G., 1982. Gilgai in Australian Black Earths and some of its effects on plants. Tropical Agriculture, 59, 149-156.

Tunny, J., 1970. The influence of Saran resin coatings on swelling of natural soil clods. Soil Sci., 109, 254-256.

USDA-NRCS, 1997. http://www2.ftw.nrcs.usda.gov/osd/dat/H/HEIDEN.html Accessed on 06/10/2009.

Vaught, R., Brye, K.R., Miller, D.M., 2006. Relationships among coefficient of linear extensibility and clay fractions in expansive, stoney soils. Soil Sci. Soc. Am. J., 70, 1983-1990.

Velde, B., 1999. Structure of surface cracks in soil and muds. Geoderma, 93, 101-124.

Wilding, L.P., Tessier, D., 1998. Genesis of Vertisols: shrink-swell phenomena. In: Wilding, L.P. and Puentes, R. (Eds.), Vertisols: Their Distribution, Properties, Classification, and Management. Texas A&M University Printing Center, College Station, TX, pp.55-79.

Yule, D.F., Ritchie, J.T., 1980a. Soil shrinkage relationships of Texas vertisols: I. Small cores. Soil Sci. Soc. Am. J., 44, 1285-1291.

Yule, D.F., Ritchie, J.T., 1980b. Soil shrinkage relationships of Texas Vertisols: II. Large cores. Soil Sci. Soc. Am. J., 44, 1291-1295.

APPENDIX A

Monthly total rainfall of the study area, located at the USDA-ARS Grassland, Soil and Water Research Laboratory, in Riesel, Texas.

Month	Rain			
	---mm---			
	2005	2006	2007	2008
January	73	64	225	31
February	78	52	9	36
March	48	104	257	106
April	14	63	51	82
May	110	151	329	117
June	12	62	163	4
July	27	98	157	19
August	262	33	8	124
September	24	84	53	22
October	30	102	65	41
November	3	8	58	26
December	6	51	55	25
Total	688	872	1429	632

APPENDIX B

Change in soil water storage (mm) at different soil layers at the measurement sites of Native prairie.

	N1			N2			N3			N4		
Date	0-30	30-60	60-90	0-30	30-60	60-90	0-30	30-60	60-90	0-30	30-60	60-90
	---------------------------- cm --											
7/16/08	-44	-40	-22	-54	-44	-24	-79	-37	-20	-46	-41	-24
7/31/08	-52	-45	-32	-55	-48	-35	-81	-42	-29	-49	-42	-31
8/15/08	-37	-42	-30	-43	-49	-37	-66	-42	-32	-42	-42	-31
8/29/08	-24	-17	-18	-29	-21	-28	-47	-15	-16	-21	-20	-20
9/19/08	-38	-34	-27	-49	-42	-35	-69	-32	-25	-31	-30	-25
10/3/08	-49	-42	-30	-59	-50	-41	-60	-38	-28	-46	-36	-28
10/17/08	-43	-47	-38	-51	-51	-42	-57	-39	-29	-41	-39	-32
12/12/08	-43	-50	-41	-53	-52	-46	-56	-41	-30	-42	-43	-34
2/3/09	-30	-49	-42	-44	-51	-46	-50	-42	-31	-36	-43	-36
4/7/09	-18	-11	-6	-19	-11	-8	-21	-4	-6	-16	-13	-7
5/28/09	-26	-13	-3	-31	-14	-8	-24	-4	-4	-23	-15	-4
6/23/09	-55	-49	-28	-58	-50	-31	-62	-40	-16	-52	-41	-21
7/10/09	-37	-53	-37	-44	-54	-41	-41	-55	-30	-37	-45	-34
7/24/09	-59	-58	-44	-61	-56	-47	-62	-62	-38	-55	-49	-39
8/6/09	-57	-60	-48	-60	-60	-50	-53	-62	-45	-54	-51	-41
8/17/09	-64	-63	-54	-64	-62	-54	-66	-71	-46	-60	-53	-44
8/28/09	-64	-66	-57	-66	-64	-58	-71	-74	-51	-60	-54	-46
9/18/09	NA	NA	NA	-16	-10	-9	0	-18	-8	-14	-12	-16
10/23/09	0	-2	-1	-1	-5	-3	11	-46	-130	-4	-6	-7
11/25/09	-1	-2	-2	-6	-1	-1	10	-14	-3	-4	-6	-7
12/21/09	-4	-1	-1	-5	-1	0	13	-12	0	-2	-4	-6

	N1			N2			N3			N4		
Date	0-30	30-60	60-90	0-30	30-60	60-90	0-30	30-60	60-90	0-30	30-60	60-90
	------------------------------ cm ------------------------------											
1/26/10	-2	0	-1	-1	-2	0	9	-15	-2	-2	-6	-6
2/19/10	-1	-1	-1	-1	-4	-2	11	-15	-1	-2	-7	-8
3/17/10	-3	-9	-11	-2	-2	-2	10	-17	-3	0	1	-1
4/8/10	-10	-3	-1	-9	-4	-1	4	-16	-1	-12	-8	-6
5/6/10	-18	-4	-3	-24	-7	-2	-11	-20	-4	-24	-11	-7
5/25/10	-53	-25	-7	-57	-30	-7	-69	-46	-6	-60	-32	-13
6/17/10	-33	-28	-14	-34	-29	-12	-27	-48	-8	-33	-37	-16
7/15/10	-50	-51	-22	-53	-51	-31	-30	-49	-8	-55	-48	-25
7/30/10	-31	-52	-29	-31	-52	-49	-22	-43	-11	-28	-48	-31
8/13/10	-70	-63	-37	-70	-64	-52	-53	-45	-10	-66	-56	-33
9/16/10	-24	-19	-15	-28	-19	-25	-18	-32	-11	-26	-19	-18

APPENDIX C

Change in soil water storage (mm) at different soil layers at the measurement sites of Grazed pasture.

	G1			G2			G3			G4			G5		
Date	0-30	30-60	60-90	0-30	30-60	60-90	0-30	30-60	60-90	0-30	30-60	60-90	0-30	30-60	60-90
	- -cm- -														
7/16/08	-81	-61	-76	-76	-54	-72	NA	NA	NA	-54	-47	-46	-70	-54	-46
7/31/08	-70	-59	-72	-64	-54	-70	-75	-61	-72	-48	-48	-46	-60	-51	-44
8/15/08	-51	-55	-73	-43	-52	-72	-53	-58	-72	-33	-44	-45	-33	-46	-44
8/29/08	-26	-38	-70	-26	-26	-67	-35	-43	-69	-18	-28	-42	-24	-30	-44
9/19/08	-50	-46	-70	-44	-36	-66	-59	-56	-72	-37	-39	-44	-47	-42	-42
10/3/08	-64	-54	-70	-56	-44	-69	-74	-66	-77	-51	-47	-46	-64	-51	-46
10/17/08	-52	-54	-72	-48	-46	-70	-63	-69	-79	-38	-47	-47	-50	-49	-46
12/12/08	-58	-56	-73	-53	-49	-71	-66	-73	-84	-41	-48	-49	-55	-51	-48
1/22/09	-46	-55	-72	-42	-48	-70	-47	-72	-82	-27	-48	-48	-37	-48	-48
2/3/09	-48	-55	-72	-44	-48	-70	-47	-73	-82	-29	-47	-47	-38	-49	-47
2/12/09	-22	-31	-67	-18	-24	-66	-24	-40	-73	-13	-29	-44	-21	-17	-39
4/7/09	-13	-10	-27	-17	-2	-22	NA	NA	NA	-11	-15	-19	-20	-6	-7
5/28/09	-22	-13	-25	-24	-4	-23	-28	-18	-24	-21	-18	-19	-29	-13	-9
6/23/09	-61	-46	-46	-55	-32	-36	-64	-54	-46	-51	-47	-37	-66	-46	-32
7/10/09	-32	-48	-54	-29	-37	-45	-38	-54	-55	-23	-32	-37	-29	-35	-40

		G1			G2			G3			G4			G5	
Date	0-30	30-60	60-90	0-30	30-60	60-90	0-30	30-60	60-90	0-30	30-60	60-90	0-30	30-60	60-90
							-cm-								
7/24/09	-60	-55	-59	-60	-48	-55	-65	-62	-68	-51	-49	-46	-65	-48	-49
8/6/09	-56	-57	-63	-59	-52	-59	-61	-63	-70	-50	-53	-50	-59	-51	-52
8/16/09	-61	-58	-65	-65	-57	-64	-70	-67	-73	-57	-57	-55	-68	-53	-54
8/28/09	-61	-60	-67	-71	-61	-68	-72	-70	-75	-60	-62	-60	-69	-57	-57
9/18/09	-10	-12	-26	-9	-12	-25	-24	-10	-27	-6	-15	-23	-14	-6	-12
10/23/09	-1	-9	-13	1	-3	-17	-1	-12	-16	-5	-9	-11	-8	2	-3
11/13/09	-1	-1	0	-2	2	-2	-3	-1	0	NA	NA	NA	NA	NA	NA
11/25/09	-7	-11	-14	-11	-8	-19	-7	-13	-17	-7	0	-12	-13	-2	-4
12/21/09	-12	-14	-15	-15	-10	-15	-10	-15	-19	-10	-12	-13	-9	-2	-4
1/26/10	-10	-13	-14	-6	-6	-9	-14	-14	-19	-5	-11	-10	-7	0	-2
2/19/10	-4	-11	-15	-7	-8	-13	-6	-13	-18	-9	-10	-12	-7	-1	-4
3/17/10	-6	-8	-14	-7	-7	-10	-6	-10	-16	-5	-10	-10	-5	-1	-3
4/8/10	-10	-14	-16	-17	-13	-15	-19	-17	-19	-13	-9	-15	-13	-5	-4
5/6/10	-17	-17	-15	-21	-17	-15	-32	-23	-22	-21	-13	-14	-22	-6	-5
5/25/10	-47	-30	-22	-47	-31	-24	-59	-39	-27	-46	-16	-22	-56	-20	-8
6/17/10	-25	-34	-32	-25	-28	-28	-31	-37	-33	-24	-32	-26	-33	-20	-15
7/15/10	-47	-57	-44	-39	-47	-42	-55	-55	-45	-33	-27	-41	-49	-45	-33
7/30/10	-27	-55	-58	-23	-41	-49	-37	-64	-57	-18	-43	-51	-31	-40	-49
8/13/10	-65	-66	-53	-57	-61	-47	-74	-68	-56	-48	-43	-51	-69	-55	-48
9/16/10	-24	-26	-33	-22	-28	-30	-30	-28	-32	-16	-55	-34	-28	-16	-25

APPENDIX D

Change in soil water storage (mm) at different soil layers at the measurement sites of Row crop.

	RC1			RC2			RC3			RC4		
Date	0-30	30-60	60-90	0-30	30-60	60-90	0-30	30-60	60-90	0-30	30-60	60-90
	cm											
8/15/08	-39	-43	-42	-41	-43	-46	-51	-50	-47	-39	-42	-41
8/29/08	-17	-24	-36	-15	-26	-42	-22	-26	-40	-18	-25	-35
9/19/08	-21	-24	-35	-24	-28	-42	-22	-28	-40	-19	-28	-35
10/17/08	-34	-34	-36	-35	-35	-43	-39	-40	-42	-19	-29	-36
10/31/08	-41	-39	-39	NA	NA	NA	-43	-42	-43	-21	-30	-38
12/12/08	-41	-40	-40	-32	-36	-43	-39	-43	-43	-17	-31	-37
1/22/09	-36	-41	-40	-31	-36	-43	-33	-43	-44	-18	-22	-38
2/12/09	-14	-32	-40	-13	-26	-42	-20	-29	-43	-13	-22	-33
4/7/09	-3	-2	-1	NA	NA	NA	-13	-10	-7	2	-28	-7
6/16/09	-25	-18	-12	NA	NA	NA	-23	-17	-15	NA	NA	NA
7/10/09	-17	-21	-16	NA	NA	NA	-15	-14	-13	NA	NA	NA
7/24/09	-21	-23	-16	NA	NA	NA	-18	-17	-15	NA	NA	NA
8/6/09	-18	-22	-15	-26	0	0	-22	-18	-16	-29	-29	-19
8/17/09	-28	-24	-18	-35	-23	-21	-36	-26	-19	-45	-45	-31
8/28/09	-51	-30	-15	-48	-41	-40	-34	-22	-14	-37	-41	NA
10/16/09	-4	-5	-7	0	1	-3	-3	-1	-1	0	-9	-8
11/13/09	-15	-11	-10	-10	-2		-4	-1	-1	-2	-8	-8
11/25/09	-8	-10	-9	-4	-1	-6	-1	-1	-1	-5	-11	-11
12/22/09	-10	-10	-8	-9	-7	-9	-3	-1	-1	-2	-9	-10
1/22/10	-8	-9	-8	-6	-3	-7	-5	-4	-2	-3	-10	-10

	RC1			RC2			RC3			RC4		
Date	0-30	30-60	60-90	0-30	30-60	60-90	0-30	30-60	60-90	0-30	30-60	60-90
						-cm-						
2/19/10	-8	-10	-10	-5	-3	-9	-4	-4	-3	-5	-12	-13
3/5/10	-7	-10	-7	-2	1	-4	-2	0	-1	-2	-12	-11
4/8/10	-15	-11	-8	-11	-6	-10	-7	-6	-1	-13	-10	-11
5/6/10	-13	-11	-8	-17	-8	-8	-13	-9	-2	-4	-10	-11
5/25/10	-32	-15	-10	-43	-14	-11	-42	-30	-18	-7	-10	-10
6/17/10	-35	-40	-25	-30	-20	-21	-23	-28	-32	-17	-10	-10
7/15/10	-55	-45	-98	-73	-52	-41	-54	-51	-51	-31	-30	-18
7/30/10	-30	-49	-45	NA	NA	NA	-28	-54	-59	NA	NA	NA
8/13/10	-54	-48	-41	-95	-70	-56	-54	-56	-57	-30	-23	-14

APPENDIX E

Soil subsidence (mm) at different soil layers at the measurement sites of Native prairie.

	NP1			NP2			NP3			NP4		
Date	0-30	30-60	60-90	0-30	30-60	60-90	0-30	30-60	60-90	0-30	30-60	60-90
	-------------cm-------------											
7/16/08	-2	-15	-7	-13	-14	-8	-16	2	-5	-13	-12	2
7/31/08	-13	-15	-9	-16	-14	-10	-22	2	-8	-14	-12	1
8/15/08	-7	-13	-9	-7	-13	-12	-21	2	-10	-10	-11	0
8/29/08	-4	-4	-6	-3	-4	-9	-9	3	-2	-4	-3	3
9/19/08	-6	-10	-7	-8	-9	-11	-15	5	-7	-7	-6	2
10/3/08	-10	-13	-9	-12	-10	-12	-18	3	-10	-10	-8	1
10/17/08	-6	-14	-9	-6	-10	-13	-15	2	-11	-6	-9	1
12/12/08	-7	-14	-9	-5	-11	-13	-14	1	-11	-7	-10	1
2/3/09	-5	-13	-9	-3	-10	-13	-12	2	-11	-6	-10	1
4/7/09	-2	-3	-1	2	-1	-4	-7	8	0	-1	-2	7
5/28/09	-4	-3	-2	-1	-2	-2	-9	9	1	-2	-3	9
6/23/09	-11	-17	-6	-7	-14	-8	-14	-4	-3	-13	-12	2
7/10/09	-3	-17	-8	-3	-12	-11	9	-22	-9	-6	-12	-1
7/24/09	-12	-19	-9	-10	-14	-11	14	-34	-11	-13	-14	-3
8/6/09	-9	-19	-10	-6	-14	-12	18	-37	-13	-10	-16	-4
8/16/09	-13	-20	-11	-10	-14	-13	22	-43	-14	-14	-18	-4
8/28/09	-13	-20	-12	-10	-15	-13	21	-44	-15	-14	-18	-6
9/18/09	2	-7	-5	3	-4	-7	32	-27	-9	0	-6	-5
10/23/09	-1	-1	-2	4	-2	1	28	-28	-1	-1	-3	-1
11/25/09	1	-1	-1	-1	-1	0	29	-28	-1	-1	0	-2

	NP1			NP2			NP3			NP4		
Date	0-30	30-60	60-90	0-30	30-60	60-90	0-30	30-60	60-90	0-30	30-60	60-90
	-cm-											
12/22/09	1	0	-1	-2	0	0	28	-28	0	-1	0	-1
1/26/10	1	1	-1	-1	0	0	26	-28	0	-1	0	-1
2/19/10	1	0	-1	-2	0	0	27	-28	0	0	-1	1
3/17/10	0	0	0	0	0	1	28	-28	0	0	1	-1
4/8/10	0	0	-1	-1	0	0	26	-30	0	-6	-1	0
5/6/10	-3	2	-3	-4	0	0	24	-30	-1	-10	-1	0
5/25/10	-11	-5	-2	-9	-7	-1	11	-37	-1	-17	-7	-2
6/17/10	-3	0	-11	-5	-7	-3	17	-37	-3	-9	-10	0
7/15/10	-9	-14	-5	-6	-11	-9	20	-40	-3	-11	-13	-5
7/30/10	-4	-13	-7	-3	-12	-12	21	-43	-4	-4	-15	-6
8/13/10	-13	-17	-9	-12	-15	-13	12	-44	-5	-13	-16	-8
9/16/10	-4	-10	-6	-4	-5	-11	24	-39	-6	-6	-4	-8

APPENDIX F

Soil subsidence (mm) at different soil layers at the measurement sites of Grazed pasture.

	G1			G2			G3			G4			G5		
Date	0-30	30-60	60-90	0-30	30-60	60-90	0-30	30-60	60-90	0-30	30-60	60-90	0-30	30-60	60-90
								----cm----							
7/16/08	-10	18	-50	-12	25	-40	NA	NA	NA	-7	-13	-13	4	-21	-18
7/31/08	-15	18	-50	-18	24	-41	-24	24	-47	-16	-14	-13	-2	-21	-19
8/15/08	-8	20	-51	-8	25	-42	-15	21	-44	-6	-14	-13	4	-18	-19
8/29/08	-3	23	-46	-4	30	-40	-12	23	-38	1	-9	-12	8	-9	-20
9/19/08	-9	21	-46	-10	26	-39	-18	18	-37	-8	-11	-12	1	-16	-17
10/3/08	-15	20	-47	-13	23	-39	-20	17	-40	-13	-12	-12	-3	-13	-21
10/17/08	-8	20	-47	-8	24	-40	-11	12	-41	-7	-12	-13	2	-14	-21
12/12/08	-8	18	-47	-8	24	-40	-9	12	-44	-7	-12	-13	0	-10	-21
1/22/09	-5	18	-45	-8	23	-37	-3	7	-40	-4	-12	-13	1	-8	-21
2/3/09	-6	18	-46	-8	24	-37	-3	7	-40	-4	-12	-13	2	-8	-21
2/12/09	-4	19	-41	-4	25	-32	-2	8	-33	-1	-6	-12	2	2	-20
4/7/09	-3	14	-28	-6	26	-19	0	5	-17	2	-6	2	2	5	-7
5/28/09	-5	13	-23	-9	29	-17	-2	4	-15	-5	-5	6	-1	0	-6
6/23/09	-16	8	-33	-13	18	-24	-14	-1	-23	-15	-12	-1	-10	-7	-11
7/10/09	-5	10	-33	-7	16	-22	-5	-5	-22	-4	-10	-5	-3	-3	-18
7/24/09	-14	10	-34	-11	15	-29	-13	2	-31	-14	-10	-9	-9	-2	-22
8/6/09	-9	7	-35	-8	13	-30	-17	3	-31	-11	-12	-11	-8	-5	-23
8/16/09	-12	6	-36	-14	11	-32	-21	4	-32	-12	-14	-13	-9	-6	-23
8/28/09	-14	5	-36	-13	10	-36	-20	4	-32	-9	-19	-14	-10	-7	-24
9/18/09	1	4	-14	5	6	-14	-23	20	-12	3	-5	-9	-1	4	-12

	G1			G2			G3			G4			G5		
Date	0-30	30-60	60-90	0-30	30-60	60-90	0-30	30-60	60-90	0-30	30-60	60-90	0-30	30-60	60-90
	cm														
10/23/09	-1	-1	-5	2	6	-13	-2	-3	1	0	0	3	-3	6	-5
11/13/09	-2	-1	-1	-4	5	-4	-3	-2	0	-1	-1	2	-1	7	-7
11/25/09	-1	-1	-1	-4	5	-12	-2	-1	0	2	-1	2	0	1	-2
12/21/09	0	-1	1	-6	5	-1	-1	-1	0	-1	-1	1	1	2	-3
1/26/10	-1	-1	1	-3	4	2	-2	0	0	0	-2	2	1	1	-2
2/19/10	0	0	0	0	2	-2	0	0	0	0	-1	1	1	1	-1
3/17/10	0	0	0	0	0	0	0	0	0	0	0	0	0	0	0
4/8/10	-2	0	-1	-2	-1	0	-3	-1	-1	-1	0	0	-1	-1	0
5/6/10	-3	-1	-2	-5	-1	0	-7	-1	-2	-5	-2	-1	-5	2	-3
5/25/10	-10	-3	-4	-9	-7	-2	-12	-5	-6	-10	-7	-2	-11	-4	-3
6/17/10	-6	-5	-7	-6	-7	-1	-5	-7	-5	-4	-9	-6	-6	0	-7
7/15/10	-7	-8	-6	-5	-10	-9	-10	-5	-12	-3	-16	-9	-6	-8	-11
7/30/10	-4	0	-16	-5	-12	-6	-6	-8	-12	3	-18	-12	-5	-3	-15
8/13/10	-10	-2	-9	-12	-28	4	-18	-7	-18	5	-31	-12	-11	-9	-14
9/16/10	-3	-1	-18	1	-15	-7	-4	-7	-9	6	-21	-5	-4	4	-17

APPENDIX G

Soil subsidence (mm) at different soil layers at the measurement sites of Row crop.

	RC1			RC2			RC3			RC4		
Date	0-30	30-60	60-90	0-30	30-60	60-90	0-30	30-60	60-90	0-30	30-60	60-90
						-cm-						
8/15/08	-27	-16	-12	-18	-10	-16	-26	-12	-12	-10	-18	-25
8/29/08	-17	-8	-12	-6	-4	-14	-17	-3	-8	-7	-9	-24
9/19/08	-17	-7	-10	-13	-4	-14	-18	-3	-7	-7	-9	-23
10/17/08	-16	-11	-11	-9	-4	-13	-17	-7	-9	-4	-7	-23
10/31/08	-21	-12	-11	NA	NA	NA	-21	-6	-9	-5	-7	-23
12/12/08	-18	-12	-11	-10	-4	-13	-18	-6	-9	-4	-7	-23
1/22/09	-18	-12	-11	-11	-4	-12	-18	-5	-9	-5	-7	-22
2/12/09	-8	-7	-11	-6	-1	-11	-16	-1	-8	-5	-6	-20
4/7/09	-6	-1	-1	0	0	0	-12	-1	-4	5	-5	-11
6/16/09	-12	-3	0	NA	NA	NA	-17	-2	-4	NA	NA	NA
7/10/09	-1	-5	0	NA	NA	NA	-8	-2	-4	NA	NA	NA
7/24/09	-7	-5	1	NA	NA	NA	-12	-2	-4	NA	NA	NA
8/6/09	-4	-5	1	-4	0	0	-10	-3	-4	6	-13	-9
8/17/09	-15	-5	0	-10	-1	-2	-13	-8	-5	1	-13	-12
8/28/09	-20	-4	-1	-14	-3	-6	-14	-11	-8	-3	-15	-12
10/16/09	-3	-1	-1	1	4	0	-4	-1	-2	1	-1	-1
11/13/09	-5	-1	-1	0	4	1	-4	-1	-1	0	-1	-2
11/25/09	-3	-1	-1	1	5	0	-4	-1	-1	0	-1	-2
12/21/09	-4	0	0	0	4	1	-3	0	-1	1	0	-2
1/22/10	-2	0	0	1	5	1	0	0	0	2	0	-1

	RC1			RC2			RC3			RC4		
Date	0-30	30-60	60-90	0-30	30-60	60-90	0-30	30-60	60-90	0-30	30-60	60-90
						-cm-						
2/19/10	0	0	0	4	6	1	0	0	0	3	0	0
3/5/10	-2	0	0	2	6	1	0	0	0	NA	NA	NA
4/9/10	-5	0	0	-1	5	1	-2	0	0	4	0	0
5/6/10	-6	0	0	-4	5	1	-3	0	-1	-7	0	0
5/25/10	-12	-1	0	-12	5	1	-9	-3	-2	1	0	-1
6/17/10	-7	-6	-6	-4	5	-1	-6	0	-5	-1	0	-1
7/15/10	-6	-10	-7	-12	-4	-6	-10	-5	-12	-6	-1	-1
7/30/10	2	-11	-7	NA	NA	NA	-1	-4	-13	-5	-5	-4
8/13/10	-11	-11	-6	-15	-7	-9	-9	-8	-13	-10	-6	-2
9/16/10	11	-3	1	4	-2	-9	-3	3	-4	3	-6	2

VITA

Name: Takele Mitiku Dinka

Address: Department of Soil and Crop Sciences
Texas A&M University
370 Olsen Blvd.
2474 TAMU
College Station, TX 77843-2474
C/o Cristine Morgan

Email Address: takele2004@yahoo.com

Education: B.S., Soil and Water Conservation, Mekelle University, Ethiopia, 2002

M.S., International Land and Water Management, Wageningen University, 2007

Ph.D., Soil Science, Texas A&M University, 2011